FACULDADE DE ENGENHARIA DA UNIVERSIDADE DO PORTO

Multibody Dynamic Analysis of a Freight Wagon

Francisca Cerqueira Manso

Master's Degree in Mechanical Engineering

Supervisor: Prof. Abílio de Jesus

Co-Supervisor: Dr. Cláudio Horas

Co-Supervisor: Prof. Francisco Andrade Pires

October 18, 2023

Multibody Dynamic Analysis of a Freight Wagon

Francisca Cerqueira Manso

Master's Degree in Mechanical Engineering

October 18, 2023

Resumo

O transporte de mercadorias está a passar por uma transformação crucial desde que os vagões articulados de mercadorias ganharam popularidade na Europa. A aceitação da expansão dos vagões articulados em toda a Europa provoca uma mudança de paradigma na eficácia e eficiência do transporte de carga, o que beneficia os operadores de transporte ferroviário de várias formas.

O aumento substancial da capacidade de carga é o benefício mais realçado no sector do transporte de carga. Os vagões articulados apresentam inúmeras qualidades, mantendo o comprimento típico do comboio, com potencial para aumentar a capacidade de carga. O número de viagens requeridas será significativamente reduzido em prol do crescimento da capacidade, que , em consequência, também aumentará a eficácia operacional e simplificará a logística. Além disso, oferece também uma eficiência optimizada, uma melhor gestão da carga, economia de custos, flexibilidade da carga e um menor impacto ambiental.

A presente dissertação de mestrado desenvolve uma investigação elaborada sobre um vagão de mercadorias, designado por Sggrss 80', modelado através da implementação de um software de simulação, Simpack, com o objetivo de conhecer as suas respostas dinâmicas. No vagão estudado foram admitidos dois cenários, um deles baseado num incidente de descarrilamento de um caso real e outro baseado num estudo de segurança de vias torcidas. O caso de estudo real teve lugar num segmento ferroviário específico situado a norte da cidade de Coimbra enquanto que o segundo cenário resultou seguindo a norma EN 14363.

Foi efectuada uma exposição de componentes do vagão sofisticados, incluindo o sistema de suspensão, a modelação do acoplamento entre o bogie e a estrutura da carroçaria, e a articulação inerente. Esta expedição intelectual atravessou a perspetiva de elementos de força complexos, em que a interação de forças como o atrito e os amortecedores foi representada no modelo. Além disso, a articulação existente também colocou um problema de modelação difícil devido ao facto de ser um componente de fricção puro.

Por fim, esta tese oferece uma compreensão sobre o tema de segurança ferroviária através da análise de cenários simulados com a presença de irregularidades intrusivas na via. Posteriormente à simulação, pretende-se avaliar cenários de tipos de descarrilamento durante o mesmo, destacando-se três critérios. Adicionalmente, realizou-se uma análise parametrica para investigar a influência da fricção no descarrilamento. Os resultados do estudo contribuem para a compreensão teórica do limite de descarrilamento e para os avanços práticos na segurança ferroviária, abrindo caminho para o aumento das directrizes operacionais e da operação de engenharia preventiva.

Abstract

Freight transportation has been going through an ongoing and crucial transformation since the popularity of articulated freight wagons was gained in Europe. A paradigm shift in the effectiveness and efficiency of cargo transportation is brought about by accepting the expansion of articulated freight wagons across Europe, which benefits rail freight operators in a variety of ways.

The substantial increase in cargo capacity is the most emphasized benefit felt in the Railway cargo industry. Articulated wagons achieve amazing accomplishments while maintaining the typical train length, with the potential to increase freight capacities. The number of railway passages necessary has also significantly decreased as a result of the rise in capacity, which will boost operational effectiveness and simplify logistics. Moreover, it also offers streamlined efficiency, improved load handling, cost saving, cargo flexibility, and reduced environmental impact.

This master's thesis undertakes an elaborate investigation of a Freight Wagon, denoted as Sggrss 80', modeled by implementing a simulation software, named Simpack, focusing on acknowledging the dynamic responses. Two scenarios were considered for the wagon, one based on a derailment incident in a real case and the other based on a safety study of twisted tracks. The real case study took place on a specific railway segment near the city of Coimbra, while the second scenario was based on EN 14363 standard.

A meticulous description of sophisticated components, including the suspension system, the modeling of the coupling between the bogie and the body frame, and the inherent articulation, was undertaken. This intellectual expedition traversed the perspective of complex force elements, where the interplay of forces such as friction and bumpstops were attempted in the model. Additionally, the existing articulation also posed a difficult modeling problem due to being a pure friction component.

This thesis offers important apprehension into the subject of railroad safety through the examination of simulated scenarios with the presence of intrusive track irregularities. Afterwards the simulation, the aim is to evaluate the types of derailment that could occur during the simulation, highlighting three criteria. In addition, a parametric analysis was carried out to investigate the influence of friction on derailment. The study's findings advance both theoretical understandings of the derailment limit as well as practical advances in railway safety by opening the way for increased operational guidelines and preventive engineering operation.

Acknowledgements

To my supervisor, Abílio de Jesus, for his support, guidance of my research, and willingness to help me as much as possible throughout this hard and challenging project dissertation. I appreciate all the efforts in making my project complete.

To my co-supervisor, Cláudio Horas, for his contribution to the development and improvement of this work, and his ability to help me. Also for providing valuable feedback, which significantly contributed to the success of this project.

To Muhammad for helping me and for wasting a lot of time with me, especially at the beginning of this project. I hope I haven't been too annoying. To Marco António, I would like to express my heartfelt gratitude for your time, knowledge and support in this work. To Hugo Magalhães, for providing all his knowledge even though he wasn't involved in the project, and for showing his willingness to participate in interesting discussions to improve my thesis.

To my friends, who, above all the good things, never forgot to look out for me when I was not doing so well. A special thanks to Ana and Daniela, for always believing in me, for putting up with and helping me with everything throughout this academic journey. For all the kind and honest words and for the friendship that will always remain. With you, I have learned to live life more freely. To Miguel, thank you for your loyalty and honesty and for always motivating me to stay strong in this difficult life. Thank you for putting up with me and always being there.

To Şevval, whom I was lucky enough to meet when I was in Romania, I thank you for being able to consider you as a sister and who, despite being in Turkey, always looked out for my happiness. Teşekkürler, Şevval.

To Catarina, Diogo and Pedro, for making my journey in Italy unforgettable and never abandoning me. Now we just have to go back to Turin and finally go to the top of the Mole Antonelliana.

To my old housemates, thank you for transforming our space into such a special home. I am grateful for meeting so many wonderful women.

To ACOMINHO, who welcomed me as family and helped me grow. Here, I've learned a lot and I've been able to escape the routine to work on something I enjoy.

To my parents, for fighting for me every day, for working so hard to provide me with everything they could. Thank you for being there with me when you can, and for teaching me all the values of life. To my sister, for all the love and affection, and all the extra attention she gives to me. I know you suffer a lot when I am not perfectly fine. To my grandmothers, for taking care of me when my parents couldn't, and for their kind heart and good food. To my family and Andreia, for being there and doing everything for me, even when life was not going well.

To my grandfather, who is no longer here, I thank you for being the best grandfather in the world, for always taking care of me, and for understanding me. For always letting me win every competition we did. You were and always will be my role model and I know you'll always be there for me.

This work is a result of Agenda “SMART WAGONS – Development of Production Capacity in Portugal of Smart Wagons for Freight”, nr. C644940527-00000048, investment project nr. 27, financed by the Recovery and Resilience Plan (PRR) and by European Union - NextGeneration EU.

Francisca Manso

"Be real,
and let them talk."

Édouard Manet

Contents

List of Figures

List of Tables

Acronyms and Symbols

AB	Axlebox
BF	Bogie Frame
BL	Back Left
BLF	Back Left Front
BLB	Back Left Back
BR	Back Right
BRF	Back Right Front
BRB	Back Right Back
DAE	Differential-algebraic equations
DOE	Design of Experiments
DOF	Degrees of Freedom
EN	European Standard
FE	Force Elements
FL	Front Left
FLF	Front Left Front
FLB	Front Left Back
FR	Front Right
FRF	Front Right Front
FRB	Front Right Back
ICE	Intercity-Experimental
Lsmo/2	Smoothing length between sections
ODE	Ordinary differential equations
Par1	Length of section
PS	Primary Suspension
SNFC	National Society of the French Railways
TEN-T	Trans-European Transport Network
TSI	Technical Specifications for Interoperability
UIC	International Union of Railways
WS	Wheelset

E Young Modulus
F$_n$ Normal force
Q Vertical wheel-rail contact force
Q$_0$ Static vertical wheel load
s Position along the track
Y Lateral wheel-rail contact force
F$_\eta$ Lateral creep force
γ Flange angle
μ Coefficient of friction
ρ Density

Horizontal Properties
CIR Circle
CLO Clothoid
Par2 Radius of curvature or start radius of curvature for transition
Par3 Radius of the transition
STR Straight

Superelevation Properties
CST Constant
LIR Linear ramp
Par2 Superelevation for constant section or start superelevation of a ramp

Vertical Properties
CLS Constant slope
Par2 Value for a constant slope or start slope for transition
Par3 End slope transition

Chapter 1

Introduction

1.1 Context

Railways were first introduced in England, to lessen the friction when carrying heavily loaded vehicles. Later the process was quickly globalized due to its opportunity for mass transportation crossing long routes. This process has created new obstacles for the transportation sector, particularly for railroads, along with the need to meet an increase in demand for the mobility of people and products. There has been a lot of pressure for faster, more effective, and yet greener trains to keep up with other modes of transportation. Not only do these improvements necessitate significant investments in engineering, but they also subject the trains to increasingly challenging and aggressive conditions as their performance improves. Hence, due to those conditions, the safety of the trains plays a crucial role in the study of the dynamic behavior in those extreme conditions.

Railway is a type of transportation that allows the movement of people and goods, fundamental to European society. By the 20th century, an unheard-of chance to develop sustainability was necessary in order to be a significant factor in the prosperity of Europe. Various countries in the EU have made an effort in the development of rail infrastructures and also created new railways, to connect the continent even more. Thus, the relevance of this for transportation is evident as it includes numerous beneficial factors for a more sustainable, united, economic, and inclusive society.

After the pandemic, financing was done to recover the economies to improve and complete with the railway lines [1]. Consequently, some projects were created in order to achieve proper innovation and technology development in this area of substantial investment, such as the current Trans-European Transport Network (TEN-T). This plan aims to implement and develop a connection of 4 different modes of transportation such as railway lines, road, inland watercourses, maritime shipping routes, ports, airports and railroad terminals, as illustrated in Figure 1.1. In this way, it will close gaps and blockage problems seeking to unite a reinforced social, economic and territorial Europe. TEN-T will also demonstrate additional European value through its contribution to the objectives under four categories: cohesion, efficiency, sustainability and increasing user benefits.

Besides the construction of new physical infrastructure, the TEN-T policy supports the application of innovation, new technologies and digital solutions to all modes of transport. The objective is the improved use of infrastructure, reduced environmental impact of transport, enhanced energy efficiency and increased safety.

For this Network, it is outlined in the regulation a 2 level of structure: the comprehensive and core networks. First and foremost, the comprehensive network, which aims to be completed by 2050, includes all TEN-T modes of transport infrastructure previosly mentioned, as well as encourages the effective, environmentally and socially responsible use of that infrastructure, particularly the related telematic applications [2]. The core network, which will be ceased by the end of 2030, consists of the comprehensive network's strategic and most significant components for attaining the TEN-T development goals. This network should serve as the foundation for the growth of an efficient multimodal transportation system and act as a catalyst for the growth of the entire extensive network. Additionally, it should make it possible for the Union to concentrate on the TEN-cross-border T's segments, missing links, multimodal interconnections, and major bottlenecks, which will help achieve the White Paper's goal of reducing greenhouse gas emissions from transportation by 60% to 1990 levels by 2050 [3].

One of the main problems in the Iberian region is the adoption of their own standardization on the gauge of the lines, and this aims to surpass this barrier. As per reports from Spanish news, European executives aspire to accelerate the interoperability of European rail networks. However, for the Iberian Peninsula, the proposed strategy requires the governments of Portugal and Spain for a two-year time frame to delineate their gauge migration plans. This strategic plan aims to enforce the migration of the Atlantic and Mediterranean corridors under the Trans-European Transport Network by 2030 and extend the same approach to the rest of the corridors by 2050 [4].

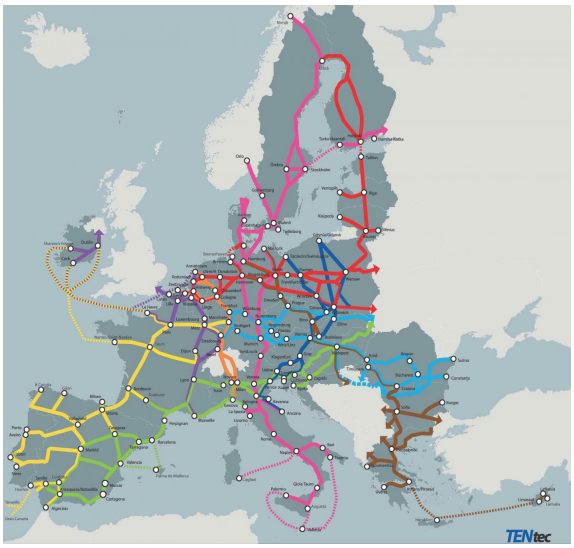

Figure 1.1: Trans-European Transport Network [5].

In Portugal, as a solution to technological barriers and market gaps in the domestic railway industry, *SMARTWAGONS* seeks to develop smart wagons for rail freight transport and production

capacity for their manufacture. In the Portuguese railway industry, the development of smartwagons and new, high-value-added technologies for their manufacture, operation, and maintenance would allow for an improvement in operational capacity, sustainability, and competitiveness. Additionally, it carries along a number of benefits, including the reinvention of the productive capability of rail carriages to change the specialization profile, increasing the productive potential and internationalization of technology, products, and services. Simultaneously, this initiative serves as an encouragement for providing qualified jobs, increasing the environmental and energy efficiency for a more appealing and competitive offer, and bringing operations that are smarter, safer, and more efficient with fewer operating/maintenance costs or issues with communication/monitoring [6].

One of the most important elements in the train is the bogie, as its function is to move the train guaranteeing safety. The Y25-type bogies is one of the most widely used for rail freight services in Europe whose fundamental idea has various applications in real life. The application of this family of bogies derives due to its easy maintenance, low-cost production, and lightweight compared to other bogies, for example, leaf springs bogies [7, 8].

1.2 Thesis Goals

This work aims to study the multibody dynamics of a freight wagon under maximum efficiency surpassing various conditions without any problem of vibrations and possibly a derailment.

For that, it was feasible to accomplish the goal by dividing the study into various parts such as:

- Modelling an 80ft freight wagon fully loaded composed with a two platformed articulated intermodal wagon on 3 bogies with steel coil springs and friction dampers using a multibody software, SimPack®;
- Simulate the model by analyzing the contact forces of the contact between the wheel and the rail, possible unwanted vibrations, and displacements, avoiding potential derailment of the cargo train;
- Imposing types of irregularities that can happen on common days of labor of the train;
- Optimization of the model by evaluating the variability of the mechanical properties of the first iteration.

All of this study will meet the requirements of TSI, EN, UIC standards with Iberian gauge distance since it is the one used in Portugal.

Overall, this aims to develop a multibody dynamics model of a freight wagon representing the selected case study. The objective of the simulation is to estimate the loading forces acting in the different substructures of the vehicle.

1.3 Outline of the Thesis

The goals outlined in the preceding part led to the division of the structure of the current thesis into five chapters, the first of which is devoted to outlining the thesis' principal goals and scope.

In Chapter 2, a bibliographic review is presented in respect of the outlook related to the freight wagons and their safety criteria. Firstly, an historical context of the introduction of Railway mechanics and railways in Portugal is introduced followed by a long and detailed description of the main structural and dynamic components. Additionally, a condensed review of the study performed on the wheel-rail contact analysis is carried out, including the contact forces displayed by the bodies. Also, an extensive overview of the types of derailments is addressed, emphasizing the wheel flange climb criteria, also known as the Nadal criteria, as a main focus in addressing railway crashes. Interconnected systems and equations of motion of multibody dynamics of a complex running wagon are introduced as a final note ending this state-of-art chapter.

An implementation of a specific flat freight wagon model is laid out in Chapter 3, by a detailed multibody model for an Sggrss Wagon, covering bumpstop stiffness and friction surfaces. Couplings between bogies and body frames are explained, including pivot and side bearers for better suspension as well as the central articulation mechanism linking the two body frames making them articulated trains. Moreover, in Section 3.3, the focus shifts to the track model of the study case, which is a segment of "Linha do Norte" in Portugal along with an illustration of the track's layout, curves, and longitudinal profiles. In essence, these sub-chapters contribute to an examination of a sophisticated and complex multibody simulation model for an increasingly growing option when choosing a freight wagon, encircling diverse aspects of component modeling, couplings, friction, articulation, and track representation aiming to acknowledge the behavior of the freight wagons and their interaction with the railway track in particular scenarios.

Chapter 4 presents the result outcomes of the simulation model described in Chapter 3 using the Simpack® post-processing tool. It is introduced firstly by explaining and detailing the simulation pathway and the respective parameters and settings. Afterward, results like displacements, Nadal criteria, Prud'homme criteria, and wheel unloading are examined and discussed. This section ends with the influence of varying properties, most specifically the coefficient of friction on axlebox friction surfaces.

In Chapter 5, delves into conducting a derailment study following the EN 14363 standard of twisted tracks. The new track is configured with varied vertical, horizontal, and superelevation inputs, as well as the excitation profile and the scenario parameters. The results expected are only applied for the Nadal criteria of the Front Left wheel that are then commented on.

Last but not least, in Chapter 6, the main conclusions of the project are done along with future developments regarded as crucial for the development and accuracy of the model and simulation results.

Chapter 2

Railway Dynamics

Railway Dynamics is present in all of the surroundings of a moving body and railway is one of them, being an important complex study of the motion and behavior of railcars as they move along the tracks [9]. It analyses the forces and stresses acting on the railcar as well as the interaction between the track and the environment, and the moving part, such as freight wagons.

Considering the dynamics of trains, they depend on circumstances such as the weight, speed and type of train, the condition of the track and the irregularities like the weather and territory [10, 11]. Firstly, the exploration of this topic assumes significance as it helps ensure safe and efficient operation by identifying potential problems such as excessive oscillation or instability. Hence, it will lead to the designing and developing of new railcars and suspension systems, aiming to improve performance and reduce maintenance costs.

In the railway industry, there are two types of trains: freight wagons and passenger trains. The development of a train will require a distinct approach of dynamics, since a freight wagon's purpose is to run safely transporting as much cargo as possible without any comfort, and a passenger train aims to transport people as fast as possible, ensuring the passenger a pleasant train ride even in rough conditions. For that, in the passenger train bogie, extra and complex suspensions and damping are used, whereas in freight wagons most of the bogies are commonly composed of friction-damped suspensions.

The suspensions are responsible for supporting the load and absorbing shocks and vibrations present in a bogie, which carries the wheels and the axles.

Nowadays, advances in computer modeling and simulation have enabled more precise and detailed analysis of railcar dynamics. This has led to the development of new technologies, such as active suspension systems and railcar condition monitoring systems, which can help improve the reliability and safety of freight cars.

2.1 The History of Railways

Once there is a moving vehicle, there is a huge demand for analyzing the dynamic behavior which was introduced at the beginning of the 19th century. This study was derived in Germany with changes in the elements of a train, for example, the replacement of the wheel for a conical profile creating a better performance in self-centering.

Germany's post-war issues have negatively affected the development of high-speed train travel. However, the contrary happened in Japan, where 120 marine experts were assigned by the Japanese government to develop the fundamental study of high-speed rail transportation in 1946. In 1905 did the French national railway company begin its studies aiming for the same objective. Sometime after, tests were made for a high-speed train, in the Bordeaux- Hendaye line, reaching 331km/h resulting in a deformation on the track [12].

Figure 2.1: Track test of SNCF train Bordeaux- Hendaye in 1955 [12].

A competition was announced in May 1955 to address the instability sinusoidal motion problem - also called the "hutting" movement – that occurred in France, often known as the issue with high-speed rail traffic in Europe. Tadashi Matsudaira, a Japanese navy engineer, was one of the three winners. The efforts of Matsudaira led to the creation of a new bogie for the Tokaido high-speed train [13].

In England, notably in Alan Wickens' group, extensive theoretical examinations into the hunting dilemma were carried out [14]. Wickens, who had a fundamental grasp of aircraft design, came to the conclusion that the equations used to represent the instability problem of sinusoidal motion could also be used to describe other instability problems, such as wing vibration caused by aeroelasticity.

Carl Theodor Müller, who at the time was the foremost authority in Germany for all issues pertaining to rail car dynamics, published a scientific study in 1969 that made a clear distinction between forced vibrations and self-excited vibrations that happen as velocity is raised [15]. Yet Müller pupil Hans-Ludwig Krugmann didn't reference Wickens' work or the publications in a volume he released in 1982. The physical reason for instability was not acknowledged, and "hunting" was presented as an issue of forced vibrations generated by stochastic track imperfections. It is assumed that, except for Müller's lectures in Munich, high-speed traffic-related topics were not covered at any German universities.

Later, in the 70s, a big investment was made in the railways followed by the development of a maglev, known as Transrapid. Because of that, in 1972, an initiative was launched whose purpose was to focus on 3 research areas, such as, the track, the vehicle and their interaction [**?**]. German study sought to comprehend the principles of running stability and contact mechanics while high-speed trains were already in service in France and Japan [16]. With the benefits of government funding, Germany's heavy industries were able to perform examinations into running stability. As a result, instruments for designing rail vehicles were created, including a test rig for entire rail cars and the Intercity-Experimental (ICE) test vehicle, which served as a prototype for the initial run of ICE-trains. Basic contact mechanics and investigations into linear and nonlinear stability, including limit cycle calculation, were made clear to the industry. Since 1976, software development has been necessary as part of the project, leading to the development of software's: Medyna® and Simpack®. This development led to further investigation in more complex studies like comfortability, stability and curving of the train.

The "Research on the boundaries of the wheel/rail system" project had the effect of turning the known boundaries of the system into daily rail traffic. However, the consequences of increased performance, higher velocities, axle loads, and design changes on the rails, vehicles, and the system were not investigated enough. The results of this project were concentrated on subsystem improvement, and it was anticipated that over time, the wheel/rail system would push itself to new boundaries. Even though there were initiatives from research institutions, universities, and the industry, a new research project was not launched. In the mid-80s, various projects at universities focused on the track and the loads that result from the interaction of the wheel and rail. A program entitled "Dystem Dynamics and Long-term Behavior of Vehicles, Rail, and Subsoil" was established by a German research organization, called DFG, to address these issues. New advancements in Europe were being driven by rail-borne high-speed traffic, according to research and development on vehicles and tracks.

In Portugal, the railway industry was launched on the 28th of October of 1856 whose event was tremendously important and revolutionary at the time, since transportation was done mostly by watercourses. Despite its late introduction, it was created primarily to facilitate the efficient movement of people and goods between the interior regions and the central city ports [17].

The development of Portugal's railway system has been the subject of numerous significant studies. To illustrate the influence of this technological achievement on the nineteenth and twentieth centuries, these studies have looked at the political and economic conditions at the time that railways were invented.

Nonetheless, it is crucial to recognize the impressive expansion of already-existing metropolitan centers as well as the quick emergence of new ones following the advent of the railway in Portugal. Therefore, new planning techniques were developed to manage this new infrastructure, as well as the resulting spatial effects on a global, regional, and urban scale [18].

2.2 Freight Wagon

In the cargo industry, the railways are one of the primary modes of transportation defined as the use of railroads and trains for on-land freight transportation, able to ship numerous and various kinds of goods.

In contrast to passenger trains, the freights wagons have several technical and working differences, with the type of transportation being the main one, where the passengers train transports people and freight moves heavy cargo. In cargo transportation, the aim is to efficiently transport as much load as possible with no need for extra investment especially in comfort and high speed.

The freight wagon structures, encompassing the wheels, axles, bogies, and suspensions, are the principal factors to consider when designing a freight wagon (see Figure 2.2).

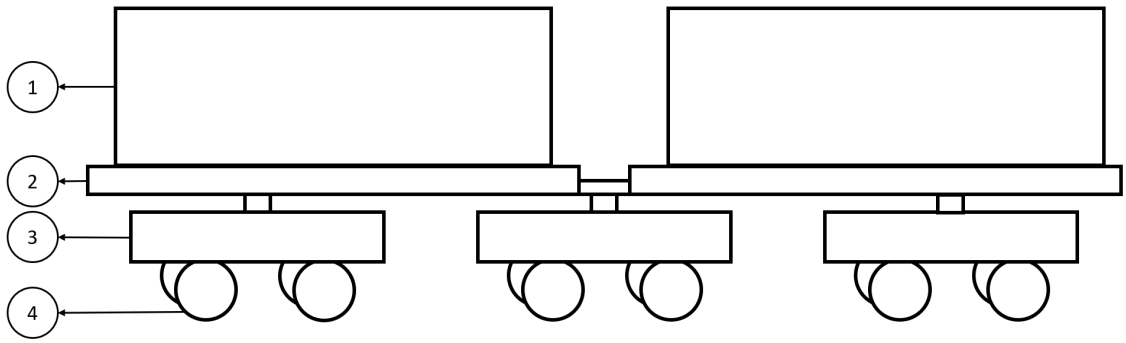

Figure 2.2: Composition of an articulated vehicle: 1 – container, 2 – body frame, 3 – bogie, 4 – wheelset.

2.2.1 Bogies

Railcar bogies are crucial for safe railroad operations and carry out duties of providing support for the railcar body, stability on all types of railroads, good damping dissipation when incurring irregularities as well as identifying them. A bogie is a chassis or frame that holds the wheelsets of a railway vehicle.

The different types of bogies are primarily categorized corresponding to their number of axles and the machine design of the suspension. Moreover, bogies are divided into single-axle, two-axle, three-axles, and more, being the two-axle the most commonly used due to its simple structure and good quality of avoiding track irregularities of the freight wagon structure [19].

2.2.1.1 Bogies on Freight Wagons

In Europe, cargo trains are specially integrated with some types of UCI 2 axle running gears as well as specific bogies [20].

Introductory, steel leaf spring suspension, presented in Figure 2.3a is also commonly used in freight wagons, such as those used for transporting goods by train. This type of suspension is in general used for 2-axle freight wagons. The leaf springs used in freight wagons are typically larger, stronger, and cheaper than those used in passenger vehicles, as they need to support much heavier loads [21]. However, they present a feeble behavior in damping capacities, leading to possible "hunting" oscillation. Hence, it remains a popular choice for freight wagons due to its durability, reliability, and cost-effectiveness. Nevertheless, newer systems are also being applied to meet better requirements which will be listed below.

Secondly, the Link bogie, depicted in Figure 2.3b was introduced in the 20s being the first bogie implemented with the UIC standardization [22].Design-wise, the spring directs the wheelset and functions on top of the axlebox. It offers better stability and ride quality compared to steel leaf spring suspension, however, results in more expensive and complex maintenance.

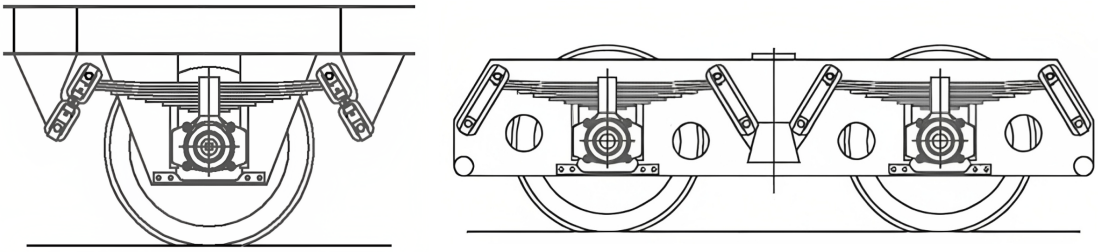

(a) (b)

Figure 2.3: Common bogies in freight transportation. (a) Steel leaf spring [22]. (b) Link bogie [22].

Finally, the Y25 bogie is a two-axle bogie with an axle load of up to 25 tons, hence the name Y25. The Y25 bogie was introduced in the 1980s as a replacement for older bogie designs, developed by the SNCF, and has since become one of the most widely used bogies in Europe [22].

The Y25 bogie, represented in Figure 2.4, features several design improvements over older bogie designs, including better performance, improved reliability, and reduced maintenance requirements. Moreover, it is designed to accommodate a range of different types of freight wagons, including open wagons, tank wagons, and container wagons. It is also compatible with a variety of different track gauges, making it a versatile choice for freight railways across Europe.

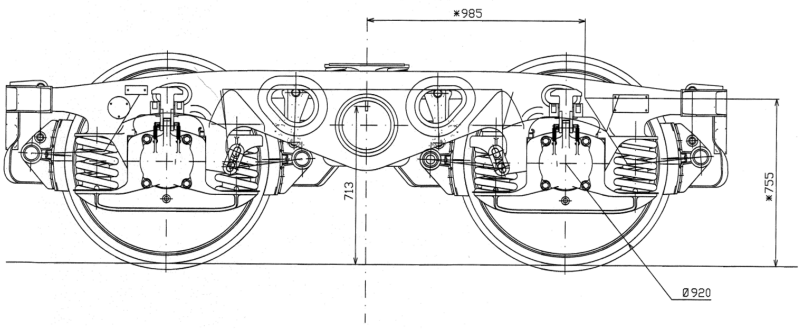

Figure 2.4: Y25 bogie drawing (supplied by MEDWAY).

To sum up, the Y25 bogie is a popular and reliable choice for European freight wagons and has helped to improve the safety and efficiency of freight transportation on the continent, becoming the most cost-effective bogie on the market.

2.2.2 Suspension

The term "suspension" describes a group of parts that operate together to support and stabilize a mechanical structure, reduce vibrations, and absorb shocks [23]. It is frequently used in automobiles, trucks, motorcycles, trains, bicycles, and other machinery, as well as in other settings where comfort, safety, and smooth motion are sought.

A suspension system usually consists of several parts, including springs, dampers, and other devices that work together to separate the body or load of a vehicle from the irregularities of the road or surface it is driving on. The vehicle's suspension system enables the wheels or other supporting components to move independently from the body or load, thereby minimizing the effects of shocks and vibrations on the vehicle and its occupants.

2.2.2.1 Springs

Springs are mechanical components that are designed to store and release mechanical energy in response to external forces [24]. Their main purpose is to provide a force that opposes an external force or deformation. When a force is applied to a spring, it compresses or stretches, storing energy in the process. When the external force is removed, the spring releases the stored energy, returning to its original shape, thereby improving the performance and safety of mechanical systems.

In this industry, there are normally two types of springs: primary springs and secondary springs to avoid derailment and to uncouple vibration and noise between the wheelsets and the vehicle body. The primary springs are the major load springs located at the wheel, between the wheelset and the bogie frame that support the weight of the vehicle and its payload. The majority of vibration is absorbed by these types of springs. In addition to supporting the primary springs and adding additional suspension and stability, secondary springs are sometimes referred to as auxiliary or assistant springs located between the wagon and the bogie frame. Secondary springs are frequently

used to prevent the primary springs from being overloaded and bottoming out while the vehicle is traveling over difficult terrain or carrying a big load thus offering great stability, comfort, and less noise on the train.

In a freight wagon bogie, it is only present primary spring, which are between the axlebox (housing for the bearings that sustain the vehicle's axle load) and the frame, that can be constructed as steel leaf or coil springs, as rubber springs or as air springs [25]. There are 4 configurations of steel springs mainly used in the industry of railway such as Leaf spring, Parabolic leaf spring, Cylindrical helical springs and Flexi-coil cylindrical helical springs, represented in Figure 2.5.

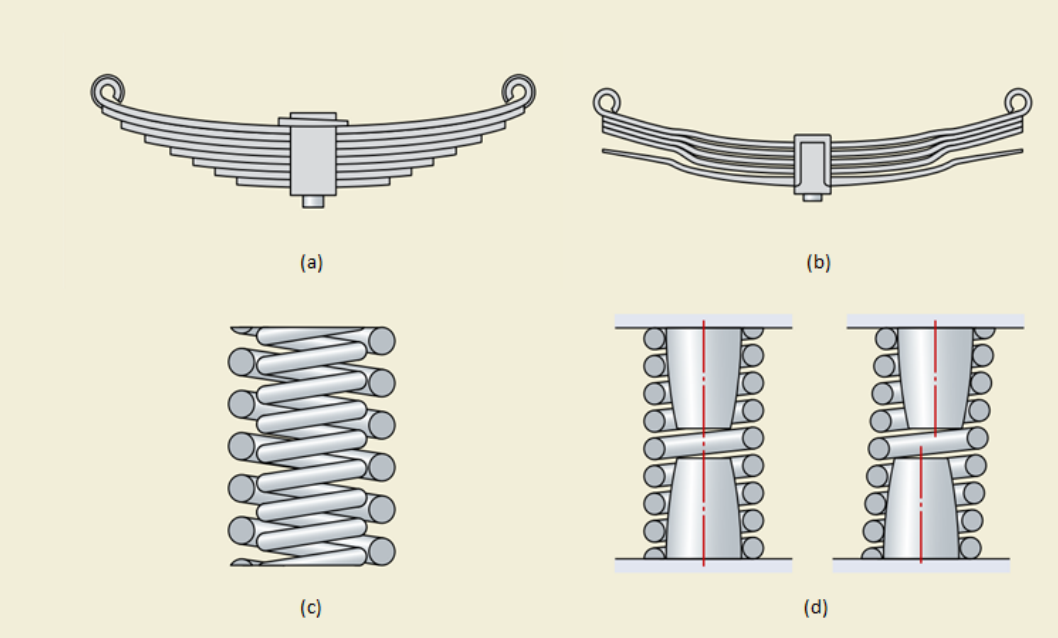

Figure 2.5: Types of steel springs: (a) leaf spring; (b) parabolic leaf spring; (c) cylindrical helical springs; (d) flexi-coil cylindrical helical springs (Adapted from [26]).

These types of springs are mainly produced of steel, where Table 2.1 presents some values adopted by manufacturers depending on the specific standard.

Table 2.1: Material properties of Steel Spring.

Material	E (MPa)	G (MPa)	$\rho(kg/m^3)$
Spring steel wire (EN 10270-1)	206000	81500	7850
Spring steel wire (EN 10270-1)	206000	79500	7850
Steel (EN 10089)	206000	78500	7850

Coil helical springs are created with a wire or rod that is wound in a helical (spiral) pattern, forming a coiled structure with spaces between the coils. Axial stiffness, which corresponds to vertical deformation, is just one component that must be taken into account, whereas others include coupling between different directions and reaction moments brought on by non-axial displacement of the vertical force. Also, compression preload can also cause destabilizing effects in the transverse plane, requiring analysis of buckling limits, which depend on how the coil spring deforms and how its ends are fixed.

To simplify an approach to model coil springs by employing a single and linear stiffness in the axial direction to achieve a more accurate portrayal, it is necessary to incorporate non-linearity related to bumpstops or vertical non-linearity, which frequently happens in the primary suspension because of inner coil springs with vertical clearance. However, to accurately depict true coil spring suspensions, simple models frequently need to be improved to include transverse effects.

Hence, as for calculating the axial stiffness, k, of a cylindrical coil spring, its computation only depends on the geometry:

$$k = \frac{Gd^4}{8D^3n} \tag{2.1}$$

where, G is the modulus of rigidity, d is the wire diameter, D is the mean coil diameter, and n number is coil windings.

For the shear stiffness, if the springs undergo small deflections, which are present in freight wagons, it can be assumed as a constant value. Its expression is complex and dependent on various factors, such as the vertical stiffness seen in the equation below:

$$k_s = k\xi \left[\xi - 1 + \frac{\frac{1}{\lambda}}{\frac{1}{2}+\frac{G}{E}} \sqrt{\left(\frac{1}{2}+\frac{G}{E}\right)\left(\frac{G}{E}+\frac{1-\xi}{\xi}\right)} \tan\left(\lambda\xi\sqrt{\left(\frac{1}{2}+\frac{G}{E}\right)\left(\frac{G}{E}+\frac{1-\xi}{\xi}\right)}\right)\right]^{-1} \tag{2.2}$$

where, ξ is the relative spring deflection, λ is the slenderness ratio, and E is the Young Modulus.

Springs play a critical role in train suspension systems, serving to absorb shock and promote stability during transportation. According to UIC standardization, leaf and coil springs are the most widely used types of springs in trains. However, contrary to the springs described above, rubber springs offer a better complexity in the design being much simpler, and normally present on both primary and secondary suspensions.

Finally, when is needed requirements of low mass, vibration and stability in string payload variations, air springs are chosen as they are composed of rubber-cord housing filled with compressed air.

2.2.2.2 Dampers

Dampers are crucial components of many mechanical systems. Their main purpose is to control or dampen the movement of a system in response to external forces or vibrations predominantly to improve the safety, comfort, and efficiency of mechanical systems by controlling and minimizing unwanted movements and vibrations.

Freight wagons are subjected to a variety of external forces and vibrations during operation as they may experience impacts from rough tracks, vibrations from the movement of the cargo, or shocks from coupling and uncoupling with other wagons. These forces and vibrations can cause the wagon to bounce, oscillate, or sway, which can be uncomfortable for passengers and may even result in cargo damage or derailment. To prevent this from happening, dampers are installed in the suspension system of freight wagons which help to absorb and dissipate the kinetic energy generated by the shocks and vibrations, thereby reducing the amount of movement and improving the stability and ride quality of the wagon.

Most of the dampers used are hydraulic to be able to withstand heavy loads carried by trains, but mechanical ones can be also considered. Dampers are supported on the axlebox in various directions, depending on the purpose of the use.

The industry of railways offers suspensions with viscous or friction damping systems, where the latter is mainly used in freight wagons. Friction damping is present when two surfaces come in contact resulting in the dissipation of energy. The force can either be constant or variable with the mass of the body, but it is always proportional to the friction coefficient, pressure and motion. However, viscous damping acts in the presence of a viscous fluid, also known as a lubricant, between two parts in hydraulic dampers. These dampers are not only usually used in passenger trains but also in modern freight bogies [12].

2.2.3 Wheelset

A wheelset is composed of two wheels that are rigidly fitted into each side of an axle shaft [27]. Its purpose is to provide a tolerance distance between the track and vehicle, a direction that decides how the rail gauge will move, including at curves and switches, and apply traction and braking forces to the rails to move the vehicle forward and backward [28].

In a straight trajectory, the wheels of a train have an equivalent rolling radius. However, this is not confirmed when a train encounters curved tracks. Thus, the outer rail, R_{out} is longer than the inner rail, R_{in}, demanding the outer wheel to cover a greater distance than the inner wheel. Therefore, the wheelset undergoes a lateral displacement, y caused by the interplay between the outer rail and the wheels themselves, as seen in Figure 2.6a.

The wheel is presented with a tapered profile, as depicted in Figure 2.6b, which transmits lateral forces to the train when the wheel deviates from its central alignment. This characteristic provides them with more effective and smooth self-centering on the track, mainly on curves. Although, this type of profile can bring "hunting" or lateral vehicle oscillations. The presence of vibrations creates forces in the system that could detriment in the rails and vehicles, make passengers uncomfortable, and raise the possibility of a derailment. Designing railroad vehicles requires knowing the critical speed, which is the longitudinal speed at which the vehicle becomes unstable [29].

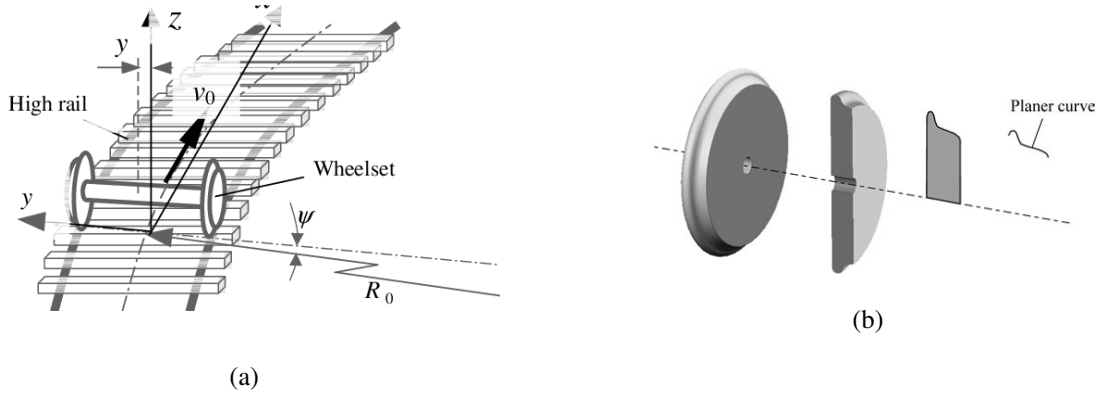

(a) (b)

Figure 2.6: Wheelset design. (a) A wheelset passing a curved track [30]. (b) Wheel surface [31].

The dynamics and stability of railroad vehicles are also significantly influenced by wheel geometry. The profile of the wheels and rails has a significant impact on a vehicle's critical speed. The curve that determines the wheel profile is completely rotated about the wheel axis to produce the surface of the wheel [31].

2.2.4 Type of Wagons

In freight wagons, it is important to account for the maximum efficiency of the volume of cargo carried and the time of loading and unloading the goods [28]. Freight wagons come in a wide range of shapes and styles, and they are typically named after the cargo they are intended to transport. Heavy haul wagons that transport bulk materials are a type of freight wagon which can transport a range of cargo, including retail goods, liquids, building materials, and general freight [27]. In the case of heavy-duty, they are chosen when there is a need of transporting substantial goods, for example, coal, gravel, wood, etc. These types of wagons are named following the type of material transported and are known to have high axle loads due to their bulkiness. In terms of geometry, they vary from the way that the cargo is unloaded. On one hand, if they are unloaded on the bottom, their name is hopper or bottom dump wagon. On the other hand, wagons called bathtub, rotary dump or gondola are required when the load is removed by a via other than the bottom.

Figure 2.7: Heavy-duty Medway wagon for transporting ballast [32].

However, general freight wagons are named within the same logic as the heavy-duty wagons, but differ when it comes to their construction. The wagon frame is incorporated into the wagon body during the building of heavy haul wagons and general freight wagons are made of a frame, which is then covered with a body on top of them. The general wagons can transport a wide variety of materials, including liquids or gases.

Figure 2.8: Medway Freight Container wagon [32].

2.2.5 Track

The railway track is an essential structure for the operation of trains and traditionally is mainly composed of 5 components illustrated in Figure 2.9: rails, sleepers, ballast, fasteners, and subgrade. This rail sketch provides information about the typical rail infrastructure design that includes ballast material. Although, the field of railway engineering encompasses a variety of track designs, which do not incorporate ballasts. These systems allow a railway vehicle to move evenly, depending mainly on wheel-rail contact, which ensures dynamic stability on the train.

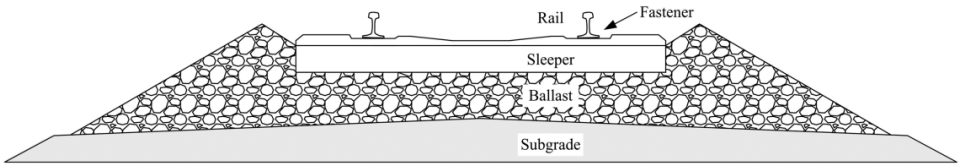

Figure 2.9: Rail track components [28].

The rails provide the contact surface for the running wheels of the vehicle and are usually produced in steel with an I shape, known as Flat bottomed Vignole rail, introduced by Charles Vignoles in Britain [33]. Moreover, rails should ensure ruggedness, high stiffness, and hardness in order to avoid serious damages, such as fractures, elastic deformation, and wheel degradation. Although this profile is dominant in worldwide use, their track gauge differs from region to region. Track gauge is the minimum nominal distance, in millimeters, between the left and right rail, within a vertical length of 14.5 mm (± 0.5 mm) from the top downwards of the rail. The most widely used track gauge globally, occupying most of the world's and Europe's rail network, is 1435 millimeters, which is known as "standard gauge", seen in Figure 2.10. In Portugal and Spain, a track gauge of 1668 millimeters is used in the majority of the territory, deferring a lot from the standard gauge [34].

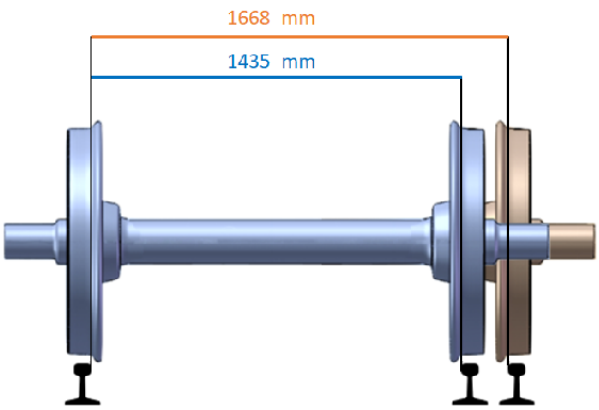

Figure 2.10: Iberic and Standard track gauge.

The sleepers are present under the rails, surrounded or not by the ballast depending on the type of track, in order to maintain the correct gauge, level, and alignment. Also, sleepers should have firmness, elasticity, and durability making them able to resist longitudinal and lateral displacements [28].

The fasteners ensure the assembly of the rails to the sleepers resulting in requiring excellent mechanical properties, which are directly associated with the behavior of rails [35]. This component system it is also operated to maintain the rail gauge and establish the safety of trains.

Ballasts represent a granular composition of the superstructure of ballasted tracks used in most of the railway structures in the world, aiming for reduced load transition in the subgrade and displacement in curves [36]. Subgrade is composed of soil crucial for the running of freight wagons, whose objective intersects with the ballast by making it possible for an even transfer of loads [37, 38].

The track line is characterized by the coordinates $x(s)$, $y(s)$, and $z(s)$, by the angles $\psi(s)$, the yaw angle about the z-axis, the $\theta(s)$, the pitch angle about the y-axis, and the $\phi(s)$, the roll angle about the x-axis. The track design is detailed by the length, curvature and cant in sections that led to a description of the track center line, s. The position and orientation are done in three principal directions: horizontal layout, vertical layout, superelevation or camber. The horizontal layout is defined by the horizontal radius or curvature; the vertical layout by the vertical slope, the vertical radius or curvature; the superelevation by the level difference along a lateral baseline, the superelevation reference length.

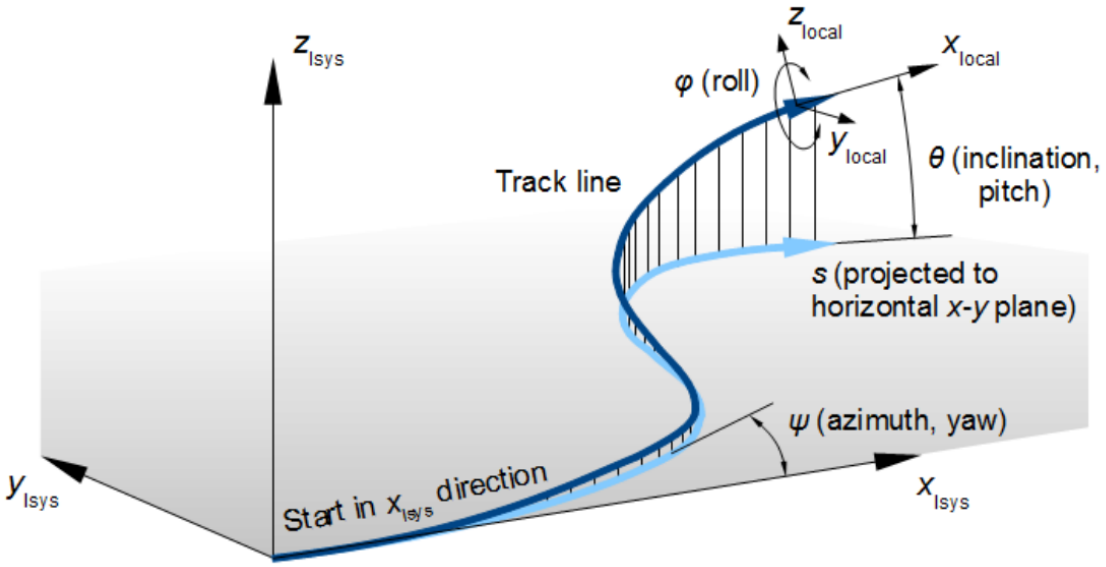

Figure 2.11: Track line in three-dimensional space [39].

Finally, the track eventually will undergo some maintenance processes due to the irregularities and the passage of the trains. Hence, when choosing between maintenance operations it is important to take into account the tolerance limitations for signs of alert, which require work planning, intervention, which require quick action, and prompt action. The values for the track geometric parameter's maximum permissible tolerances are shown in Table 2.2.

Table 2.2: Tolerances of geometric parameters of the track for 1668 mm gauge lines [40].

Class	IV			III		
Velocity [km/m] / Parameter [mm]	80<v<=120			120<v<=160		
	Alert	Intervention	Immediate Action	Alert	Intervention	Immediate Action
Gauge	-7/+25	-9/+30	-11/+35	-6/+25	-8/+30	-10/+35
Average Gauge	-5/+22	-6/+25	-8/+27	-3/+16	-4/+18	-6/+20
Longitudinal level D1	+-16	+-19	+-26	+-15	+-17	+-23
Longitudinal level D2	n.a.	n.a.	n.a.	n.a.	n.a.	n.a.
Alignment D1	+-11	+-13	+-17	+-9	+-10	+-14
Alignment D2	n.a.	n.a.	n.a.	n.a.	n.a.	n.a
Bending (3 meters base)	+-12	+-15	+-21	+-12	+-15	+-21

2.3 Wheel-Rail Contact

The contact between the wheel of a train and the track is a fundamental interaction to ensure safety in the dynamic behavior of the vehicle. Hence, the conical shape surface of the wheel contacts location in the rail is critical for computing the contact Forces, with the formulation of the normal and tangential forces, illustrated in Figure 2.12. In the interference between both bodies, there is a high-stress concentration which can be exposed to damage [41].

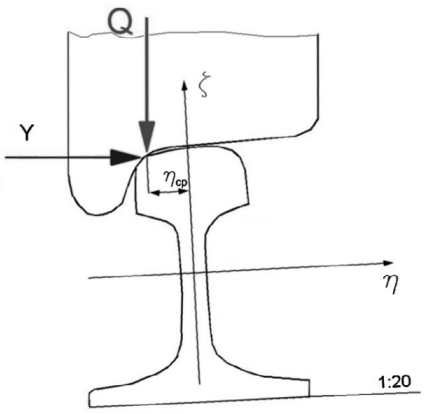

Figure 2.12: Normal Force, Q, and Creep Force, Y [42].

The Normal contact forces can be formulated by elliptical contact areas and non-elliptical contact areas. The elliptical contact areas are characterized by the Hertz solution. This was made with some assumptions for the contact of the bodies: Bodies can be viewed as an elastic half-space

loaded over a small contact area; The Contact area's dimensions must also be small in relation to the sizes of the individual bodies and the relative radii of curvature of the surfaces; Friction-less smooth surfaces, disregarding other possible loads excepting the normal load; Possible to apply Hooke's law due to minimal strains [43]. Although this method is widely used in simulation and reveals calculations with reasonable efficiency and accuracy, these assumptions are often not respected.

When the rail and wheel are in rolling contact, it will create zones in the contact where it may slip and further where it may stick. The slip phenomenon, also known as creepage, is then caused by the tangential strains of both bodies in the adhesion area and will create creep moments and Tangential creep forces that depend on the kinematic of the wheel-rail [31]. Railcar stability and steering are significantly impacted by these creep forces and moments. It is possible to use many creep-force theories that can be based on linear models, while others make use of nonlinear force-creepage correlations. In multibody railway softwares, it is also presented various tangential forces theories for dynamic analysis.

2.4 Derailment

A derailment occurs when a train or other rail vehicle deviates from the track on which should be traveling. Derailments can happen for a number of reasons, such as mechanical breakdowns, track flaws, excessive speed, poor maintenance, human mistake, or environmental issues like inclement weather or obstructions on the rails. Wheels climbing off the rail, rail gauge widening or rail rollover that causes wheels to fall between rails are some examples of common derailments in the railway.

Derailments were primarily caused by damaged rails or welds in all speed ranges. At low speeds, some track and human element causes, such as faulty train handling, brake operations, and inappropriate usage of switches, are predominant leading to derailment. However, when the speed is high derailment occurs due to equipment factors such as bearing failure, broken wheels, and axle and journal flaws [44]. In Appendix E the leading causes of freight train derailments in the United States between 2001 and 2010 are presented.

Based on how lateral restrictions at the wheel-rail interface are eliminated, railway derailments caused by this can be divided into four basic mechanisms: wheel flange climb; gauge widening; wheel unloading; and track panel movement. The Wheel Flange Climbing derailment mechanism causes the wheels to climb onto the top of the rail head. Its mechanism will be described more precisely in Section 2.4.1. The Track Panel Shift derailment mechanism results in a lateral displacement on the track explained particularly in Section 2.4.2. The derailment mechanism named Wheel Unloading happens when the wheels lose contact with the rail, thoroughly outlined in Section 2.4.3. Finally, the Gauge Widening derailment mechanism occurs by rail deflection, exhibited in Section 2.4.4.

In Table 2.3 and Figure 2.13 it is possible to see all the types of derailments analyzed in the industry of railways industry as a summary of what was mentioned before.

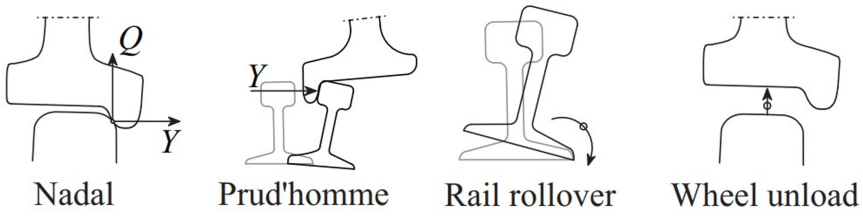

Figure 2.13: Types of derailments (Adapted from [45]).

Table 2.3: Derailment limits for the running safety (Adapted from [46]).

Derailment mechanism	Criteria	Safety factor	Country Region	Limit Value	Reference
Wheel flange climbing	Nadal	$\xi_N = \frac{Y}{Q}$	Europe	0.8	TSI
			Japan	0.8 (more than 15msec)	RTRI
			China	0.8	TB 10002-2017
			North America	1.0 (more than 50 msec/ 3 feet)	AAR
Track panel shift	Prud'homme	$\xi_P = \frac{\sum Y_{WS}}{10+\frac{2Q_0}{3}}$	Europe	1.0	TSI
Wheel unloading	Unloading wheelset	$\xi_{U,ws} = 1 - \frac{Q}{Q_0}$	Europe	0.9	EN 14067-6
			Japan	0.8	RTRI
			China	0.6	TB 10002-2017
			North America	0.9	AAR
	Unloading bogie	$\xi_{U,bg} = 1 - \frac{Q_i+Q_j}{2Q_0}$	Europe	0.9	EN 14067-6
Gauge widening	Rail roll	$\xi_P = \frac{\sum_{bgside} Y}{\sum_{bgside} Q}$	North America	0.6	AAR

2.4.1 Wheel Flange Climb

Wheel flange climbing is a type of derailment mechanism, that generally occurs on curves, caused by high lateral forces when the vertical force is reduced or high vibrations of both forces mentioned before result in the wheels climbing onto the top of the rail head [28, 46]. Tangential forces in the contact can reach high values with rapid variation in intensity and direction due to the high contact stiffness caused by the type of material used and by altering contact properties of the geometry of the profiles. When modeling, it is important to take into account the values of contact forces for a better evaluation of the dynamic behavior [47].

A wheel climb derailment criteria was introduced known as Nadal's criterion, which was developed from 1896 to 1908 [48]. The criteria is evaluated by the ratio between the lateral contact force, Y, and the vertical contact force, Q. For a typical flange angle of 65º and a coefficient of friction, $\mu = 0.5$, the Nadal limit in Europe is 0.8.

The link between the (Y/Q) necessary for derailment and the angle of attack and longitudinal creep was explored by Gilchrist and Brickle in 1976 [49] using the most recent theory of wheel-rail interaction forces in conjunction with observations from laboratory tests. These outcomes demonstrated that Nadal's findings were accurate for high attack angles and little longitudinal creep.

The ratio between the contact forces is expressed as:

$$\frac{Y}{Q} = \frac{tan(\gamma) - \frac{F_\eta}{F_n}}{1 + \frac{F_\eta}{F_n} tan(\gamma)} \tag{2.3}$$

where, γ is the contact angle between the wheel and rail. Also, Nadal suggested an expression in the saturation condition:

$$\frac{Y}{Q} = \frac{tan(\gamma) - \mu}{1 + \mu tan(\gamma)} \tag{2.4}$$

since is known that:

$$F_\eta = \mu F_n \tag{2.5}$$

where, F_η is the lateral creep force and F_n is the normal force in the wheel-rail contact. When analyzing the equation it is possible to see that, if the friction coefficient and the maximum contact angle are fixed, the derailment ratio never surpasses its limit.

The maximum contact angle can be also plotted for variable friction coefficient (from 0.1 to 1) and Y/Q ratio. As it is possible to see in Figure 2.14 the grater the maximum contact angle, the higher the Nadal criteria limit is for derailment by Wheel Flange Climb.

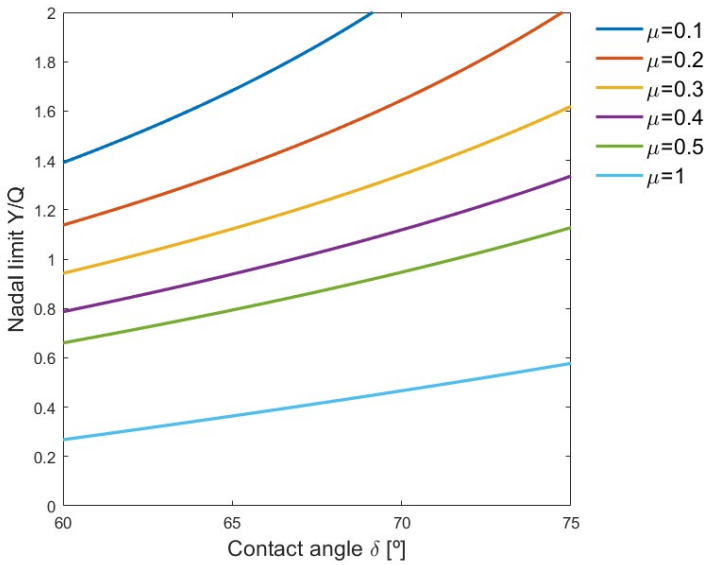

Figure 2.14: Relation of limiting wheel Y/Q ratio and maximum wheel-rail contact angle.

2.4.2 Track Panel Shift

The track shift derailment happens due to track degradation in the lateral plane on the track, causing lateral displacement usually in the ballast. For high-speed trains, this type of criterion is important to analyze, according to [50].

The SNCF has made the largest impact on the discussion of track shift by restricting the lateral load generated by a wheelset, in order to prevent excessive track panel displacement. After several years of research, a study of Prud'homme was started by investigating experimentally the lateral strength of a wood tie track under a moving lateral load [51]. This led to the creation of the Prud'homme criteria limit, expressed as:

$$\xi_P = \frac{\sum Y_{WS}}{10 + \frac{2Q_0}{3}} \frac{[kN]}{[kN]} \tag{2.6}$$

2.4.3 Wheel Unloading

A derailment by wheel unloading may happen when a vehicle experiences vibrations for some of the wheels causing it to lose contact with the rail. Numerous excitation sources, including track imperfections, earthquakes, and crosswinds, among others, have been implicated in the development of these extreme vibrations [46]. The criteria for wheel unloading can be determined by the unloading of the wheelset or the bogie, giving many more paths for this analysis. When referring to the Wheelset, the limit is calculated by the ratio of dynamic and static vertical loads, calculated by:

$$\xi_{U,ws} = 1 - \frac{Q}{Q_0} \tag{2.7}$$

The study related to the bogie is a less conservative method that is also reflected in the European standard [52]. The wheel unloading in this instance is determined by:

$$\xi_{U,bg} = 1 - \frac{Q_i + Q_j}{2Q_0} \tag{2.8}$$

where Q_i and Q_j are the vertical loads on the first and second wheels for one side, respectively.

2.4.4 Gauge Widening

The gauge widening derailment mechanism occurs by merging two causes: wide gauges and considerable lateral deflections caused by rail rollover. Hence, the gauge widens by rotating in the outward side corner of the foot of the rail due to fatigue, causing progressive failure over time. This can be determined by accounting or not for the restraints provided by the rail fasteners and the torsional stiffness of the rail section. The limit of this type of derailment not accounting for the torsional stiffness [53] is calculated by:

$$\frac{Y}{Q} = \frac{d}{h} \tag{2.9}$$

where, h is the height of the rail, and d is the horizontal distance between the roll point and the contact point. The other criterion [54], is calculated by the ratio of the combined effects of one side of the bogie:

$$\xi_P = \frac{\sum_{bgside} Y}{\sum_{bgside} Q} \tag{2.10}$$

2.5 Multibody Dynamics

Multibody dynamics is the study of the motion and behavior mechanics of connected bodies, known as multibody systems, with the presence of force elements and constraints. The topic can be explored through flexible or rigid bodies emphasizing the effects of contact forces, friction, and constraints [39].

Railway dynamics systems are a very complex but important context for understanding the interactions between the train components and track infrastructure. Freight wagons are intricate multibody systems made up of locomotives, body frames, containers, bogies, wheels, and axles, all of which are coupled by a variety of mechanical links. For a train to run safely, effectively, and dependably, these interrelated parts must behave in the right way.

The equations of motion of a multibody system emerge from the imposition of constraints that govern the interactions between various bodies together with motion equations. This process gives rise to a set of crucial components, including generalized coordinates, constraint equations, and connection forces.

As example and according to [55], for a particle of mass m constrained to move on a spherical surface, its positions, in Cartesian coordinates, in the x-y-z inertial reference frame, $\mathbf{q}$, is represented in matrix form as:

$$\mathbf{q} = \begin{bmatrix} q_1 & q_2 & q_3 \end{bmatrix}^\top = \begin{bmatrix} x & y & z \end{bmatrix}^\top \tag{2.11}$$

The kinematic constraint that the particle referent of the center of the inertial coordinate system moves on the surface is:

$$\Phi(\mathbf{q}) = \frac{(\mathbf{q}^\top \mathbf{q} - 1)}{2} = \frac{(q_1^2 + q_2^2 + q_3^2 - 1)}{2} = 0 \tag{2.12}$$

Defining the constraint Jacobian, a partial derivation of the constraint equation:

$$\Phi_\mathbf{q}(\mathbf{q}) = \begin{bmatrix} \frac{\partial \Phi}{\partial q_1} & \frac{\partial \Phi}{\partial q_2} & \frac{\partial \Phi}{\partial q_3} \end{bmatrix} = \begin{bmatrix} q_1 & q_2 & q_3 \end{bmatrix} = \mathbf{q}^\top \tag{2.13}$$

And using time order differentiation, resulting firstly in the velocity constraint equation and, secondly, in the acceleration constraint equation written respectively as:

$$\Phi_\mathbf{q} \dot{\mathbf{q}} = 0 \tag{2.14}$$

$$\Phi_\mathbf{q} \ddot{\mathbf{q}} = -\dot{\Phi}_\mathbf{q} \dot{\mathbf{q}} = -\dot{\mathbf{q}}^\top \dot{\mathbf{q}} = (\dot{q_1^2} + \dot{q_2^2} + \dot{q_3^2}) \tag{2.15}$$

To apply the Principle of Virtual Work, a virtual displacement is defined as $\partial \mathbf{q} = \begin{bmatrix} \partial q_1 & \partial q_2 & \partial q_3 \end{bmatrix}^\top$ and is independent of time and satisfies the linearized form of Equation (2.12),

$$\Phi_\mathbf{q} \partial \mathbf{q} = 0 \tag{2.16}$$

The Principle of Virtual Work not considering the connection forces, based on d'Alembert's principle, is defined as :

$$\partial \mathbf{q}^\top (m\ddot{\mathbf{q}} + mg\mathbf{u}_z) = 0 \tag{2.17}$$

where, $\mathbf{u}_z = \begin{bmatrix} 0 & 0 & 1 \end{bmatrix}^\top$ is the unit vector in z direction.

There are two distinct approaches for using Equations (2.16) and (2.17) to derive equations of motion. The first approach involves transforming the differential algebraic equations (DAE) of motion into the Lagrange multiplier form. This is achieved by introducing dependent generalized coordinates, denoted as $\mathbf{q}$, which may not fully adhere to the constraints outlined in Equations (2.12), (2.14) and (2.15). The second method entails defining independent generalized coordinates, also referred to as Lagrangian coordinates. These coordinates possess dimensions less than 3 and are carefully selected to satisfactorily address all three types of constraints imposed by Equations (2.12), (2.14) and (2.15). This selection process results in the formulation of ordinary differential equations (ODE) of motion.

The differential algebraic equation (DAE) assumes that both Equations (2.16) and (2.17) are linear concerning $\partial\mathbf{q}$. According to the Lagrange multiplier theorem, this linearity implies the existence of a unique multiplier λ, resulting in the emergence of $\partial\mathbf{q}^\top(m\ddot{\mathbf{q}}+mg\mathbf{u}_z)+\lambda\Phi_\mathbf{q}\partial\mathbf{q}=0$. Since $\partial\mathbf{q}$ is arbitrary, this further underscores the following point:

$$m\ddot{\mathbf{q}}+\Phi_\mathbf{q}^\top\lambda+mg\mathbf{u}_z=0 \tag{2.18}$$

Equation (2.18) comprises three scalar equations wherein λ appears algebraically in each of the four variables of $\mathbf{q}$ and λ itself. This equation, in conjunction with the algebraic constraint equation of (2.12), forms a system of four equations encompassing both differential and algebraic elements within the four variables $\mathbf{q}$ and λ.

In computational dynamics, some opt to augment the expression (2.15) to Equation (2.18), effectively creating a matrix equation [55]:

$$\begin{bmatrix} m\mathbf{I} & \Phi_\mathbf{q}^\top \\ \Phi_\mathbf{q} & 0 \end{bmatrix}\begin{bmatrix} \ddot{\mathbf{q}} \\ \lambda \end{bmatrix}=\begin{bmatrix} -mg\mathbf{u}_z \\ -(\dot{q_1^2}+\dot{q_2^2}+\dot{q_3^2}) \end{bmatrix} \tag{2.19}$$

Lagrange multipliers will have the physical meaning of reaction forces. This system of equations can be solved numerically for a given set of initial conditions. Equation (2.19), which was derived for the simple case of a particle, can be expanded for multibody systems by adding more generalized coordinates, constraint equations, and Lagrange multipliers.

The Simpack® software used in the project performs implicitly the methods to solve the system of equations, providing the flexibility to handle a diverse range of constraints and force elements without requiring a comprehensive and complex algebraic calculation.

Chapter 3

Wagon Model and Track

This chapter presents the model developed in Simpack® for which this project is aimed, as well as various multibody simulations.

3.1 Sggrss Wagon general characteristics

The Sggrss 80' wagon (see Figure 3.1), whose characteristics are mentioned in Table 3.1, is two-platformed and supported by three Y25 bogies, two at the end of each platform and the third in the middle connected by an articulation. This type of Y25 family bogies is very common for rail freight services in Europe following the UIC standard. This type of freight wagon is a flat wagon where the containers are removable and allow different sizes of containers, such as 20',30', and 40', fixed along the numerous spigots present in the train [56].

The letters on this wagon designation comply with the UIC classification system, which is indicated in uppercase and lowercase letters to represent various categories and their corresponding meanings. The classification assigns a capital letter standing for the category, while the remaining letters are typically in lowercase, varying based on the specific category [57]. Hence, the *Sggrss* will stand for a special flat wagon with bogies- S- for containers up to 80 feet- gg- articulated train- r- speeds up to 120km/h- ss.

Table 3.1: Main characteristics of the Sggrss wagon

Characteristic of Wagon	
Type of Wagon	Sggrss
Type of bogie	Y25
Track gauge	1668 mm
Wagon length	26390 mm
Distance between bogies	10425 mm
Bogie wheelbase	1800 mm
Bogie tare	4.6 t
Wagon tare	28.5 t
Maximum load per axle	22.5 t
Maximum allowed weight	135.0 t

Figure 3.1: Sggrss 80' Freight Wagon [58].

3.2 Sggrss Multibody model

The model of the Freight Wagon is obtained by Multibody Simulation in a commercial software called Simpack®, which allows evaluation of the behavior of the model designed by simulating and solving the equations of motion in three dimensions. For the rolling vehicle multibody model, the bodies will be connected to each other by joints or constraints. Therefore, the various bodies have specific Degrees of Freedom (DOF) which can be defined in the software by joints, constraints, forces, etc. According to [24], a degree of freedom is characterized as an independent coordinate required to ascertain the location of a system component at any given time. The lowest number of independent coordinates necessary to establish the positions of all system components at any one time is known as the number of degrees of freedom of a system.

The dynamic behavior of the model is influenced by the applied forces and the inertia properties of the bodies, such as their mass, moments of inertia, and where their centers of gravity are located. For this reason and illustrated in Table 3.2, containers, body frames, bogie, wheelsets, and axleboxes will be the components most taken into account in the inertial system. However, the kinematic joints will be represented mainly by the Primary Suspension, which includes the Shear springs and Lenoir link, the car body-to-bogie connections and body frame, and the articulation in the middle of the Freight wagon between body frames.

Table 3.2: Mass and Inertia of the Center Mass.

Body	Mass [kg]	Ix [kg m^2]	Iy [kg m^2]	Iz [kg m^2]
Container 40'ft	53250	50001.43	667866.11	666960.32
Body Frame	7350	6689	154833	161001
Bogie Frame	2700	1904.18	1843.25	3679.72
Wheelset	1000	1000	100	1000
Axlebox	1	1	1	1

Figure 3.2 presents the final loaded model with two 40 ft containers - one of the possibilities of cargo distribution - designed in Simpack® with the inertial and mass properties, in which components such as the primary suspension, couplings, and articulation will be analyzed with more detail in the next sections. Additionally, Annex A can assist in providing a more comprehensive spatial interpretation of these components.

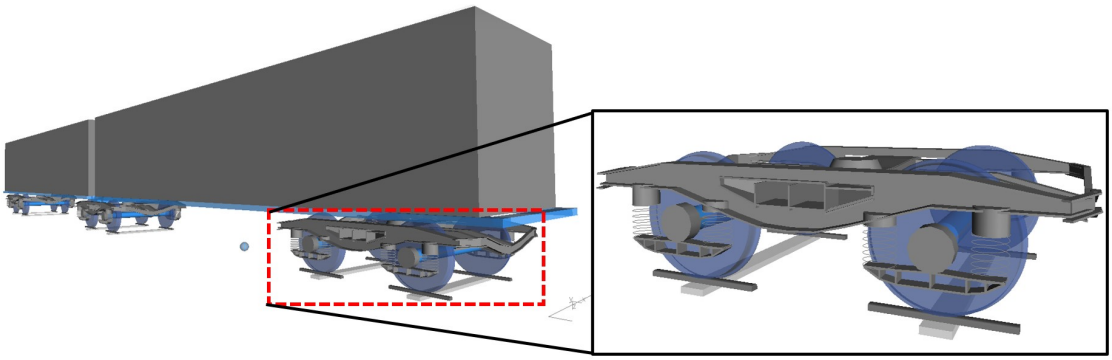

Figure 3.2: Sggrss 80' Freight Wagon model loaded with bogie detail.

3.2.1 Primary suspension

For the freight wagons in question, the Y25 bogie weight is approximately 4.6 t, the wheelbase of 1800 mm and it supports a maximum axle load of 22.5 t. Moreover, but not less important, it has a wheel diameter of 920 mm, and a maximum speed of about 100-120 km/h. Design-wise, it is composed of the bogie frame, two wheelsets, each with a pair of axleboxes, a welded bolster, braking equipment, and, finally, a suspension system. The suspension system per axlebox is composed of two pairs of cylindrical helical springs where the frame lays on and a Lenoir link with inclination seen in Figure 3.3.

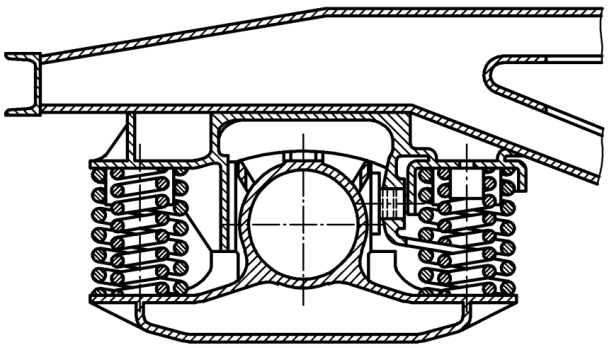

Figure 3.3: Y25 bogie [59].

3.2.1.1 Component Spring

The suspension per axlebox consists of four springs in 2 pairs, having, thus, internal and external springs. The concentric side pair that is composed of a Lenoir link is compressed between the spring cap and the axlebox, while, the other pair springs connect the bogie frame directly to the axlebox. The outer springs present some pre-load, causing a pre-deformation compared to the initial free spring. Nonetheless, the inner springs present no initial deformation and clearance from the upper support. Hence, when the innerspring acts on the suspension, generating a non-linear vertical stiffness behavior. These eight par sets are considered as parallel mounts. Moreover, the primary suspension is composed of a two-level stiffness spring suspension system that enhances the vertical stability of the tare wagon.

As for the spring behavior, the vertical stiffness has accounted for a benchmark analysis done in a D-Rail report [60], while the shear stiffness is based only on the literature of a study done by J. Pagaimo [61]. In Table 3.4, the stiffness parameters of each pair of springs are for 22.5 ton/axle bogie.

Figure 3.4: Stiffness of PS for 22.5 ton/axle bogie.

Direction	Pagaimo*		D-Rail		Adopted Value		Unit
	Outer Spring	Inner Spring	Outer Spring	Inner Spring	Outer Spring	Inner Spring	
k_x	469	555	-	-	469	555	[N/mm]
k_y	469	555	-	-	469	555	[N/mm]
k_z	-	-	997	1557	997	1557	[N/mm]

[*] Values of stiffness per spring.

Using the established EN 13906-1:2013 standard [62] described in Section 2.2.2.1, a thorough calculation of vertical stiffness was conducted using values from UIC 517 standard [63]. This generated results, represented in Table 3.3, that remarkably resembled each other and served as an authenticating and discriminating assessment of the values described in the D-Rail study.

Table 3.3: Stiffness of PS based on EN 13906-1:2013.

	Outer Spring	Inner Spring	Unit
Wire diameter, d	163	90	[mm]
Mean coil diameter, D	31	24.4	[mm]
Number coil windings, n	4.2	5.9	-
Modulus of rigidity, G	78500	78500	[MPa]
Stiffness per spring, k	498	808	[N/mm]

The Simpack® model incorporates a force element called Shear Spring Component, describing a helical spring with shear forces and bending torques coupled. This component is applied in the z-axis, acting for the vertical direction. In order to simplify the analysis, all pairs of this model are from the axlebox to the bogie frame, for a less complex analysis, since not all elements are represented in the model itself. Regarding the parameters, it is represented in the FE, vertical, lateral and longitudinal stiffness with the adopted values of Table 3.4. All this description can be seen in Figures 3.5 with a clear 3D and 2D view.

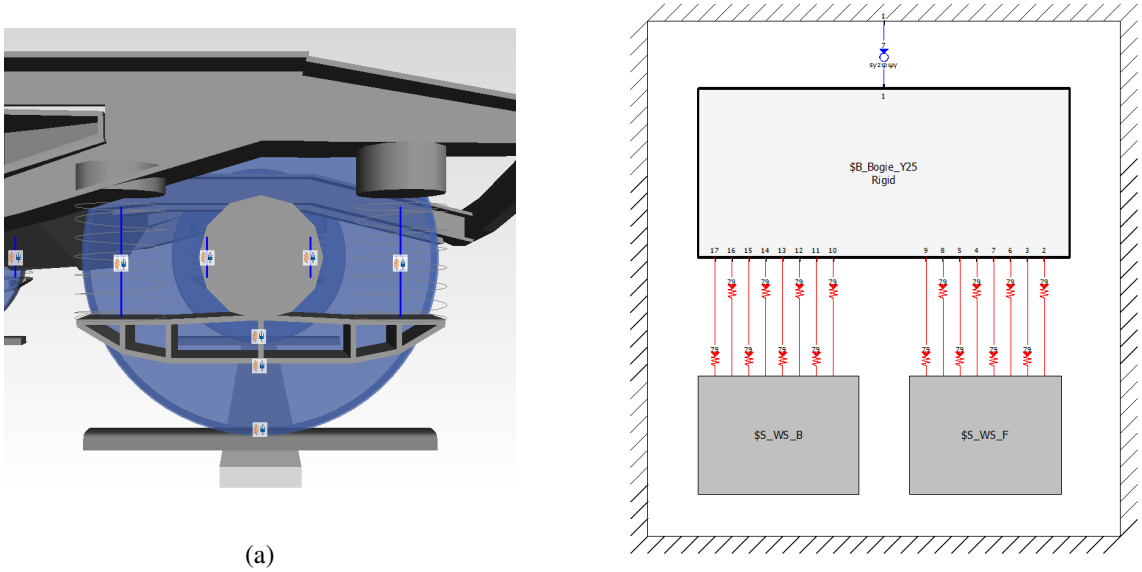

(a) (b)

Figure 3.5: Representation of the Spring component (a) 3D view. (b) 2D view.

3.2.1.2 Component damping

Bogies are equipped with diverse types of dampers to improve their performance and stability. One type of damper that is commonly used in Y25 bogies is the Lenoir friction damper, outlined in Figure 3.6. This damping component will act according to Lenoir link which creates a load-dependent longitudinal force on the spring that will be transmitted by the pusher to eventually the axlebox [64].

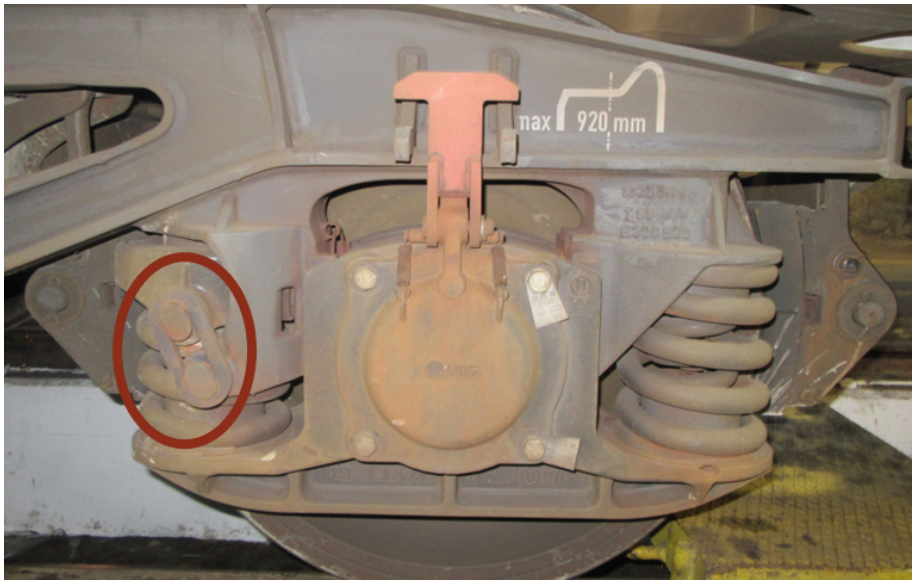

Figure 3.6: Lenoir link of Y25 bogie.

Since the link has a diagonal inclination, θ, it will be possible to decompose in horizontal and vertical dependent forces, F_H and F_V, respectively, representing the force transmitted by the pusher and the spring. The Horizontal force is a normal force operating on the friction surfaces on both sides of the axle box subject to the damping in the friction surfaces. Hence, considering an almost fixed inclination, the higher the force transmitted, the higher the horizontal force leading to greater friction damping.

Friction damping is caused when two surfaces rub against one another producing resistance to relative motion. However, in the axleboxes, there are some bumpstops that grant a specific clearance in both longitudinal and lateral directions, making it possible to perform irregularities without any concern. As illustrated in Figure 3.7, the axlebox allows a one-sided 4 mm clearance in the inner guide and no clearance in the outer guide, and in the lateral direction will have a $\pm$ 10 mm clearance.

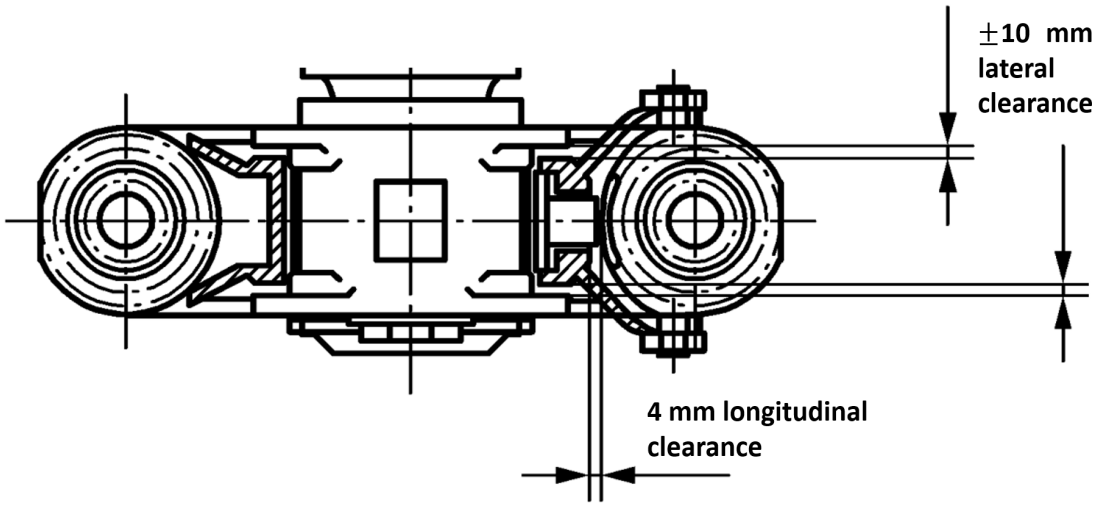

Figure 3.7: Horizontal cut view of the axlebox (Adapted from [59]).

In Simpack®, as for the clearance, a force element typically used when representing bumpstops called Spring-Damper Parallel Component, was introduced to limit the lateral and longitudinal motion of the axlebox relative to the bogie frame. These components are applied in the x-axis and y-axis of the From Marker, with a graphical input of the non-linear stiffness characteristics.

For the longitudinal direction, the bumpstop is displayed approximating a linear stiffness of about 60000 N/mm in only compression. The inner bumpstop graph will act when surpassing a clearance of 4mm, and the outer acts when the contact exists. Figures 3.8 and 3.9 represent the graphs of the front wheelset detailed before, and for the back wheelset, the graphs will be symmetric.

For the lateral direction, the bumpstop is displayed with the same value of linear lateral stiffness of 23000 N/mm, but this time in both directions and will act when surpassing a clearance of $\pm$ 10 mm. Additionally, the graph depicted in Figure 3.10 will be applied in the Front and Back wheelsets.

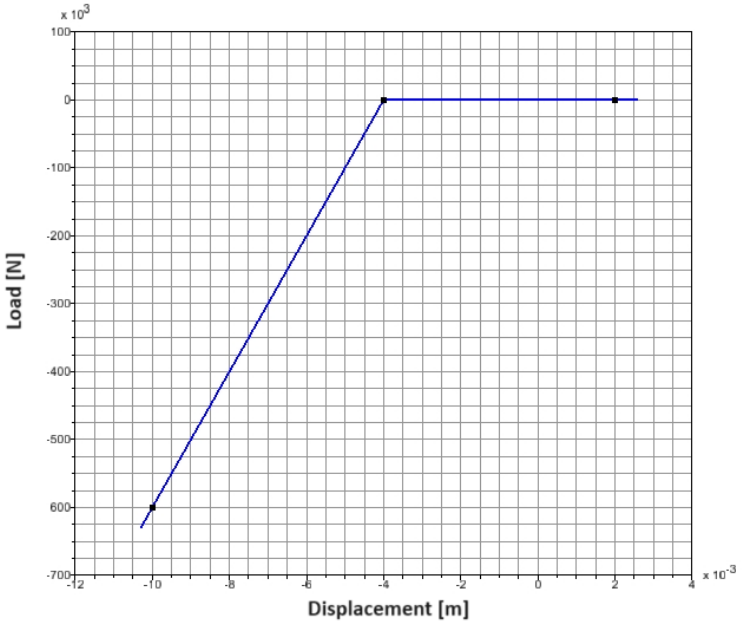

Figure 3.8: Stiffness characteristics of bumpstops - inner longitudinal guide.

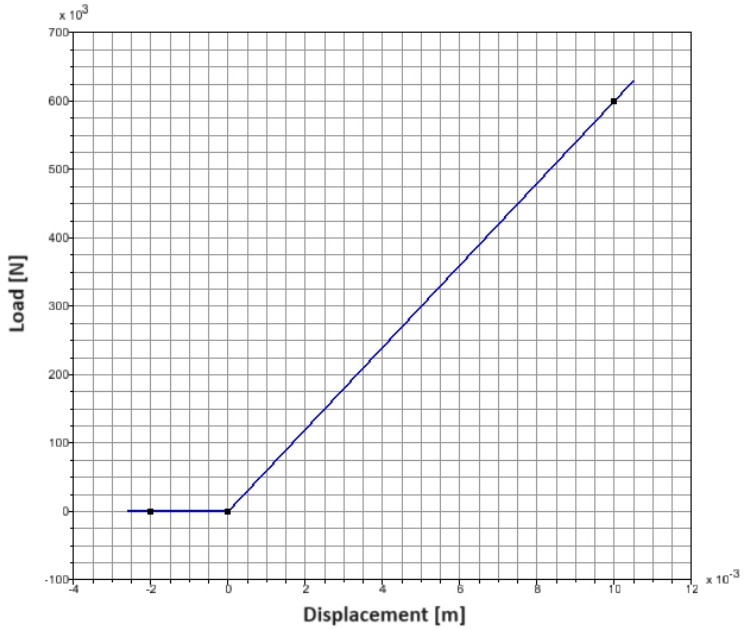

Figure 3.9: Stiffness characteristics of bumpstops - outer longitudinal guide.

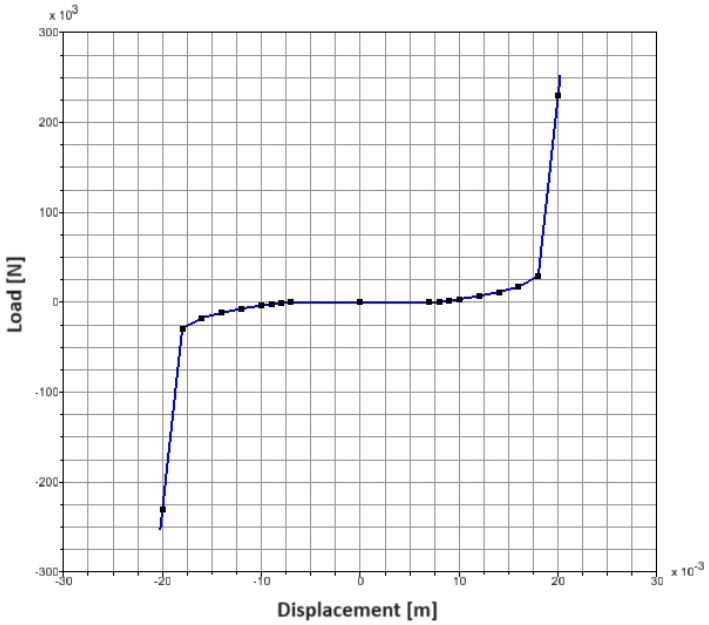

Figure 3.10: Stiffness characteristics of lateral bumpstop.

Finally, as for the friction surfaces, a Force element named Coulomb Friction is used in the model, and various approaches can be done depending on the case. Table 3.4 describes the inputs chosen for this type of friction force used.

Table 3.4: Force Element Properties of Coulomb Friction of the Axlebox.

Description			Value
Friction Force	Direction		Translational
	Force axis		x
Dynamic Friction	Friction type		Constant
	Coefficient		0.4
Static Friction	Friction type		Constant
	Coefficient		0.4
	Advanced	Enforcement	Regularized dyn fric
		Static velocity limit	1e-05
		Dynamic velocity limit	0.001
Normal Force	Input		Force/ Control output value

3.2.2 Couplings

The three bogies present in the Freight Wagon are connected to the body frames by a pivot and two side bearers, acting as a "secondary suspension" for better curve performances and reducing the chances of creating a moment around the x-axis, set out in Figure 3.11.

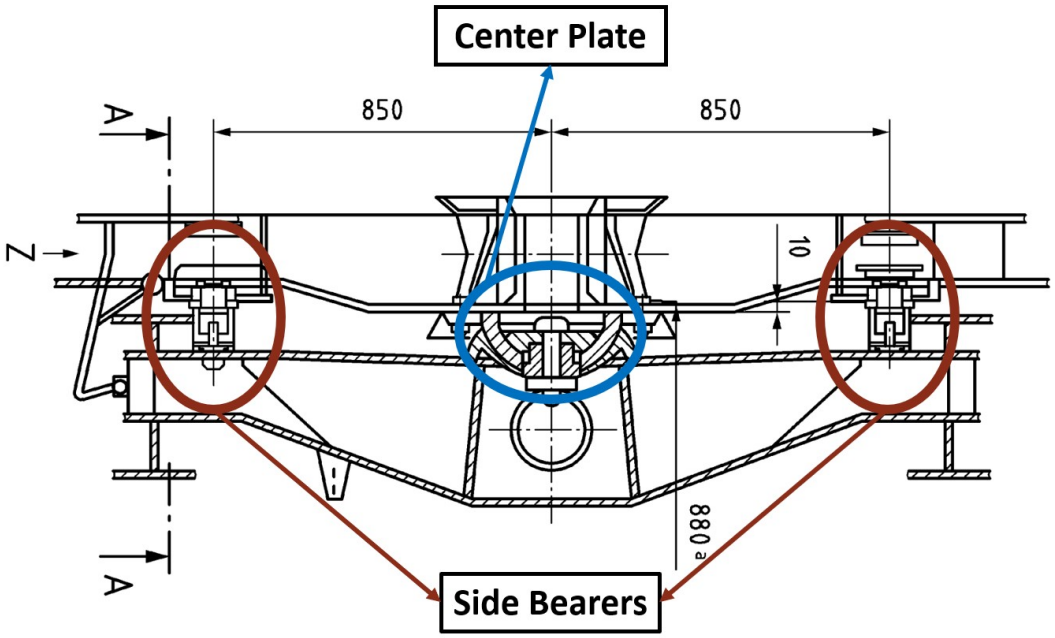

Figure 3.11: Cut view of the connection between the Bogie and Body Frame (Adapted by [59]).

3.2.2.1 Spherical Center Bowl

The spherical center bowl presents a pivot to ensure the connection and spherical surface contact area. As a result, the development was done by assigning a spherical joint between the bogie frame and body frame proved by Figure 3.11, and an elastic force element, characterized in Table 3.5. The connection linking the two bodies has friction which is not taken into account in this simulation.

Table 3.5: Elastic elements of the pivot [61].

Direction	Value	Unit
k_x	60000	[N/mm]
k_y	60000	[N/mm]
k_z	60000	[N/mm]

3.2.2.2 Side Bearer

A pair of side bearers are fixed between the bogie and the body frame, where their main role is to constrain the vehicle to roll moment and allow a better curve behavior. Each side bearer is placed 850 mm away from the center bowl pivot and its housing is mainly composed of two elastic springs, bumpstop inside the vertical springs and friction surfaces on the top. Presented in standardization of EN 16235 [59], parallel springs have a vertical spring along the z-axis of 570 kN/m and a pre-load with a nominal force of 16 kN. Additionally, a bumpstop will restrict the vertical motion when it is reached a 12 mm clearance and, also, limit longitudinally with $\pm$ 1 mm clearance.

As for the multibody model, two force elements to represent each pair of parallel springs with the stiffness and pre-load mentioned before were selected. Furthermore, the longitudinal bumpstop is considered with its minimal clearance and a stiffness of 50000 N/mm, illustrated in Figure 3.12. On the other, the vertical bumpstop is not displayed, but, as an alternative it was selected a force element with pre-load of 16 KN, a vertical stiffness of 570 KN/m, representing the springs present on the side bearers and with relatively high clearance of 40 mm.

Figure 3.12: Side Bearer: Stiffness characteristics of longitudinal bumpstop.

3.2.3 Articulation

Finally, the Talbot Type Articulation is a traditional commonly used in articulated freight wagons, in which one bogie under the coupler serves to couple both sides. However, it is a conventional and purely friction design but one of the most effective alternatives in the Railway cargo industry.

Hence, when modeling in the software, a connection of the back body frame was done dependent on the front one. The connection chosen was a universal connection allowing motion in the yaw and pitch axis since it articulates mostly in these degrees of freedom, otherwise, it will derail or break. Furthermore, it is considered an almost negligible stick and slip Coulomb friction, shown in table 3.6.

Table 3.6: Friction properties of Articulation.

Friction	
Type	Stick-Slip Coulomb
Dynamic friction coefficient	0.1
Static friction coefficient	0.2
Reference diameter	0.1
Slip velocity	1e-05
Stick stiffness	10e8
Stick damping	10000

3.3 Track Model

In the simulation, it was chosen to embrace a segment of one of Portugal's most important railway lines, known as "Linha do Norte," renowned for its vital role in connecting the cities of Lisbon and Porto across a span of 336 kilometers. This specific stretch, situated in the surroundings of Coimbra, served as the backdrop for an incident involving the derailment of a freight train comprised of twelve wagons. To evaluate the performance of the wagon both prior to and following the accident, the track was sketched by several different segments. These segments start with a 721 m straight section preceding the transition curve, which was subsequently followed by the entry transition curve, a circular curve, and the exit curve where the accident took place. All these curves are 140 m in length. Between PK 222.400 and PK 220.730, a total of 1670 m of the track was modeled. The total track length includes modeling the following straight portion of 140 m, the entrance transition curve of 149 m, and the circular curve of 250 m.

During the process of meticulously configuring the track within the software, the input data was structured into three types of table formats, laid out in Figure 3.13, including the longitudinal and vertical profile of the track, the scales and radii of both the transition and circular curves, and the levelness (NivLD1) and longitudinal alignment (AlinD1) parameters documented for each side of the track, illustrated in Annex C. In Table 3.14, a visually compelling graphical representation of top view of track output.

Given the lack of information on data for AlinD1 and NivLD1 within the post-accident region during the post-accident assessment conducted on April 4, 2017, measurements from December 16 of 2016, were operated in the simulations within the framework of this study [65].

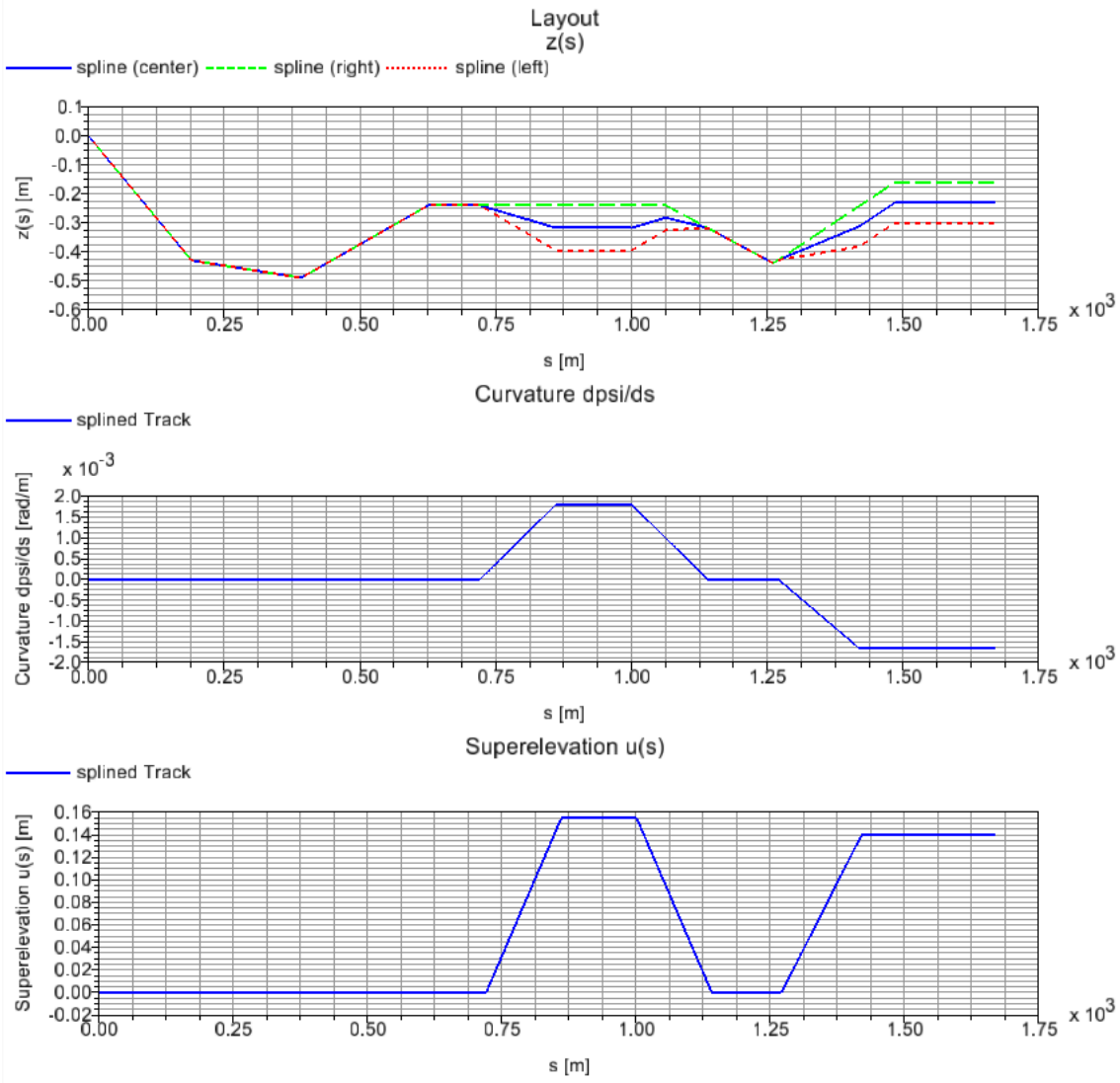

Figure 3.13: Track layout of Coimbra line: $z(s)$, Curvature $dpsi/ds$, Superelevation $u(s)$.

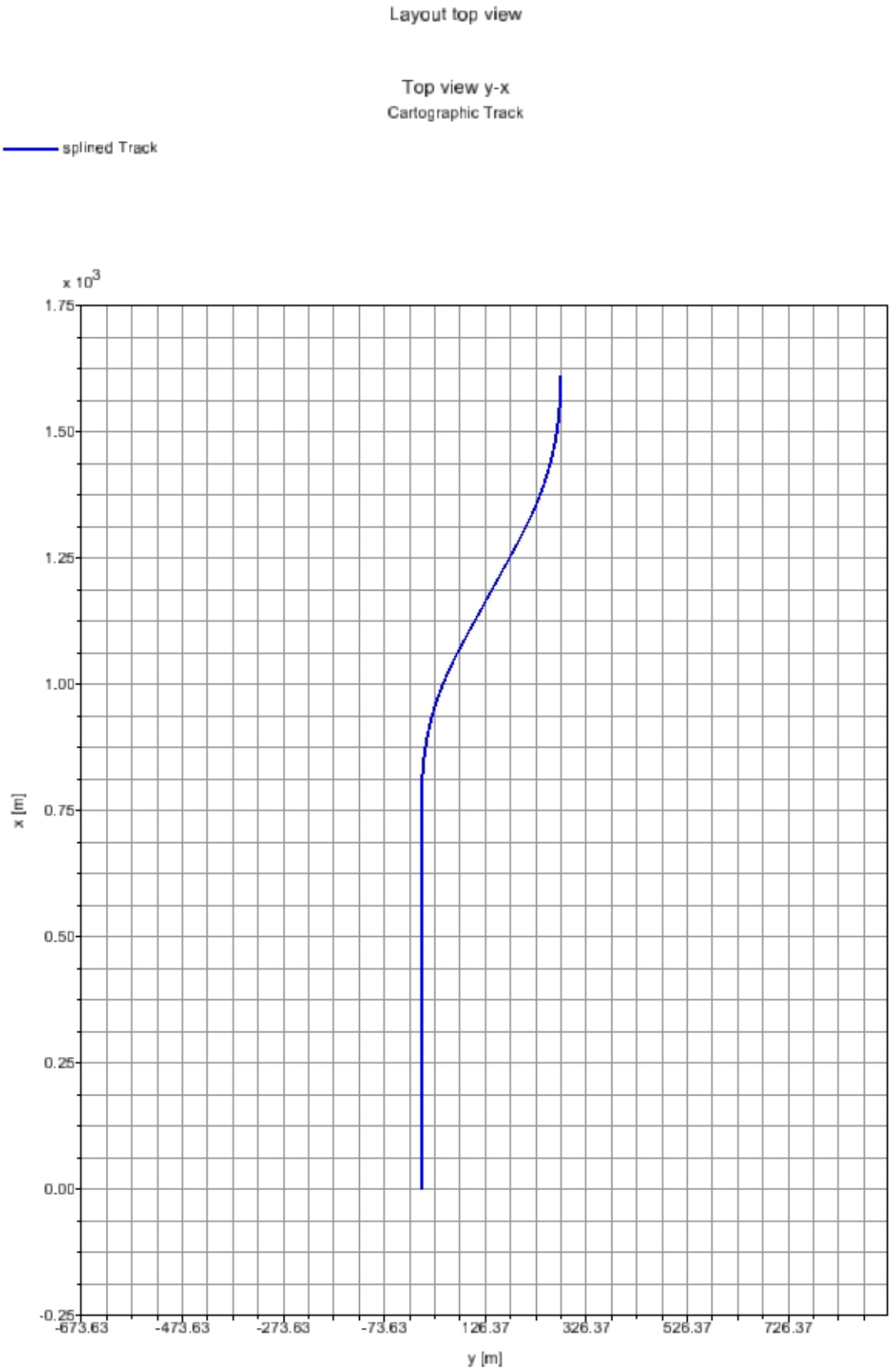

Figure 3.14: Top view of track layout of Coimbra line.

3.4 Further Remarks

The present chapter aims to conduct a description of the Sggrss 80' wagon implementation in the Simpack® Software. Due to a lack of familiarity with multibody software and the complexities brought on by the model's complexity, the modeling portion of the project ended up taking the longest.

In line with the narrative of this chapter, the initial focus was on modeling the primary suspension, which consists of springs and dampers. With easily available stiffness data, modeling the spring component turned out to be rather simple. The damping component, however, posed an issue because friction shock absorbers display non-linear behavior and there is little thorough literature on this topic. As a result, dampers were one of the last parts of the wagon model to be addressed.

With support from the Simpack® help manual, the bumpstops, which are crucial for minimizing movement in the bogies, were effectively modeled since the manual provides a thorough overview and concrete examples of various topics.

Later, the majority of the couplings created significant challenges and lacked sufficient supporting research. Despite knowing that this may not have been the best course of action, it was used a single article as the main source of information for the center plate. Regarding the articulation, the attempts to get information on the DOF and their friction were unsuccessful, which forced the author to make conservative estimates about what values were appropriate. However, modeling the Side Bearers greatly sped up the procedure. This component was well-documented in a standard for "Testing for the Acceptance of Running Characteristics of Railway Freight Wagons."

This finding provides a solid basis for moving forward to the next stage of analysis, where the behavior of the Freight wagon in a real-world case study will be examined, as outlined in Chapter 4.

Chapter 4

Simulation and Results

This chapter will present the results using the help of the post-processor Simpack® after running the model described in Chapter 3, with respective excitation and sensors.

Simpack® post can process plots in two or three dimensions, which allows a deeper interpretation of the behavior of the model. Hence, aspects that can be examined include the existence of derailment, accelerations of specific parts of the model, and the dynamic forces along the track irregularities. Moreover, it has the ability to generate animations providing further insights into the model's behavior. For instance, animations can be created to illustrate lateral and normal forces exerted on the model adding up a better understanding of the dynamic interactions between different components and helping identify critical areas of concern.

Thus, the post-processing tool enables a comprehensive analysis of the simulation results, facilitating the identification of crucial factors influencing the overall performance and safety of the system. By utilizing its graphical capabilities, Simpack® post enhances the interpretation of the results, providing valuable insights into derailment risks, localized accelerations, and dynamic forces acting along the track irregularities.

For the simulations in this section, four scenarios were considered within five different types of results. Table 4.1 displays a simplified summary of the results evaluated in each simulation. In the analysis of different simulations done, the main attention was given to safety criteria, centering on derailment risk, and the lateral and longitudinal displacements. Within the range of derailment analysis, notable criteria such as Nadal, Prud'homme, and Wheel unloading emerged, each giving distinct denotations and factors contributing to the overall assessment.

Table 4.1: Simulation scenarios considered for results analysis.

Simulation Scenario	Displacement	Nadal Criteria	Prud'homme Criteria	Wheel Unloading Criteria	Influence of variation in properties
"Accident"	✓	✓	✓	✓	✓
"2016-12-16"		✓	✓	✓	
"Intervention Limit"		✓	✓	✓	
"Alert Limit"		✓	✓	✓	

4.1 Simulation Assumptions

In order to conduct the simulation, a Loadcase model was introduced allowing the circulation of the train in accordance with the previously outlined track properties. This model contains a spherical body with a nominal radius of 0.1 m. Furthermore, it incorporates a Driven Rail Track Joint characterized by a constant velocity operating mode, exhibiting zero degrees of freedom. This joint is positioned at the midpoint of the front Body Frame, and it imparts a velocity of 95 km/h to the system.

To ensure the accurate representation of physical interactions, it was added a force element connecting between the Freight Wagon and the Loadcase. This force element is characterized by a Spring-Damper Parallel Component, with a substantial stiffness of 1E7 N/m and a damping coefficient of 5E4 along the track axis.

Lastly, in the Global Settings of Simpack®, adjustments were made from the default configurations, each tailored to the specific requirements. These modifications are detailed in Figure 4.1, offering a comprehensive view of the customized parameters that facilitate the execution of our simulation with precision and accuracy.

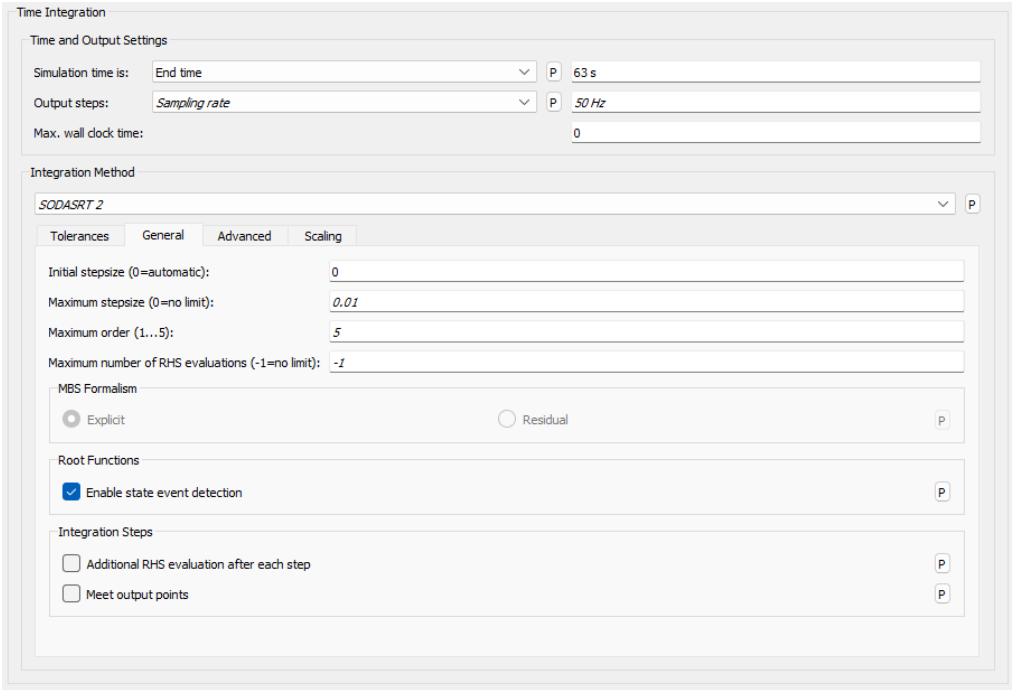

Figure 4.1: Global setting of Loadcase.

Four scenarios were evaluated based on the irregularities measured on the sample track. Since December 16, 2016, after the accident there was an unavailability of leveling and longitudinal alignment data to introduce in the calculation program. These scenarios were developed by scaling the irregularities by a given factor until the desired twist was obtained (see Annex C). The first scenario is the "Accident Scenario", where the longitudinal leveling undertook a substantial scaling by a factor of 1.425 only within the critical region of the accident. The intent behind

this adjustment was to obtain a maximum twist of approximately 29 mm. Subsequent to this, the "2016-12-16 Scenario" was then developed, in which the longitudinal leveling data measures were obtained on December 16, 2016, leading to the resultant maximum twist of approximately 21 mm. Additionally, the "Intervention Limit Scenario" was formulated by a scaling factor of 0.645, in the entire length of the rail. This adjustment was searched to limit the maximum deflection to about 15 mm. Lastly, the "Alert Limit Scenario" emerged, involving only applying a factor of 0.42 to the longitudinal leveling along the track aiming to induce a maximum deflection in the affected accident area of approximately 12 mm.

4.2 Results: Displacements

This section is completely dedicated to the analysis of the Freight Wagon, whose model was described carefully in Chapter 3.

For the analysis of the lateral displacement of the Freight wagon, and lateral and longitudinal displacements of the bogie bumpstops will only be used the "Accident Scenario" simulation since it presents the most aggressive excitation. The importance of evaluating the lateral displacement of the train is due to the Gabarit, which is the transversal section of the axis that establishes the maximum area possible to be occupied by the train. Hence, by complying with the dimensions, it is granted a safe rolling vehicle. The limits are different from country to country due to the different gauges and can be seen in the EN 15273-2:2013+A1 standard [66] (see Figure 4.2).

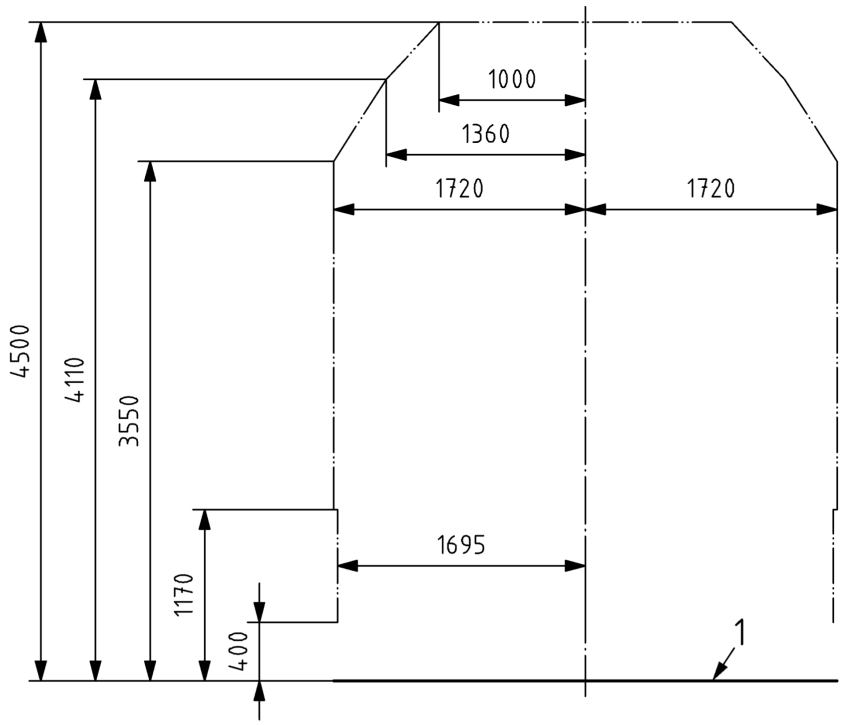

Figure 4.2: Reference profile of kinematic gauge PTb (dimensions in mm) [66].

In the Simpack® model, for this topic, a position sensor was used to monitor the center position of the Container relative to the center of the track which was then simulated to obtain the graph in Figure 4.3. The containers are about 2.395 meters wide, i.e. 1.1975 m for each side. Adding up the maximum displacement, whose value is about 0.18 m, it will not reach the Gabarit Limit.

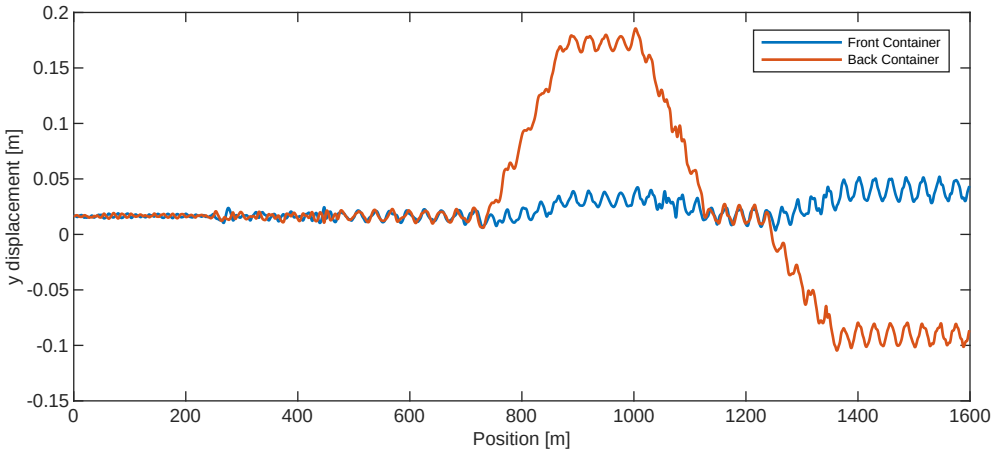

Figure 4.3: Lateral displacements of the containers.

Shifting the focus to the bumpstops displacements of the bogie, in Figures 4.4 and 4.5 are the values obtained according to the longitudinal bumpstop and, in Figure 4.6 the values obtained according to the lateral bumpstop, all from the Center Bogie. The results for the remaining axles are Annexed to F. The generation of graphs was possible through the utilization of the Simpack® post-processing tool, utilizing the output values of the force elements delineated in Table A.2 within Annex A.

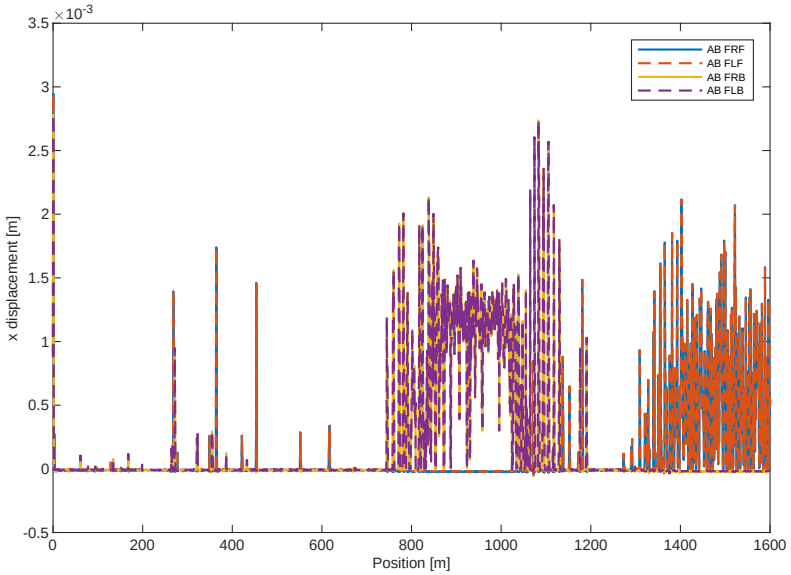

Figure 4.4: Longitudinal Bumpstops: Center Bogie - Front Axleboxes.

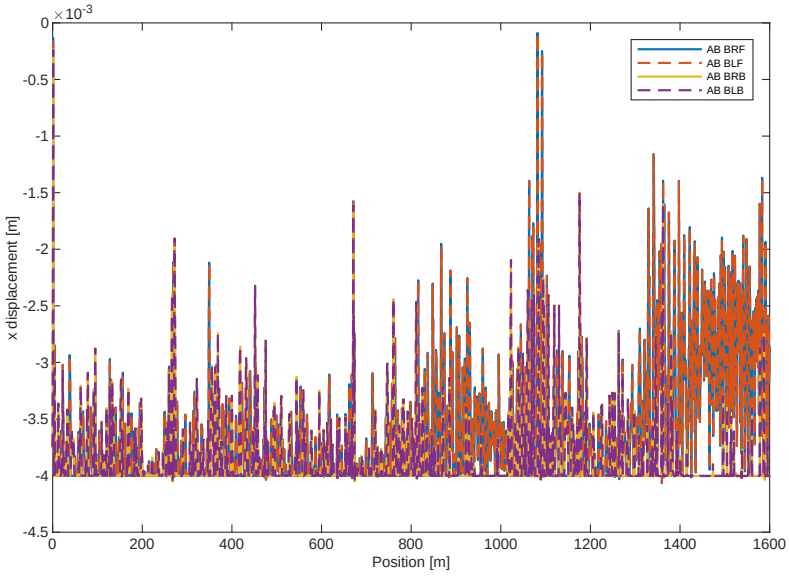

Figure 4.5: Longitudinal Bumpstops: Center Bogie - Back Axleboxes.

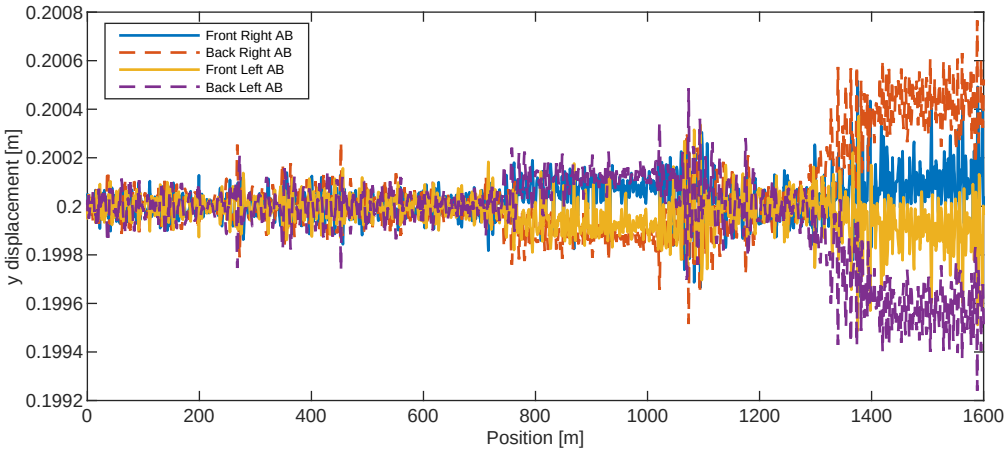

Figure 4.6: Lateral Displacement: Center Bogie

As mentioned before, the longitudinal bumpstops allow the body of the axlebox to move the bare minimum of 4 mm. It can be noticed that the limits are exceeded in the Front, Center and Back Bogie. However, considering the Center Bogie as an example, throughout all the track, the gap of 4 mm is surpassed by a minimum value, representing the friction plane collision. In a positive way, for the lateral bumpstops the limits are not exceeded in any of the Bogies, as seen in Figure 4.6 and Annex F, even though the was simulated using the most aggressive track irregularities. Hence, the Bogie will not have major problems with maintenance for the bumpstops.

4.3 Results: Nadal Criteria

This section compares the results of the Wheel Flange Derailment criteria of the four simulations ran in Simpack®: "Accident Scenario", "2016-12-16 Scenario", "Intervention Limit Scenario" and "Alert Limit Scenario". As mentioned before, this type of derailment is described by a wheel climbing the rail head, which usually exists at track curves. A comparison between simulations is done along with the most critical places of the freight wagon in the accident zone of the track design.

In order to extract the values required for the Nadal criterion, an initial step involves filtering the results by the utilization of a low-pass filter of cut-off frequency set at 20Hz. This method is integral for the testing and approval of rail vehicles. Additionally, the Y/Q values are statistically involved by the implementation of a sliding average method, with a window length of 2 m and step length of 0.5 m [67].

Figure 4.7 illustrates the Nadal criterion values specifically for the rear left wheel of the front bogie from the comprehensive evaluation of all scenarios investigated in the study, while the values for the other wheels are represented in Annex G. After running the simulations, the results in the accident section do not show any problem, not exceeding the conventional limit, recalling that this wheel represents the highest value of Y/Q in the accident scenario. Notably, Figure 4.7a stands out as the graph where this increase is most pronounced.

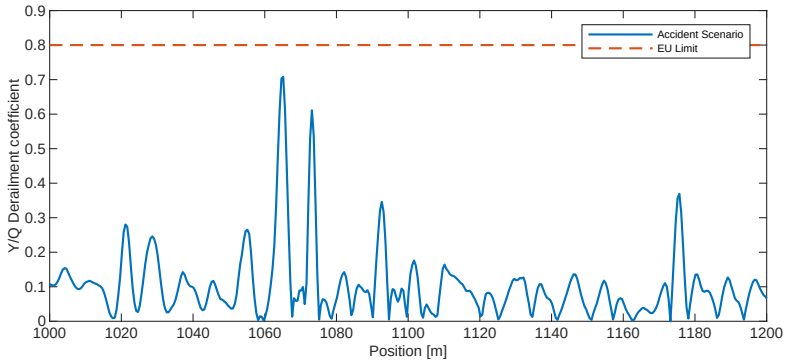

(a)

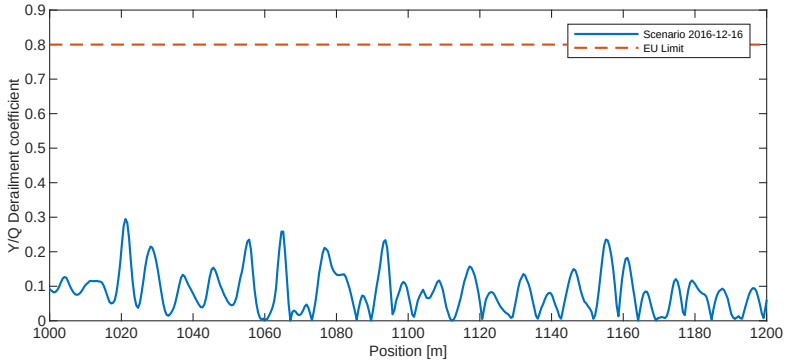

(b)

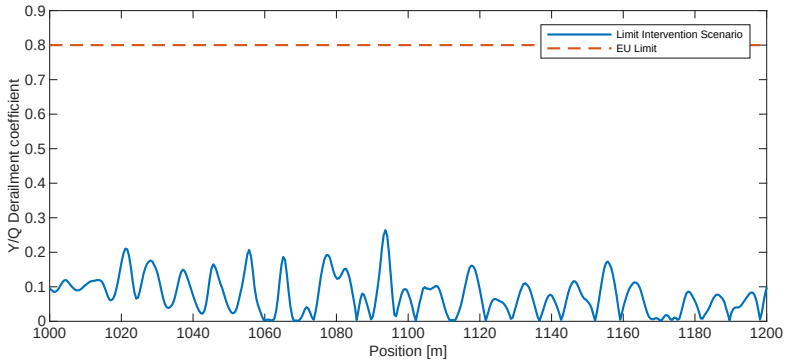

(c)

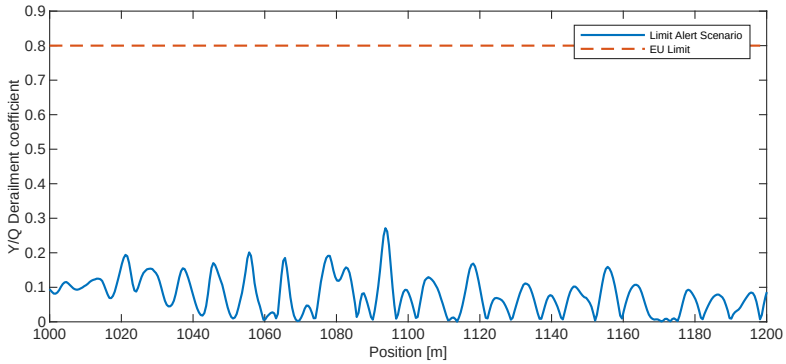

(d)

Figure 4.7: Nadal criterion for the Sggrss wagon in the scenarios: (a) accident, (b) 2016-12-16, (c) intervention limit, and (d) alert limit.

4.4 Results: Prud'homme Criteria

Within this Chapter, an in-depth comparative analysis of the Prud'homme criteria is undertaken, paralleling the methodology applied to the Nadal criteria. The investigation extends to four distinct simulations, each meticulously detailed in Section 4.1 and executed using the Simpack® software.

The Prud'homme criterion also recognized as "track panel shift derailment," centers on the lateral track displacement. Like its Nadal counterpart, the evaluation and comparison of Prud'homme criterion results and application of filters on the results are approached using consistent and rigorous methodologies.

Specifically, the Prud'homme results from all four simulations are extracted from the Back Wheelset of the Back bogie. These results are thoughtfully presented in Figure 4.8, shedding light on the behavior of this critical component within the context of the Prud'homme criteria. Furthermore, for a comprehensive overview of how other axles perform in relation to the Prud'homme criterion within the pertinent track section, illustrated in Annex H, where these additional results are thoughtfully documented.

Upon close examination of the graphical representations provided, it becomes evident that the limit values set by the Prud'homme criteria are exceeded in the accident scenario. This observation underscores the significance of these criteria in assessing rail vehicle safety. Furthermore, it is noteworthy that the remaining scenarios, namely, 2016-12-16, intervention, and alert, do not approach the limit value, thereby indicating a substantial margin of safety in these scenarios. This comparative analysis offers valuable insights into the performance and safety considerations associated with these simulations and their implications for rail vehicle operations.

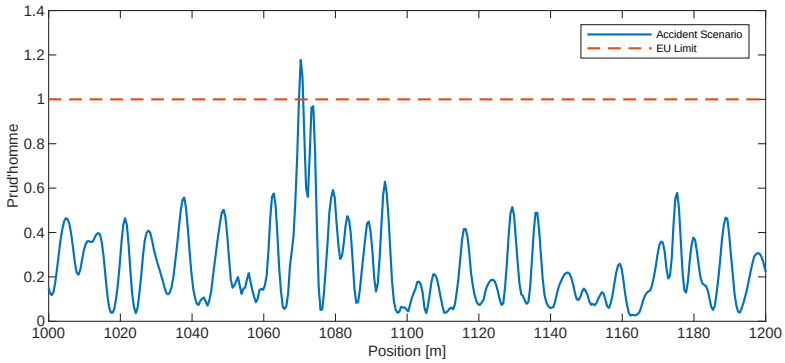

(a)

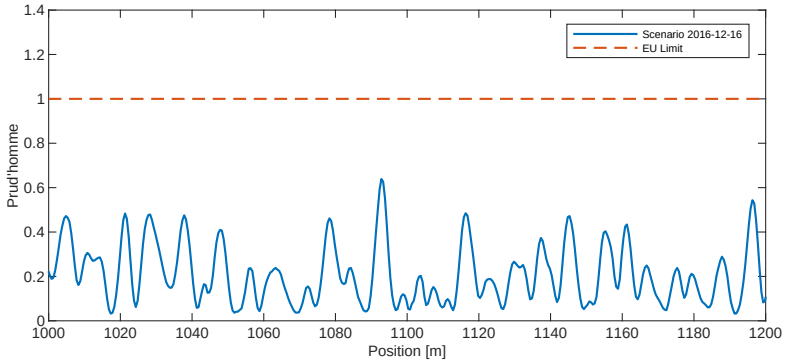

(b)

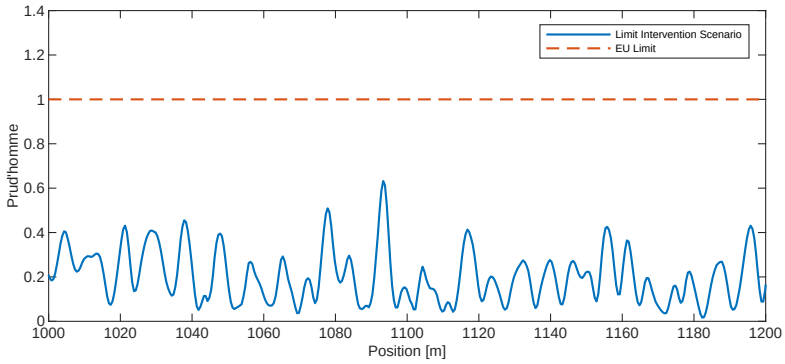

(c)

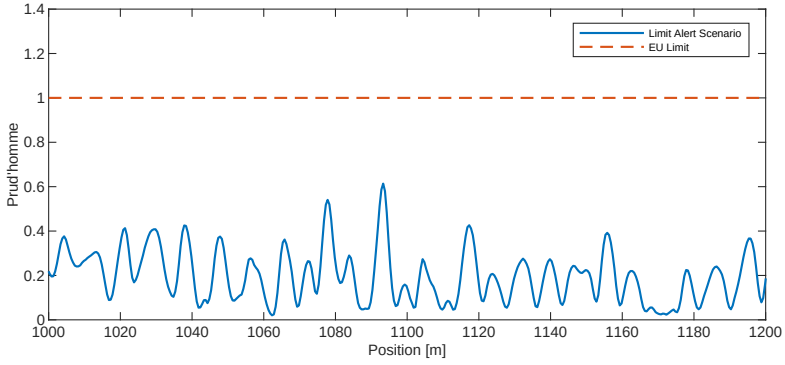

(d)

Figure 4.8: Prud'homme criterion for the Sggrss wagon in the scenarios: (a) accident, (b) 2016-12-16, (c) intervention limit, and (d) alert limit.

4.5 Results: Wheel Unloading Criteria

In this chapter, a comprehensive comparative analysis was undertaken of the Wheel Unloading Criteria, a critical aspect of railway safety. This analysis is substantiated through a series of four distinct simulations, as elucidated in Section 4.1, all meticulously conducted within the Simpack® simulation environment. The essence of this criterion revolves around the occurrence of extreme vibrations experienced by train wheels, which can ultimately lead to the loss of contact with the rail, with potentially catastrophic consequences.

The investigation centers on the results derived from these four simulations, with a specific focus on the front right wheel of the rear bogie. These results are thoughtfully presented in Figure 4.9. It's important to note that while the front right wheel is the primary focus, data pertaining to the remaining axles is thoughtfully cataloged in Annex H for the sake of completeness and reference.

As it is scrutinized the graphical representations of the findings, a salient pattern emerges. The limits prescribed by the Wheel Unloading Criteria are exceeded in specific scenarios, notably the accident scenario, which transpired on 2016-12-16, and the intervention scenario. These instances of limit breaches underscore the severity of the situation, suggesting that immediate attention and action are warranted to rectify potential safety concerns. Conversely, in the alert scenario, it is observed that the recorded values do not approach the established limit.

In conclusion, this chapter emphasizes the critical importance of assessing and understanding the Wheel Unloading Criteria within the context of railway safety. By conducting thorough simulations and adhering to established criteria, valuable insights were gained into the potential risks and vulnerabilities that can arise during rail operations.

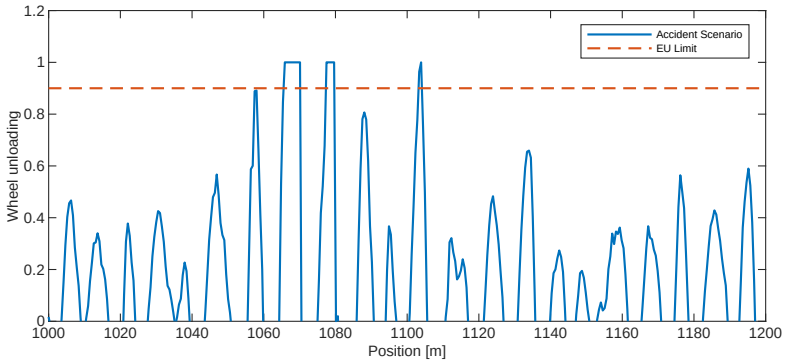

(a)

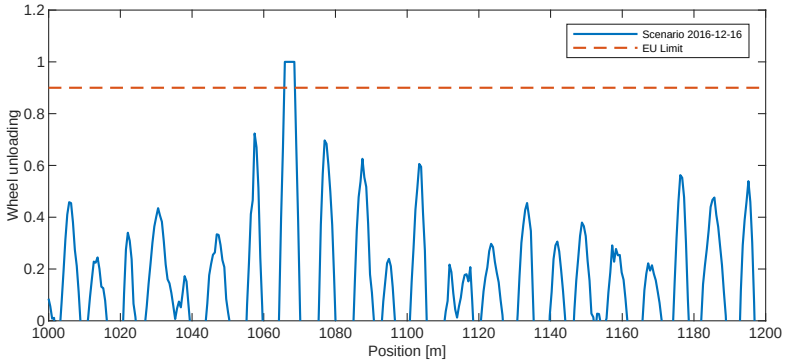

(b)

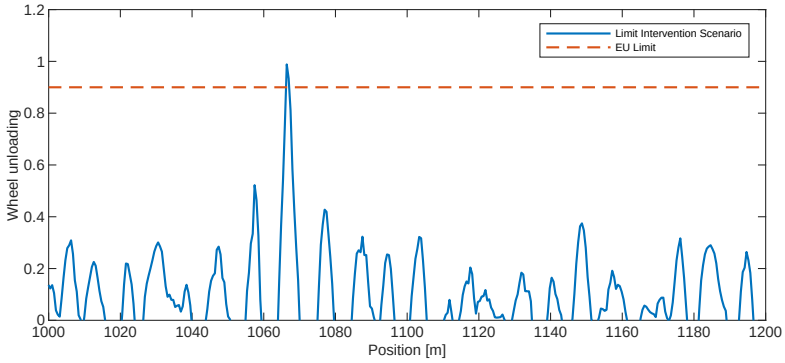

(c)

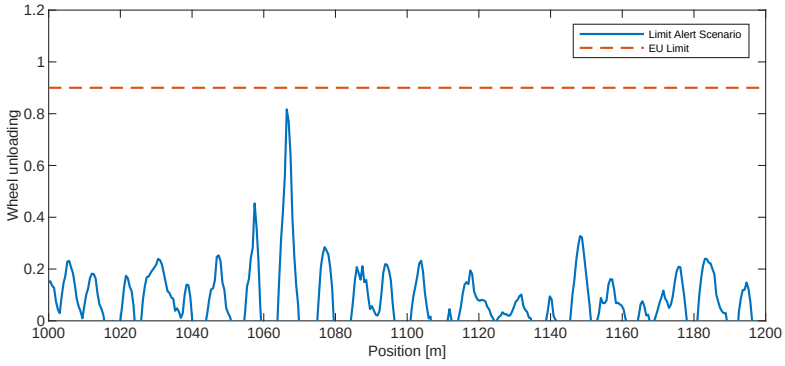

(d)

Figure 4.9: Wheel unloading criterion for the Sggrss wagon in the scenarios: (a) accident, (b) 2016-12-16, (c) intervention limit, and (d) alert limit.

4.6 Results: Influence of variation in properties

In order to conduct a comprehensive evaluation, this particular section has been created with the specific aim of scrutinizing the fluctuations in the coefficient of friction pertaining to all the friction surfaces of the axlebox, which, in their capacity as shock absorbers, play a pivotal role. Table 4.2, presents a visual representation of the new data deliberated herein, compared with the previously designated values expounded upon in Section 3.2.1.2. Additionally, it is worth noting that the data under consideration here pertains to the selected track associated with the Accident Scenario.

Table 4.2: Coefficient of friction, μ opted.

	Wagon_v1	Wagon_v0	Wagon_v2
μ	0.2	0.4	0.6

The results derived from Simpack® simulations, specifically pertaining to the maximum Y/Q values in the Front, Center, and Back Bogie, have been thoughtfully illustrated and presented for comprehensive review in Figures 4.10, 4.11, and 4.12, respectively.

Intriguingly, when considering the variation of the friction coefficient within the axlebox, a noteworthy observation comes to light. In the case of the Front and Back Bogies, especially concerning the left wheels, this variation appears to have a minimal impact on the maximum Y/Q values (see Figures 4.10 and 4.12). However, the Center Bogie presents a divergent scenario, where the coefficient of friction exerts a notably influential role in damping the system. This observation is substantiated by the data illustrated in Figure 4.11, where the decrease in wheel flange climb derailment with increasing friction is proven.

In conclusion, it becomes evident that elevating the coefficient of friction within the axlebox plays a pivotal role in enhancing the overall stability of the Freight Wagon. This finding underscores the criticality of friction-related factors in the context of system dynamics and safety considerations, offering valuable insights for optimizing rail vehicle performance and safety.

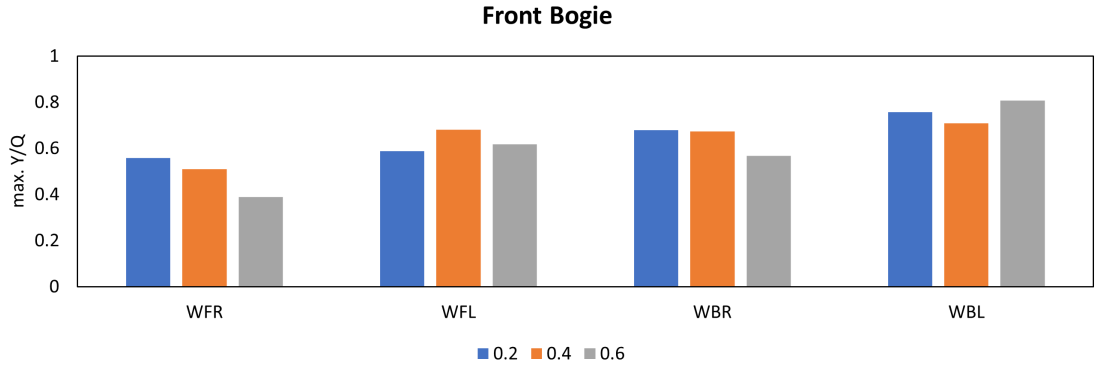

Figure 4.10: Front Bogie: Maximum Y/Q as function of the coefficient of friction.

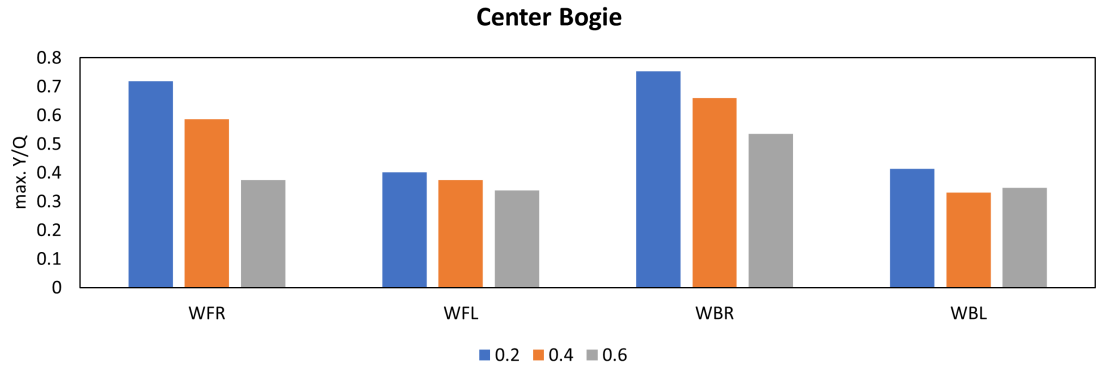

Figure 4.11: Center Bogie: Maximum Y/Q as function of the coefficient of friction.

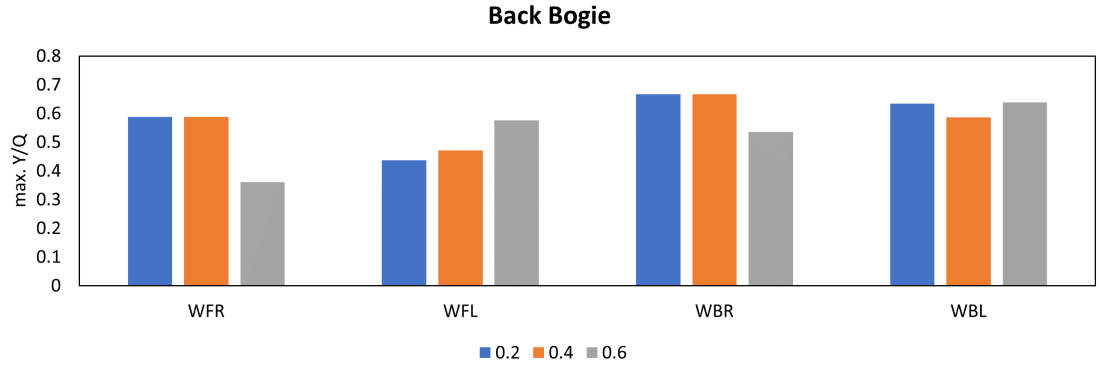

Figure 4.12: Back Bogie: Maximum Y/Q as function of the coefficient of friction.

4.7 Concluding Remarks

In this chapter, a comprehensive analysis of simulation results is obtained using Simpack®, following the model described in Chapter 3. These simulations involved various scenarios and excitation conditions, enabling it to evaluate critical aspects of the system's performance and safety.

Simpack® post-processing capabilities allow to visualize and interpret the behavior of the model such as derailment risk, accelerations at specific points of the model, and dynamic forces acting along track irregularities.

In the section dedicated to displacement analysis, it was examined the lateral displacement of the freight wagon and the lateral and longitudinal displacements of the bogie bumpstops, particularly in the "Accident Scenario." The results indicated that the lateral displacements of the containers remained within safe limits, ensuring compliance with Gabarit standards. While longitudinal bumpstop limits were minimally exceeded in certain cases, indicating manageable maintenance requirements, lateral bumpstop limits were not.

Results of Nadal, Prud'homme, and Wheel Unloading criteria were explored, comparing the performance of the system across different scenarios. These criteria provided valuable insights into derailment risks, lateral displacement of ballast, and wheel unloading issues. Notably, the accident

scenario raised concerns in almost all the criterias, emphasizing the need for further analysis and potential modifications to improve safety.

After the simulations, it is possible to conclude that the train does not face any problems of derailment by the wheel climbing the rail, even when surpassing in presence of high level of irregularities. However, the freight wagon can present problems leading to intermittent loss of contact between the wheels and the rail and track panel shift. This intriguing disparity can be attributed to various factors, including the train's traversal of curved tracks featuring superelevation transitions and slope variations. These complex track conditions, coupled with pronounced vertical irregularities, are believed to contribute to the phenomenon of wheel unloading and track panel shift. Also, the critical zones of the results fit perfectly with the prevision, since the derailment accident of the case study took place in the same zone.

Finally, it was investigated the influence of variations in the coefficient of friction within the axlebox. The results highlighted the importance of friction-related factors, particularly in the Center Bogie, where increasing the coefficient of friction played a significant role in damping the system and reducing wheel flange climb derailment risks.

In conclusion, this chapter's comprehensive analysis of simulation results using Simpack® has shed light on critical factors affecting the performance and safety of the Freight Wagon. These insights will guide a further simulation present in Chapter 5 for a wider study of the potential derailments.

Chapter 5

Derailment scenario according to EN 14363

For this chapter, Standard EN14363 offers a derailment study for vehicles to run safely on twisted tracks. The importance of the twist simulation is due to the existence of leveled tracks, canted tracks, and cross-level deviations, known for the maintenance limits interventions.

Firstly, referring back to the preceding information, a new track was used with different track properties of vertical, horizontal and superelevation inputs, illustrated in Annex D. In addition, there were alterations in both the track's levelness and longitudinal irregularities compared to the previous configuration of the Coimbra line. The changes seen in Figure 5.1 were applied in levelness in the left part of the track. For the right levelness and right and left longitudinal parts of the track, no irregularities were taken into account.

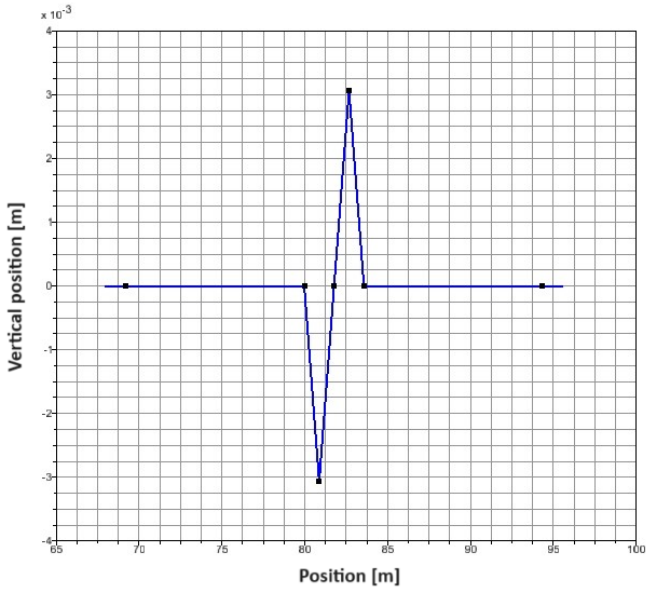

Figure 5.1: Input function of Twist test [67].

Secondly, a loadcase was also imposed with the same geometrical and joint properties, only changing the velocity of 26.39m/s (95 km/h) to 1m/s, which is the velocity suggested in the standard. Last but not least, certain modifications to the Global Settings default and Coimbra simulation menu were made, as seen in Figure 5.2. The value of the Simulation is not directly depicted because it is calculated according to the velocity and track length, valued at approximately 119.42 seconds.

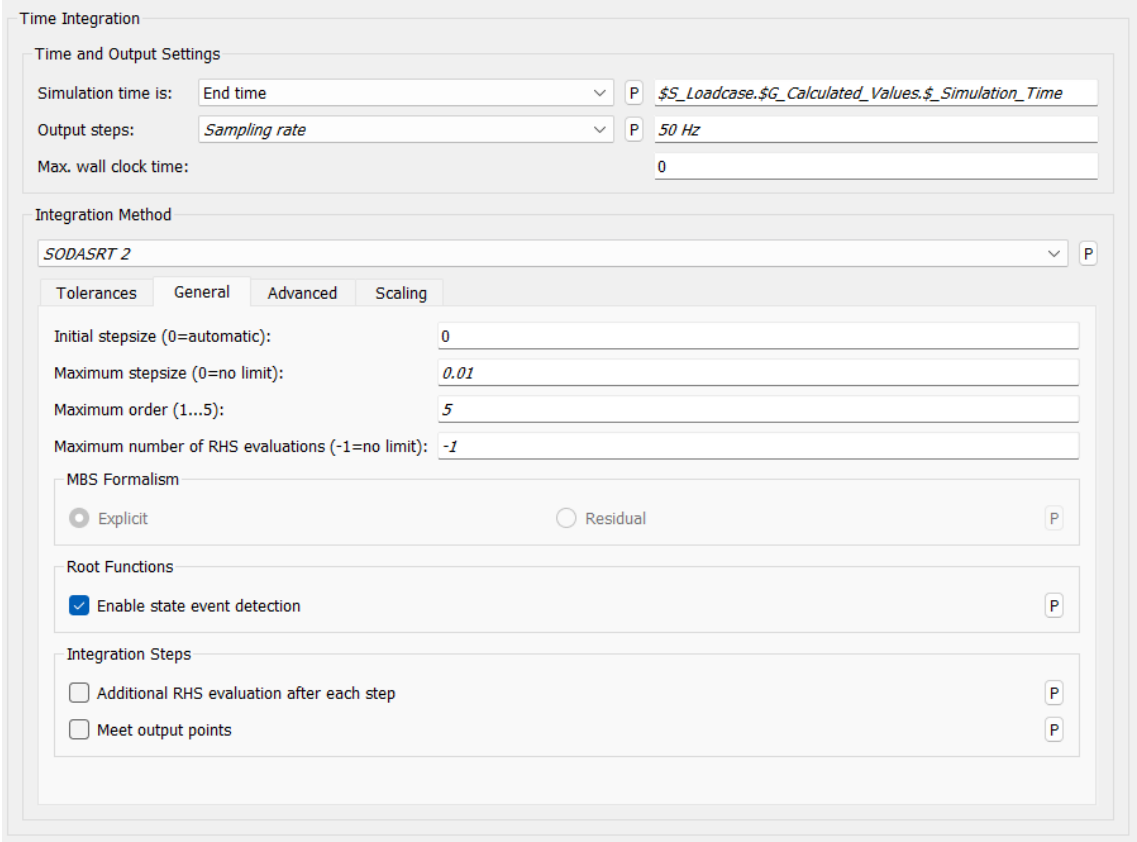

Figure 5.2: Global setting of Loadcase.

5.1 Simulation Results

Trains running on twisted rails increase the chance of derailment of flange climbing due to the presence of high lateral forces and low vertical wheel force. Hence, it is only going to be taken into account the Nadal limit of the Front Left wheel, where the irregularity was placed. In this simulation, it was considered an S1002 wheel, which has 70 degrees of contact angle, with a coefficient of friction of 0.4. These values alter the typical and conservative Nadal limit value to a greater amount of about 1.18. For the calculation of the new Nadal criteria, it was used Equation (2.4) that was explained in Sub-section 2.4.1.

It should be noted that in Figures 5.4 and 5.5 of the Central and Back Bogies, the restrictions are not exceeded, despite being exceeded in the Front Bogie, depicted in Figure 5.3. This low instability of the wheel behavior can be due to a not enough precise modeling approach.

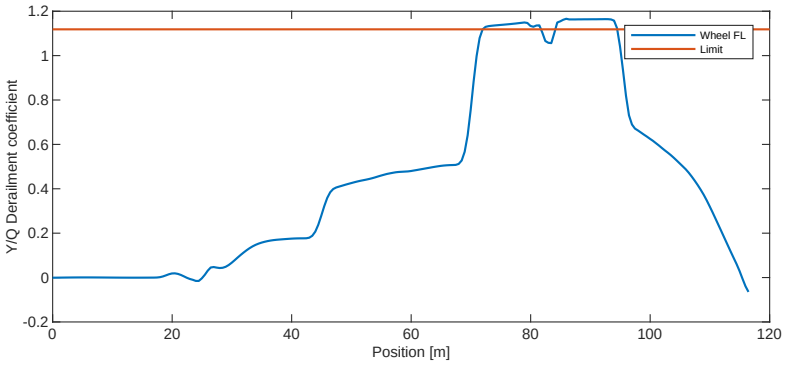

Figure 5.3: Y/Q in the Front Left Wheel of Front Bogie.

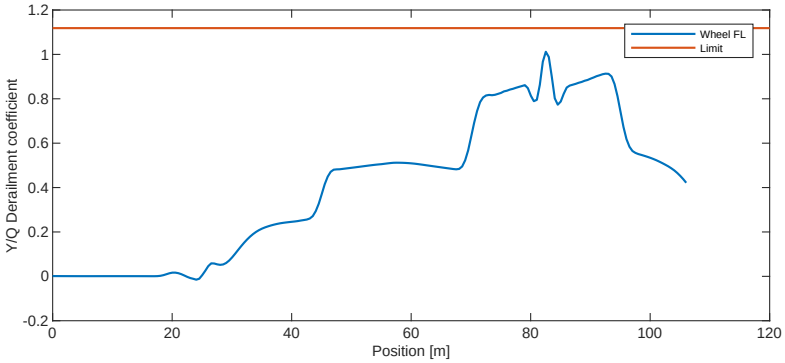

Figure 5.4: Y/Q in the Front Left Wheel of Center Bogie.

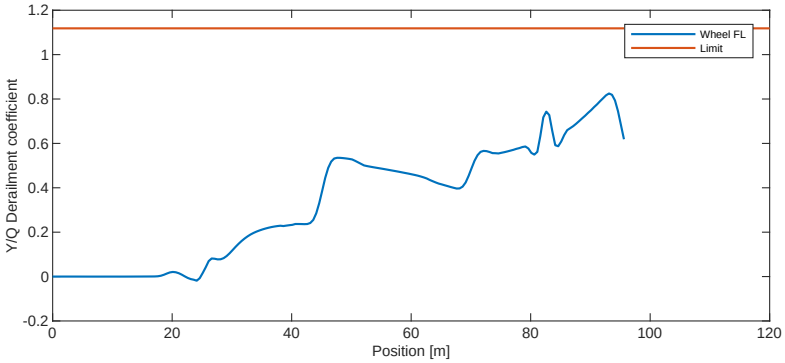

Figure 5.5: Y/Q in the Front Left Wheel of Back Bogie.

5.2 Concluding Remarks

This chapter has explored the critical aspect of ensuring the safe operation of railway vehicles on twisted tracks, as addressed by Standard EN14363. The significance of simulating track twists stems from the presence of various track configurations, such as leveled tracks, canted tracks, and cross-level deviations, which pose maintenance challenges and require well-defined intervention limits.

The simulation results were focused on the critical issue of derailment risk due to flange climbing when trains operate on twisted rails. The Nadal limit was examined for the Front Left wheel considering a less conservative value of the limit.

Central and Back Bogies did not exceed the imposed restrictions, however, the Front Bogie displayed limitations exceeding the defined criteria. This discrepancy in wheel behavior stability may be attributed to certain limitations or approximations in the modeling approach.

In summary, this chapter has highlighted the intricate nature of ensuring rail vehicle safety on twisted tracks, emphasizing the need for precise and improvement of the model and analysis to determine and mitigate derailment risks effectively. The results obtained serve as a basis for further refinement and optimization in pursuit of safer rail operations.

Chapter 6

Conclusions

6.1 Concluding Remarks

The present thesis's main goal was to meticulously scrutinize the running safety of a Freight Wagon. This entails in evaluating different types of derailment, crucial spots affected by high impacts, and even different ranges of properties and their affection on the behavior. The Wagon is a Sggrss composed of Y25 bogies modeled and investigated computationally. Even though these wagons present a simple suspension spring component, it also made up of friction surfaces and joints with clearance, which grant a non-linear behavior that also influences the running vehicle. Therefore, the modeling pathway will affect how accurate the simulation is. Hence, to achieve the goal proposed it was used a commercial software named Simpack®, which is a multibody software set for railway and road dynamics.

For the first study, it has opted to analyze the Sggrss with a case study of a derailment that took place near Coimbra composed of 4 scenarios: Accident, 2016-12-16, intervention and alert. In the displacement analysis section, it was found that the lateral displacements of the freight wagon and the lateral and longitudinal bumpstops of the bogies generally met safety standards, with some minor exceptions, leading to not having major problems with high maintenance. Additionally, three types of derailment are studied to identify the possible causes of derailment of the Freight Wagon. Subsequently, the Nadal criteria represented excellent and low value, meaning no problem of wheel climb type of derailment for any wheel of the wagon. Consequently, as the Prud'homme and Wheel Unloadin criteria are evaluated, and limits are exceeded, matching the derailment accident location, in some scenarios. The wagon's rolling over curved tracks with superelevation transitions, slope fluctuations and severe vertical anomalies could be the main causes of these remarkable discrepancies.

Lastly in the Coimbra topic, a variation of the coefficient of friction was done on Axlebox friction surfaces. The analysis illustrated that while the Front Bogie had the highest Y/Q, the coefficient had almost no impact on the Front and Back Bogies, although, the Center Bogie, had the most positive results in damping.

Finally, a standardized track for the evaluation of the Nadal criteria was performed. Focusing

initially on the Front Left wheel it revealed that it exceeded the limit while the Center and Back Bogies prevailed within acceptable limits. These conclusions can be due to potential areas of the model that need posterior improvement.

6.2 Future works

In the course of this work, various research perspectives have emerged which, may be worthy of future attention, since the software presents a wide range of selections when modeling. Therefore, different pathways can be reconsidered for future analysis addressing aspects including friction analysis, articulation dynamics, parameter variation studies, modeling limitations, and adherence to safety standards that can lead to a distinct behavior.

Starting on the bogie model, a significant improvement can happen in remodeling the friction in the axlebox. The friction force is dependent on the direction of the relative velocity, so the dry Coulomb's friction approach is unable to explain the majority of frictional effects and shows a discontinuity for the friction force at zero velocity. Instead of using this traditional model that is specifically displayed in the software, a more complex approach named the Threlfall model [68] can be more accurate, considering that it relies on avoiding a discontinuity between the two parts of the function.

The creation of new models implies various simplifications in the model for computational feasibility and efficiency, but can also frequently lead to inaccurate results. A noteworthy aspect of this matter are the incorrect and imprecise inertia, which has a very important role in multibody simulation. Moreover, a crucial aspect is the role of friction that was not considered in the connection between the bogie frame and body frame, more specifically the center plate. In the vehicle model, future studies could focus on refining the articulation degrees of freedom by creating more complicated models that better represent the various interactions between wagon parts. Therefore, incorporating an independent articulation component that realistically represents the existing mechanism can lead to a more authentic representation of wagon behavior.

The occurrence of asymmetric loading in the vehicle can be attributed to the inadequate positioning of the cargo leading to an imbalanced distribution of static wheel loads. Consequently, one of the studies that could be beneficial for this project is the impact of asymmetric loading on the derailment potential based on a parametric study as it was done in Section 4.6.

In order to conduct a more thorough investigation, the use of the Design of Experiments (DOE) methodology to include variations of multiple parameters is imperative. Hence, such a broad approach provides a more complete understanding of the interactions that influence wagon dynamics, leading to optimized design configurations.

Overall, Simpack® is a very user-friendly software, although executing some of the simulations led to a number of issues, mainly in the beginning. Implementing these improvements requires additional and in-depth research of the software capacities.

References

[1] European Commission. Accessed on June 2023. Available at https://cinea.ec.europa.eu/news-events/news/transport-infrastructure-european-commission-accelerates-shift-sustainable-and-smart-mobility-ten-t-2023-06-22_en.

[2] European Commission. Accessed on March 2023. Available at https://transport.ec.europa.eu/transport-themes/infrastructure-and-investment/trans-european-transport-network-ten-t_en.

[3] European Commission. Accessed on March 2023. Available at https://climate.ec.europa.eu/eu-action/european-green-deal/european-climate-law_en.

[4] Transportes e Negócios. Accessed on March 2023. Available at https://www.transportesenegocios.pt/ue-quer-migracao-da-bitola-iberica-ate-2030/.

[5] The core network corridors: Trans european transport network 2013, 2013.

[6] Projeto PRR SMART WAGONS Desenvolvimento de Capacidade Produtiva em Portugal de Vagões Inteligentes para Mercadorias. Accessed on June 2023. Available at https://transparencia.gov.pt/pt/fundos-europeus/prr/beneficiarios-projetos/projeto/02-C05-i01.02-2022.PC644940527-00000048/.

[7] Shift2Rail. Definition of scenarios for cbm on wagon bogies and definition of subsystem architecture report, 2020.

[8] Tomáš Lack and Juraj Gerlici. Y25 freight car bogie models properties analysis by means of computer simulations. EDP Sciences, 2018.

[9] Sirong Yi. *Dynamic Analysis of High-Speed Railway Alignment*. Elsevier, 2018.

[10] Lei Xu and Wanming Zhai. A three-dimensional dynamic model for train-track interactions. *Applied Mathematical Modelling*, 76:443–465, 2019.

[11] Ary Vinicius Nervis Frigeri, 2021.

[12] Klaus Knothe and Sebastian Stichel. *Rail Vehicle Dynamics*. Springer International Publishing, 2016.

[13] T. Matsudaira. *Shimmy of axles with pair of wheels (in Japanese)*. J. Railw. Eng. Res, 1952.

[14] A. H. Wickens. *The dynamics of railway vehicles on straight track: fundamental consideration of lateral stability*. Proc. I. Mech. Eng, 1965.

[15] CTh Müller. Das schlingerproblem in der sicht von vergangenheit und gegenwart. *Glasers Annalen*, 93:329–336, 1969.

[16] W. Michels. Theoretische Untersuchungen der Laufstabilität des Radsatzes (Theoretical investigations of the running stability of a wheelset. Status seminar III, 1976.

[17] CP-Comboios de Portugal. Accessed on March 2023. Available at https://www.cp.pt/institucional/pt/cultura-ferroviaria/historia-cp/cronologia.

[18] Teresa Marat-Mendes Inês de Azevedo Isidoro and Vera Regina Tângari. The portuguese railway in time and space – mapping phases of growth, stagnation, and decline (1845–2015)*. *Planning Perspectives*, 33(3):363–384, 2018.

[19] Isao Okamoto. How bogies work. *Japan Railway Transport Review*, 18:52–61, 1998.

[20] S Stichel. On freight wagon dynamics and track deterioration. *Proceedings of the Institution of Mechanical Engineers, Part F: Journal of Rail and Rapid Transit*, 213(4):243–254, 1999.

[21] S.D. Iwnicki, S. Stichel, A. Orlova, and M. Hecht. Dynamics of railway freight vehicle, 2015.

[22] Per-Anders Jönsson. *On the influence of rail vehicle parameters on the derailment process and its consequences*. 2005.

[23] Ayman A. Aly and Farhan A. Salem. Vehicle suspension systems control: A review. *International Journal of Control, Automation and Systems*, 2:46–54, 2013.

[24] José Dias Rodrigues. *Apontamentos de Vibrações de Sistemas Mecânicos*. 2021.

[25] N. Bosso, A. Gugliotta, and N. Zampieri. Design of a test rig for railway axle-boxes. *Procedia Structural Integrity*, 12:344–352, 2018. AIAS 2018 international conference on stress analysis.

[26] SKF. *Railway technical handbook - Bogie designs*, volume 1. 2011.

[27] Maksym Spiryagin, Colin Cole, Yan Quan Sun, Mitchell McClanachan, Valentyn Spiryagin, and Tim McSweeney. *Design and Simulation of Rail Vehicles*. CRC Press, 2014.

[28] Simon Iwnicki, Maksym Spiryagin, Colin Cole, and Tim McSweeney. *Handbook of Railway Vehicle Dynamics*. CRC Press, 2020.

[29] Paulo R. R. de Campos, Debora N. Higa, and Alfredo Gay Neto. Lateral stability of railway vehicles and new contact formulations, 2017.

[30] Xuesong Jin, Kaiyun Wang, Zefeng Wen, and Weihua Zhang. Effect of rail corrugation on vertical dynamics of railway vehicle coupled with a track. *Acta Mechanica Sinica*, 21:95–102, 2005.

[31] Ahmed A. Shabana, Khaled E. Zaazaa, and Hiroyuki Sugiyama. *Railroad vehicle dynamics: a computational approach*. CRC Press, 2008.

[32] MEDWAY. Saiba mais sobre o transporte ferroviário de mercadorias. Accessed on May 2023. Available at https://www.medway-iberia.com/pt/services/category/transporte-ferroviario.

[33] British Steel. Profile selector - vignole. Accessed on March 2023. Available at https://britishsteel.co.uk/what-we-do/rail/flat-bottomed-vignole-rail/profile-selector-vignole/.

[34] Alberto García Álvarez, Documentos De Explotación Económica, Y Técnica, and Del Ferrocarril. Automatic track gauge changeover for trains in spain, 2010.

[35] Yong Huang, Junjie Wang, Weijie Le, Liang Zhang, and Junsheng Su. Study on mechanical behaviours of rail fasteners and effects on seismic performance of urban rail viaduct. *Structures*, 33:3822–3834, 2021.

[36] M. Sol-Sánchez and G. D'Angelo. Review of the design and maintenance technologies used to decelerate the deterioration of ballasted railway tracks. *Construction and Building Materials*, 157:402–415, 2017.

[37] D. Li and E. T. Selig. Transportation research record no. 1489, railroad transportation research. *Transportation research record*, 1489:17–25, 1995.

[38] João Nogueira Alves. Evaluation of design of railway's sub-structure in high-speed.

[39] Simpack. *SIMULIA User Assistance 2023x.3*.

[40] Transporte ferroviÁrio descarrilamento de comboio de mercadorias na linha do norte, próximo de adémia, 01-04-2017, 2019.

[41] Matin Shahzamanian Sichani. Wheel-rail contact modelling in vehicle dynamics simulation, 2013.

[42] D. Milković, G. Simić, Ž. Jakovljević, J. Tanasković, and V. Lučanin. Wayside system for wheel–rail contact forces measurements. *Measurement*, 46(9):3308–3318, 2013.

[43] Carlos Fernandes. Gears, 2021-2022.

[44] Xiang Liu, M. Rapik Saat, and Christopher P. L. Barkan. Analysis of causes of major train derailment and their effect on accident rates. *Transportation Research Record*, 2289(1):154–163, 2012.

[45] Pedro Aires Moreira Montenegro Almeida. A methodology for the assessment of the train running safety on bridges, 2015.

[46] P.A. Montenegro, H. Carvalho, D. Ribeiro, R. Calçada, M. Tokunaga, M. Tanabe, and W.M. Zhai. Assessment of train running safety on bridges: A literature review. *Engineering Structures*, 241:112425, 2021.

[47] Luiza Dalpasquale. Análise da equação de nadal pela teoria de propagação de erros. Bachelor's thesis, Universidade Federal de Santa Catarina, 2019.

[48] Herbert Weinstock. *Wheel Climb Derailment Criteria for Evaluation of Rail Vehicle Safety*. 1984.

[49] A. O. Gilchrist and B. V. Brickle. A re-examination of the proneness to derailment of a railway wheel-set. *Journal of Mechanical Engineering Science*, 18(3):131–141, 1976.

[50] J.A. Elkins and A. Carter. Testing and analysis techniques for safety assessment of rail vehicles: The state-of-the-art. *Vehicle System Dynamics*, 22(3-4):185–208, 1993.

[51] G. Samavedamand, D. Thomson, and F. Blader. Safety of high speed ground transportation systems track, 1996.

[52] António Abel Henriques João M. Rocha and Rui Calçada. Probabilistic assessment of the train running safety on a short-span high-speed railway bridge. *Structure and Infrastructure Engineering*, 12(1):78–92, 2016.

[53] Association of American Railroads. *Manual of standards and recommended practices: Section C, Part II - Design, Fabrication, and Construction of Freight Cars*. Washington, DC, USA, 2015.

[54] J. A. Elkins and A. Carter. Testing and analysis techniques for safety assessment of rail vehicles: The state-of-the-art. *Vehicle System Dynamics*, 22(3-4):185–208, 1993.

[55] Edward J. Haug. *Computer-Aided Kinematics and Dynamics of Mechanical Systems Volume II: Modern Methods*. 2021.

[56] Tatravagónka Poprad. Sggrss 80‘. Accessed on March 2023. Available at http://tatravagonka.sk/wagons/sggrss-80-2/?lang=en.

[57] UIC. Accessed on March 2023. Available at https://uic.org/freight/.

[58] Ostravské opravny a strojírny. Accessed on June 2023. Available at http://www.oossro.cz/en/sggrss-80-eng/.

[59] Railway application - Testing for the acceptance of running characteristics of railway vehicles - Freight wagons - Conditions for dispensation of freight wagons with defined characteristics from on-track tests according to EN 14363. British standard, BSI Standards Publication, United Kingdom, 2013.

[60] Francesco Braghin, Anders Ekberg, Björn Pålsson, Dimitri Sala, Dirk Nicklisch, Elena Kabo, Paul Allen, Philip Shackleton, Tore Vernersson, and Michel Pineau. Development of the future rail freight system to reduce the occurrences and impact of derailment, 2013.

[61] J. N. Costa J. Pagaimo, H. Magalhães and J. Ambrósio. Derailment study of railway cargo vehicles using a response surface methodology. *Vehicle System Dynamics*, 60(1):309–334, 2022.

[62] Cylindrical helical springs made from round wire and bars: Calculation and design – part 1: Compression springs, 2013.

[63] Wagons-suspension gear-standardisation. International union of railways, 2007.

[64] Sebastián Solčanský. Lenoir friction damper and its applications. *Transportation Research Procedia*, 55:744–751, 2021. 14th International scientific conference on sustainable, modern and safe transport.

[65] Rui Calçada, Pedro A. Montenegro, and Marco Antonio Peixer. Avaliação e simulação numérica do descarrilamento do comboio de mercadorias na linha do norte a 01-04-2017, 2020.

[66] Railway applications-gauges-part 2: Rolling stock gauge, 2016.

[67] Railway applications — testing and simulation for the acceptance of running characteristics of railway vehicles — running behaviour and stationary tests, 2016.

[68] Filipe Marques, Paulo Flores, J. C. Pimenta Claro, and Hamid M. Lankarani. A survey and comparison of several friction force models for dynamic analysis of multibody mechanical systems. *Nonlinear Dynamics*, 86:1407–1443, 11 2016.

Appendix A

Simpack model of the vehicle

Table A.1: Y25 front bogie: spring properties of the Primary Suspension.

Bodies		Undef. height [m]	Stiffness [N/mm]			Coordinates [m]					
From	To		k_x	k_y	k_z	X_f	Y_f	Z_f	X_t	Y_t	Z_t
BF	AB FRF	0.260	469	469	498	-0.945	1.1	-0.571	-0.945	1.1	-0.326
BF	AB FRF	0.234	555	555	778.5	-0.945	1.1	-0.56	-0.945	1.1	-0.326
BF	AB FRB	0.260	469	469	498	-1.575	1.1	-0.571	-1.575	1.1	-0.326
BF	AB FRB	0.234	555	555	778.5	-1.575	1.1	-0.56	-1.575	1.1	-0.326
BF	AB FLF	0.260	469	469	498	-0.945	-1.1	-0.571	-0.945	-1.1	-0.326
BF	AB FLF	0.234	555	555	778.5	-0.945	-1.1	-0.56	-0.945	-1.1	-0.326
BF	AB FLB	0.260	469	469	498	-1.575	-1.1	-0.571	-1.575	-1.1	-0.326
BF	AB FLB	0.234	555	555	778.5	-1.575	-1.1	-0.56	-1.575	-1.1	-0.326
BF	AB BRF	0.260	469	469	498	-2.745	1.1	-0.571	-2.745	1.1	-0.326
BF	AB BRF	0.234	555	555	778.5	-2.745	1.1	-0.56	-2.745	1.1	-0.326
BF	AB BRB	0.260	469	469	498	-3.375	1.1	-0.571	-3.375	1.1	-0.326
BF	AB BRB	0.234	555	555	778.5	-3.375	1.1	-0.56	-3.375	1.1	-0.326
BF	AB BLF	0.260	469	469	498	-2.745	-1.1	-0.571	-2.745	-1.1	-0.326
BF	AB BLF	0.234	555	555	778.5	-2.745	-1.1	-0.56	-2.745	-1.1	-0.326
BF	AB BLB	0.260	469	469	498	-3.375	-1.1	-0.571	-3.375	-1.1	-0.326
BF	AB BLB	0.234	555	555	778.5	-3.375	-1.1	-0.56	-3.375	-1.1	-0.326

Table A.2: Y25 front bogie: longitudinal and lateral Bumpstops.

Bodies		Preload [kN]	Clearance [mm]	Coordinates [m]					
From	To			X	Y	Z	X	Y	Z
BF	AB FRF	9.6	-	-1.06	1.1	-0.46	-1.06	1.1	-0.46
BF	AB FRB	-	4	-1.46	1.1	-0.46	-1.46	1.1	-0.46
BF	AB FR	-	$\pm$ 10	-1.26	1.2	-0.46	-1.26	1.1	-0.46
BF	AB FLF	9.6	-	-1.06	-1.1	-0.46	-1.06	-1.1	-0.46
BF	AB FLB	-	4	-1.46	-1.1	-0.46	-1.46	-1.1	-0.46
BF	AB FL	-	$\pm$ 10	-1.26	-1.2	-0.46	-1.06	-1.1	-0.46
BF	AB BRB	9.6	-	-3.26	1.1	-0.46	-3.26	1.1	-0.46
BF	AB BRF	-	4	-2.86	1.1	-0.46	-2.86	1.1	-0.46
BF	AB BR	-	$\pm$ 10	-3.06	1.1	-0.46	-3.06	1.1	-0.46
BF	AB BLB	9.6	-	-3.26	-1.1	-0.46	-3.26	-1.1	-0.46
BF	AB BLF	-	4	-2.86	-1.1	-0.46	-2.86	-1.1	-0.46
BF	AB BL	-	$\pm$ 10	-3.06	-1.1	-0.46	-3.06	-1.1	-0.46

Table A.3: Sggrss: Bumpstops and spring properties of Side Bearer.

Bodies		Preload [kN]	Stiffness [N/mm]	Clearance [mm]		Coordinates [m]					
From	To			x-axis	z-axis	X_f	Y_f	Z_f	X_t	Y_t	Z_t
Body Frame	BF	16	570	$\pm$1	40	-2.16	0.816	-0.89	-2.16	-0.816	-0.7
Body Frame	BF	16	570	$\pm$1	40	-2.16	-0.816	-0.89	-2.16	-0.816	-0.7

Table A.4: Central Plate: elastic coupling properties.

Bodies		Stiffness [N/mm]			Coordinates [m]					
From	To	k_x	k_y	k_z	X_f	Y_f	Z_f	X_t	Y_t	Z_t
Body Frame	CP	60000	60000	-	-2.16	0	-0.739	-2.16	0	-0.739
Body Frame	CP	-	-	60000	-2.16	0	-0.78	-2.16	0	-0.689

Table A.5: Sgrrss: friction elements of the friction damper and the articulation between body frames.

Bodies		Coordinates [m]					
From	To	X	Y	Z	X	Y	Z
Bogie Frame	AB FRF	-1.06	1.1	-0.46	-1.06	1.1	-0.46
Bogie Frame	AB FRB	-1.46	1.1	-0.46	-1.46	1.1	-0.46
Bogie Frame	AB FLF	-1.06	-1.1	-0.46	-1.06	-1.1	-0.46
Bogie Frame	AB FLB	-1.46	-1.1	-0.46	-1.46	-1.1	-0.46
Bogie Frame	AB BRF	-2.86	1.1	-0.46	-2.86	1.1	-0.46
Bogie Frame	AB BRB	-3.26	1.1	-0.46	-3.26	1.1	-0.46
Bogie Frame	AB BLF	-2.86	-1.1	-0.46	-2.86	-1.1	-0.46
Body Frame	AB BLB	-3.26	-1.1	-0.46	-3.26	-1.1	-0.46
Body Frame F	Body Frame B	-12.58	0	-0.975	-12.58	0	-0.97

Appendix B

Track Properties - Derailment in Coimbra

B.1 Horizontal properties

Horizontal					
Type	Par 1	Par 2	Par3	Lsmo/2	Comment
STR	721	-	-	1.5	1400-679_km221
CLO	140	0	556	1.5	679-539_km221
CIR	140	556	-	1.5	539-339_km221
CLO	140	556	0	1.5	399-259_km221
STR	130	-	-	1.5	259-129_km221
CLO	149	0	-603	1.5	1129-980_km220
CIR	250	-603	-	1.5	980-730_km220

B.2 Superelevation properties

Superelevation					
Type	Par 1	Par 2	Par3	Lsmo/2	Comment
CST	721	0	-	1.5	1400-679_km221
LIR	140	0	0.155	1.5	679-539_km221
CST	140	0.155	-	1.5	539-339_km221
LIR	140	0.155	0	1.5	399-259_km221
CST	130	0	-	1.5	259-129_km221
LIR	149	0	0.14	1.5	1129-980_km220
CST	250	0.14	-	1.5	980-730_km220

B.3 Vertical properties

Vertical					
Type	Par 1	Par 2	Par3	Lsmo/2	Comment
CLS	189.29	0.002265	-	1.5	400-210.71_km222
CLS	202.89	0.0002296	-	1.5	210.71-7.82_km222
CLS	234.12	-0.001068	-	1.5	773.7-336.26_km221
CLS	437.44	0	-	1.5	773-336.26_km221
CLS	197.97	0.00101	-	1.5	336.26-138.29_km221
CLS	224.39	-0.001248	-	1.5	1138.29-913.9_km220
CLS	183.9	0	-	1.5	913.9-730_km220

Appendix C

Track Excitations - Derailment in Coimbra

C.1 Accident Scenario

Longitudinal leveling was scaled by factor 1.425 only in the critical area of the accident in order to obtain a maximum deflection of approximately 29 mm.

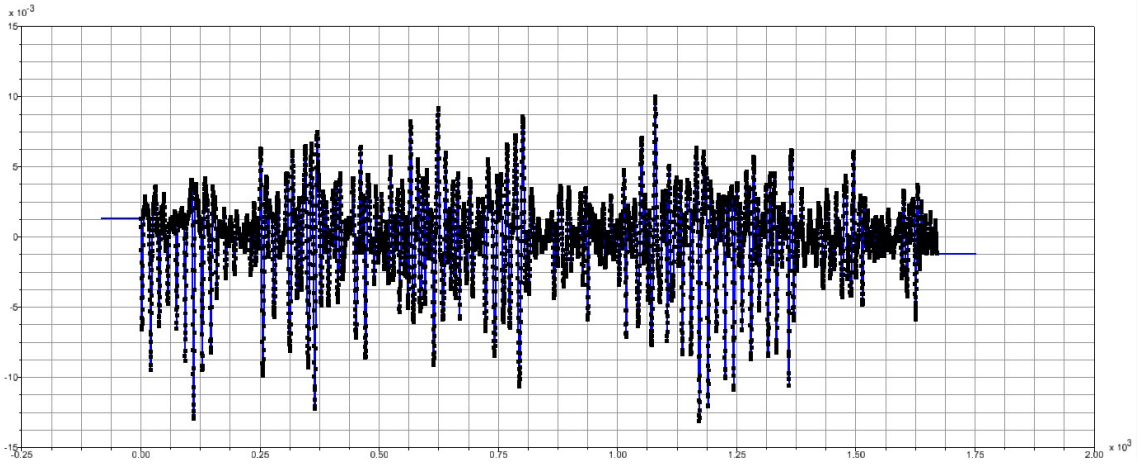

Figure C.1: Accident Scenario: Excitation Vertical Left.

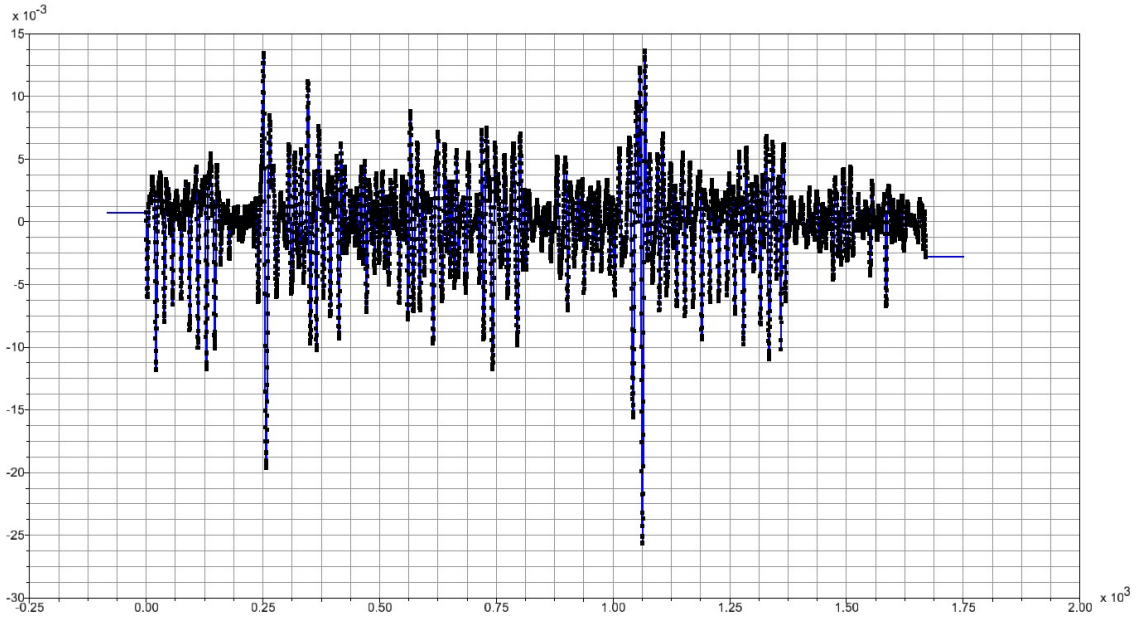

Figure C.2: Accident Scenario: Excitation Vertical Right.

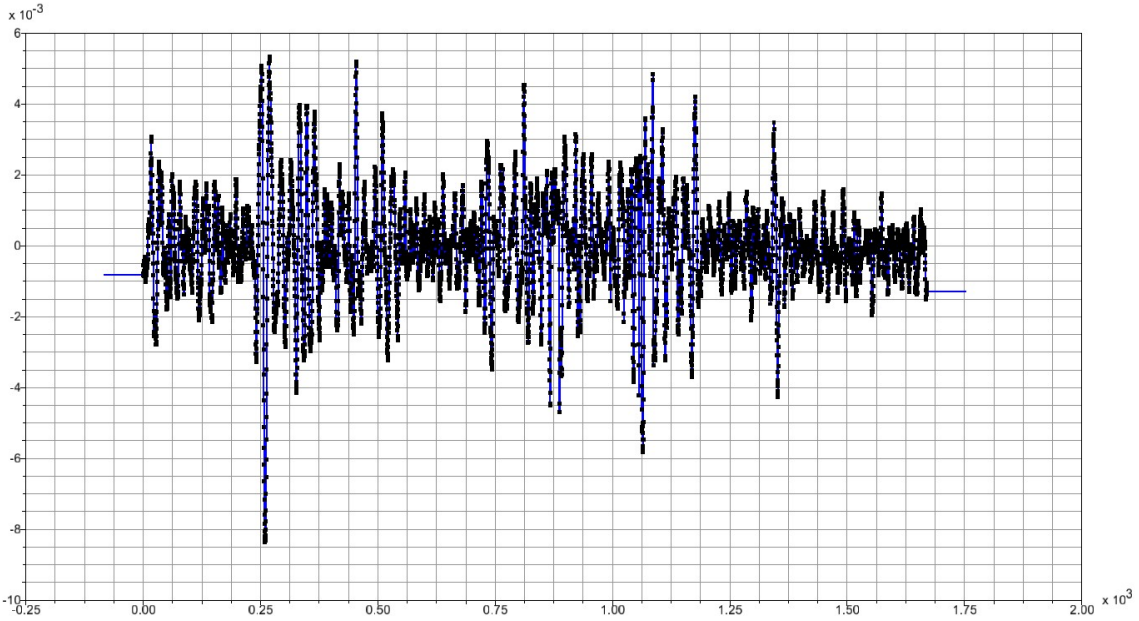

Figure C.3: Accident Scenario: Excitation Lateral Left.

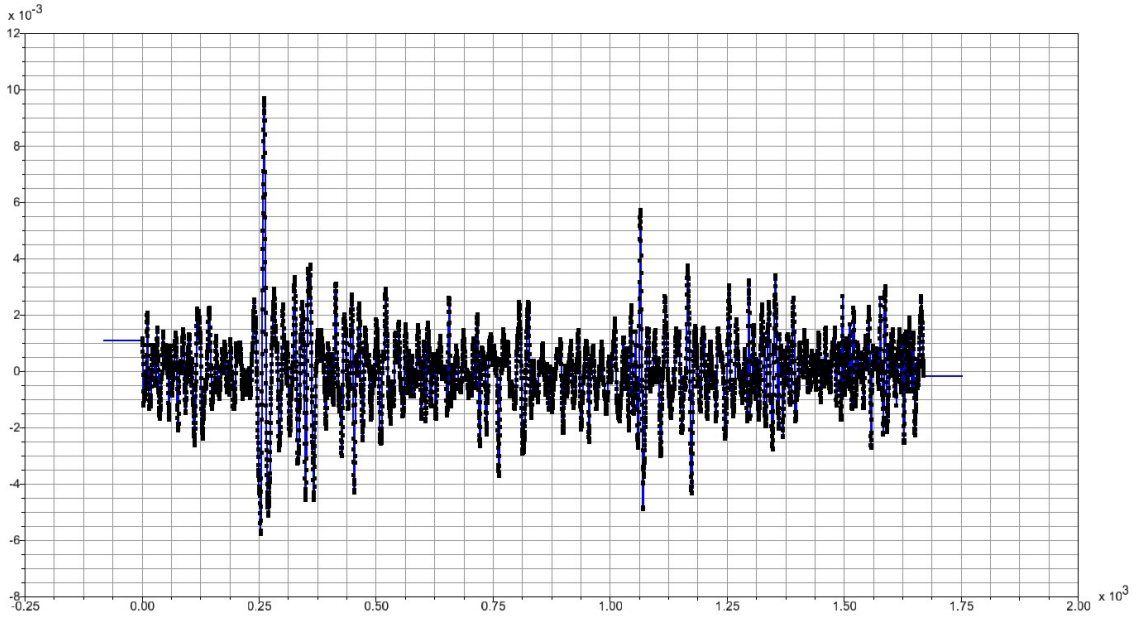

Figure C.4: Accident Scenario: Excitation Lateral Right.

C.2 Scenario 2016-12-16

Measured longitudinal levelness and maximum calculated deflection of approximately 21 mm.

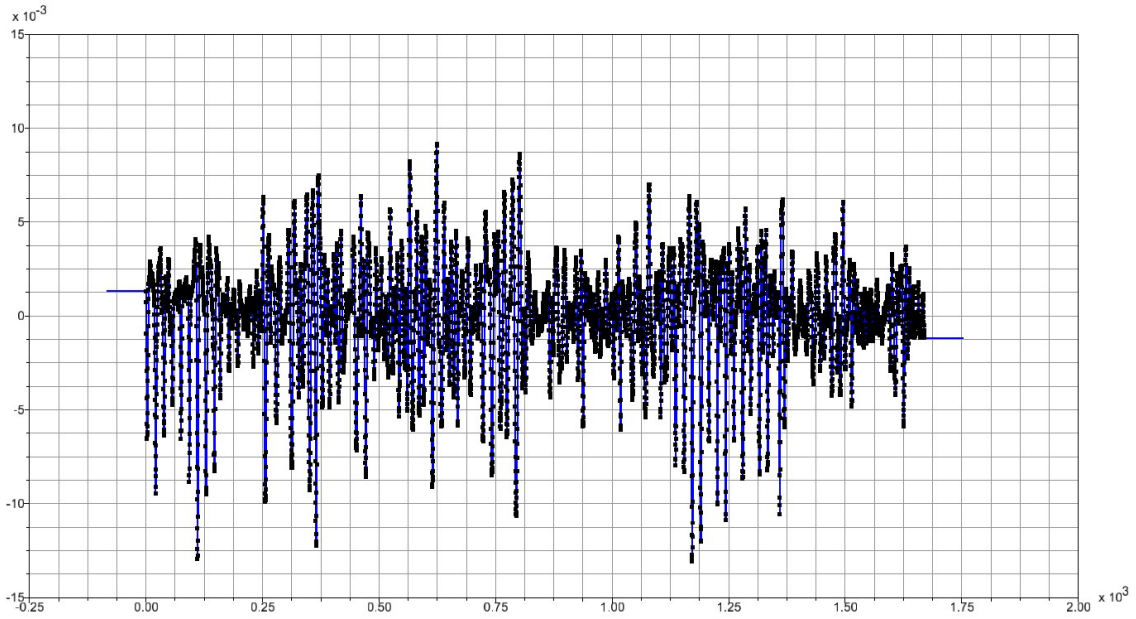

Figure C.5: Scenario 2016-12-16: Excitation Vertical Left.

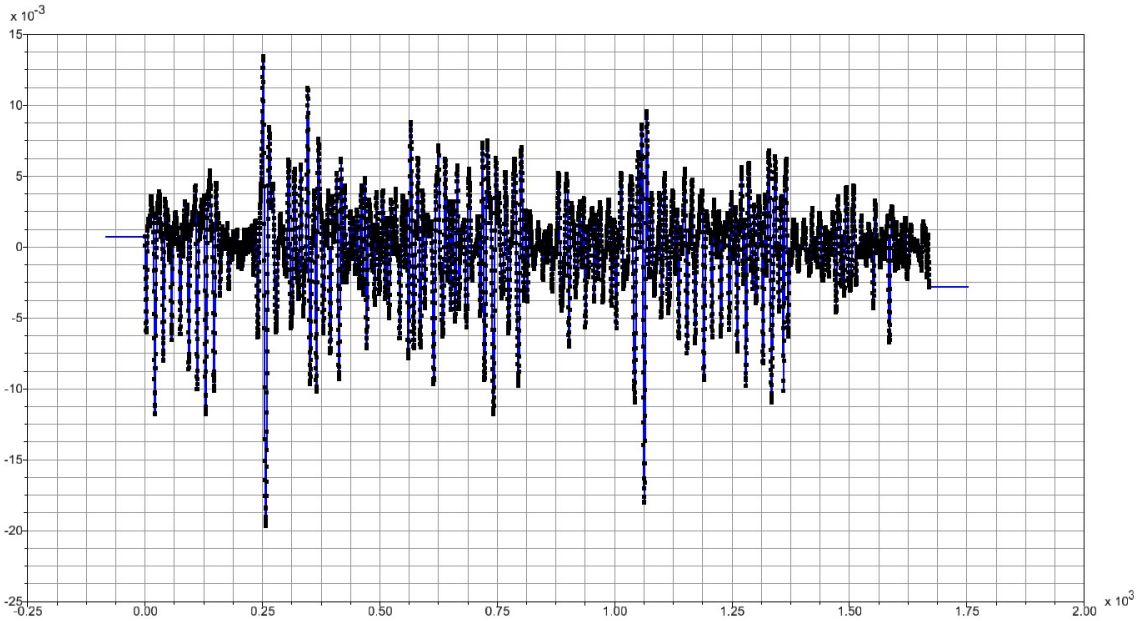

Figure C.6: Scenario 2016-12-16: Excitation Vertical Right.

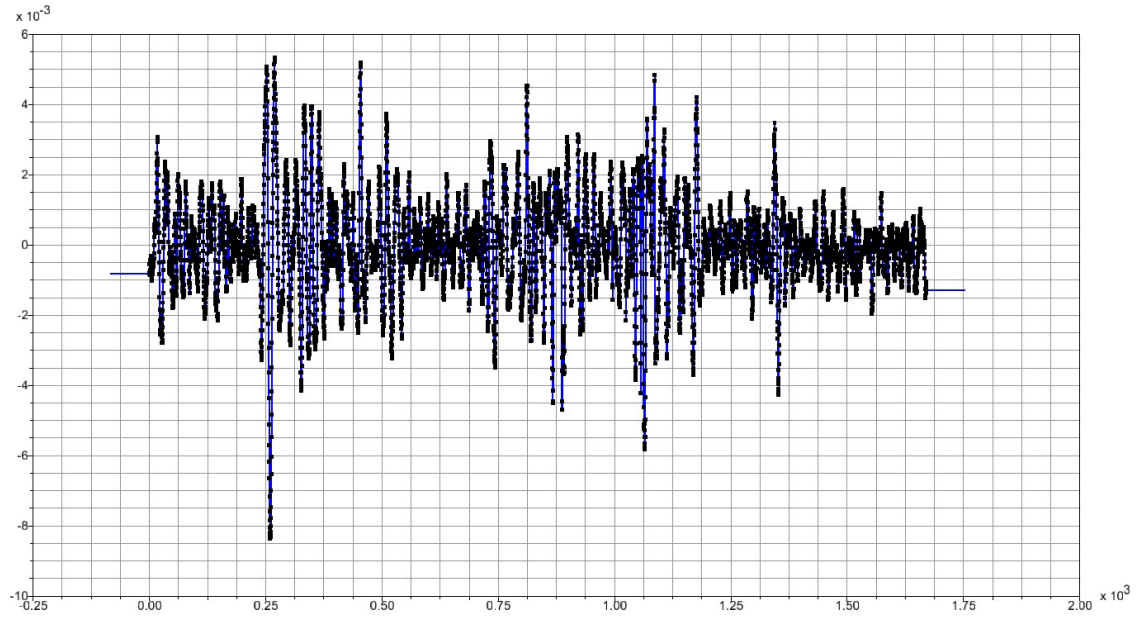

Figure C.7: Scenario 2016-12-16: Excitation Lateral Left.

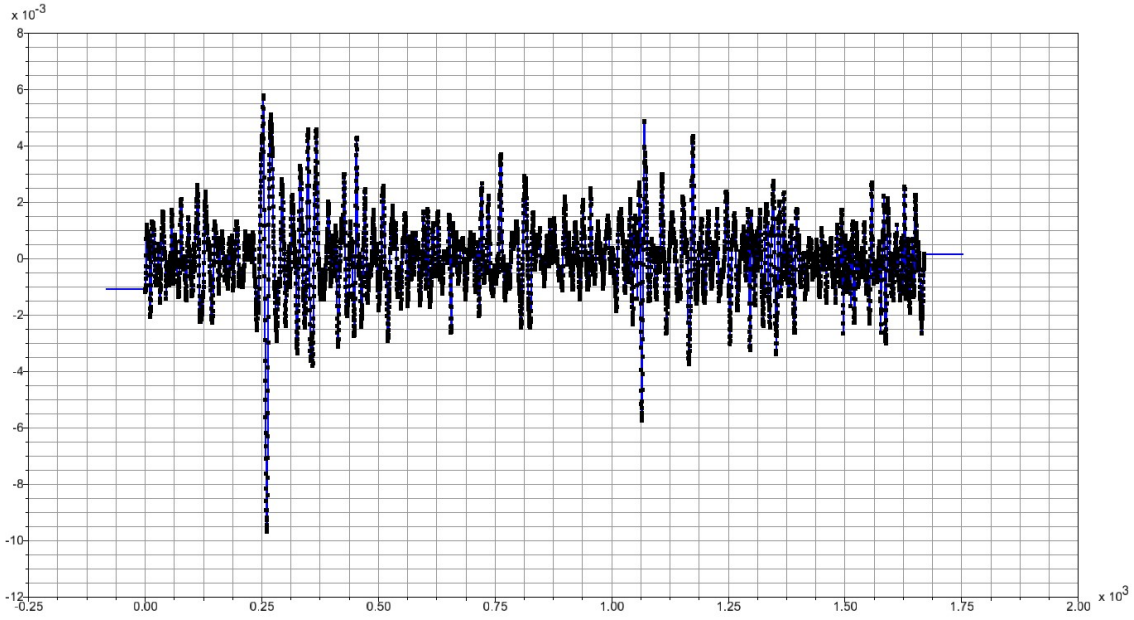

Figure C.8: Scenario 2016-12-16: Excitation Lateral Right.

C.3 Limit Intervention Scenario

Longitudinal leveling was scaled by a factor of 0.645 along the whole track in order to obtain a maximum of approximately 15 mm.

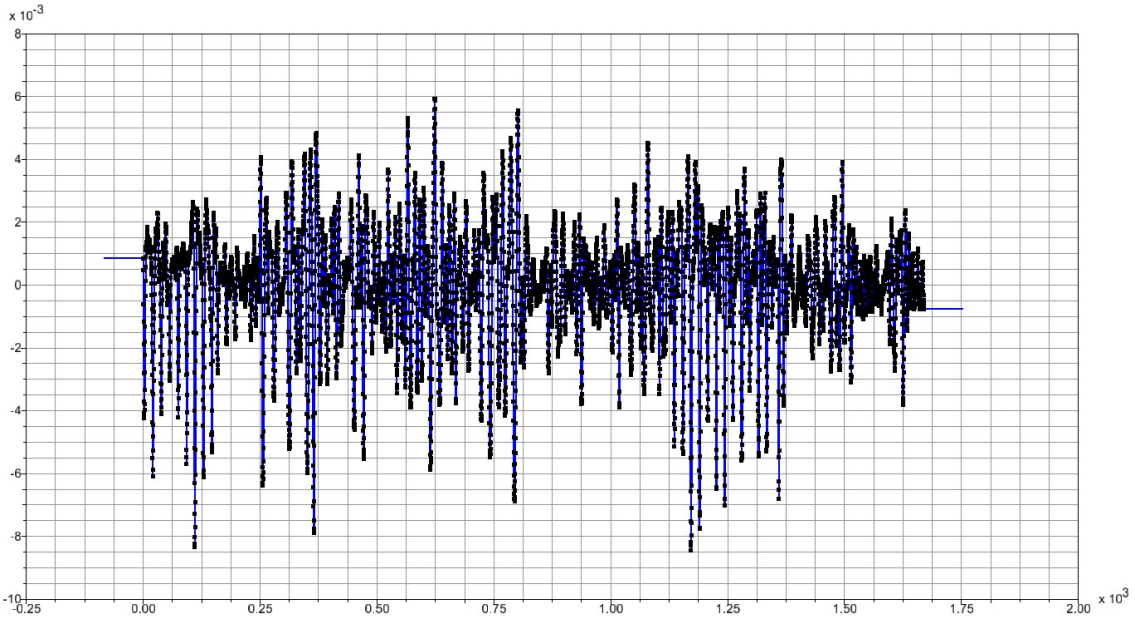

Figure C.9: Limit Intervention Scenario: Excitation Vertical Left.

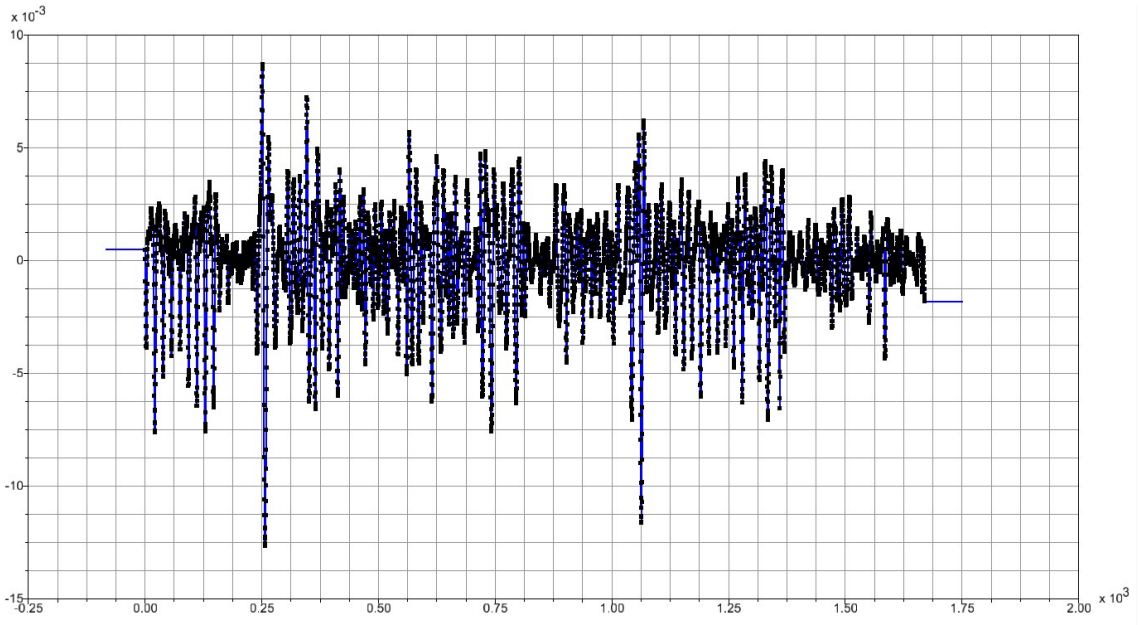

Figure C.10: Limit Intervention Scenario: Excitation Vertical Right.

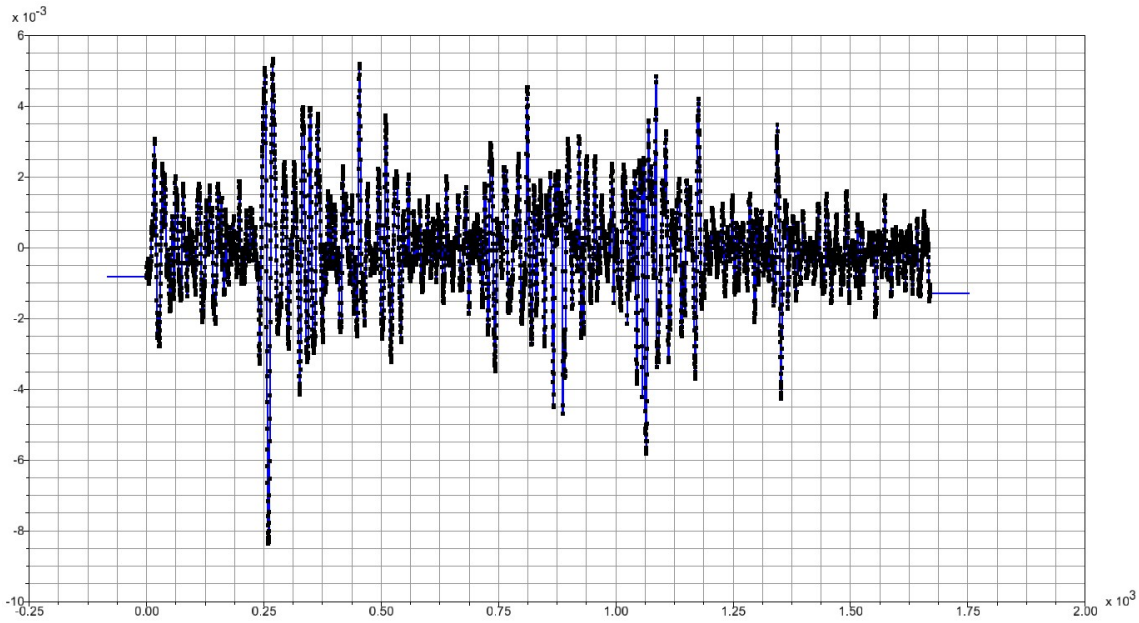

Figure C.11: Limit Intervention Scenario: Excitation Lateral Left.

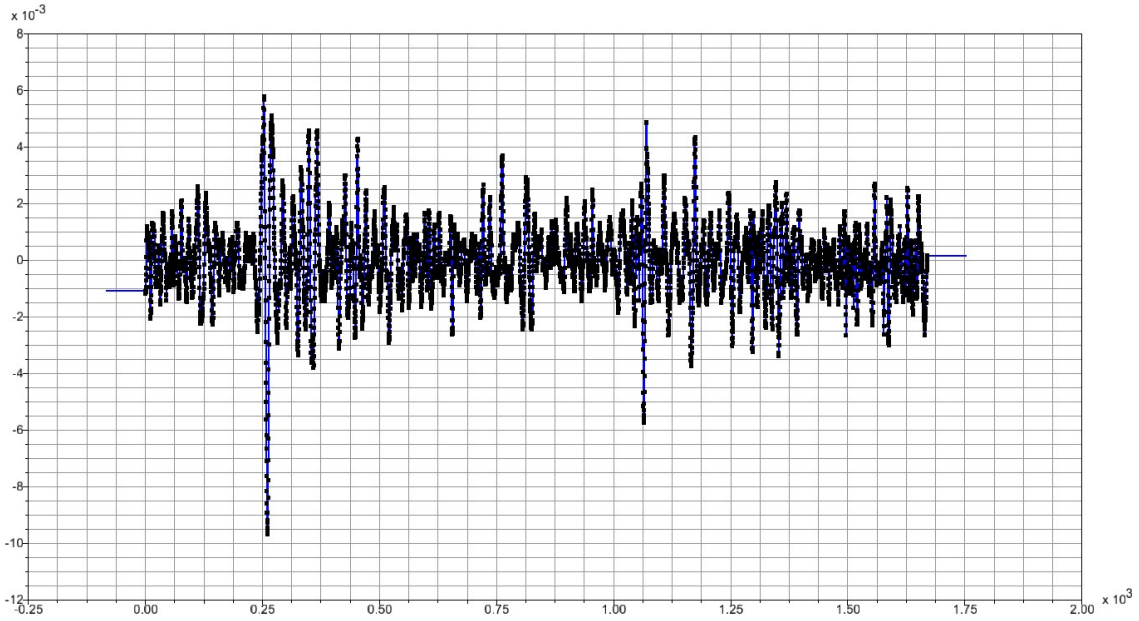

Figure C.12: Limit Intervention Scenario: Excitation Lateral Right.

C.4 Limit Alert Scenario

Longitudinal leveling scaled by a factor 0.42 along the entire track in order to obtain maximum deflection in the accident area of approximately 12 mm.

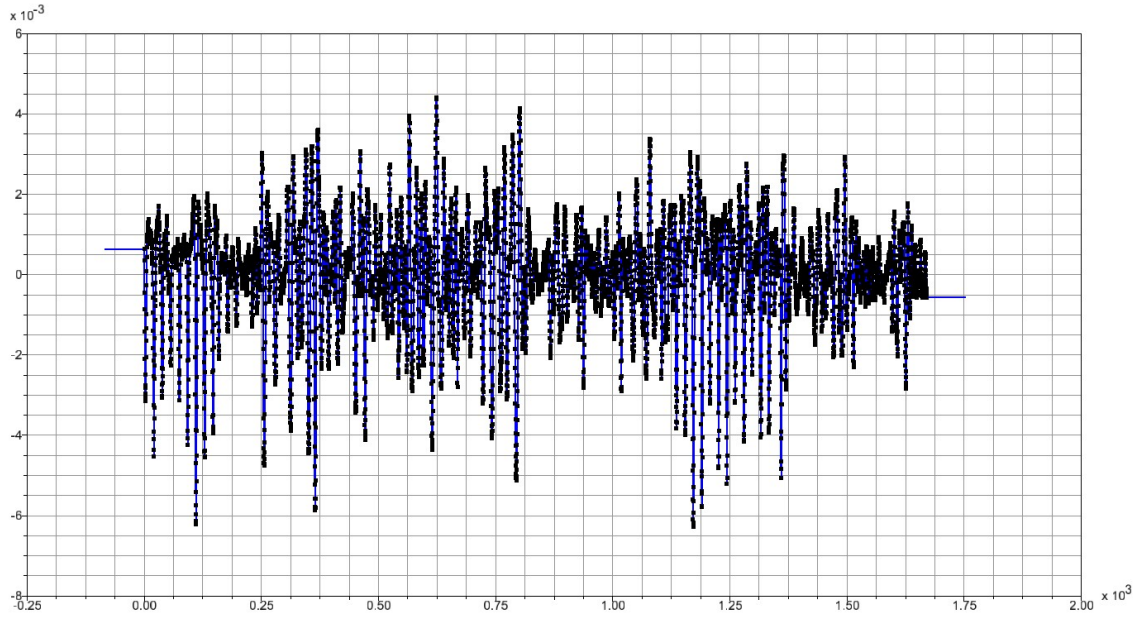

Figure C.13: Limit Alert Scenario: Excitation Vertical Left.

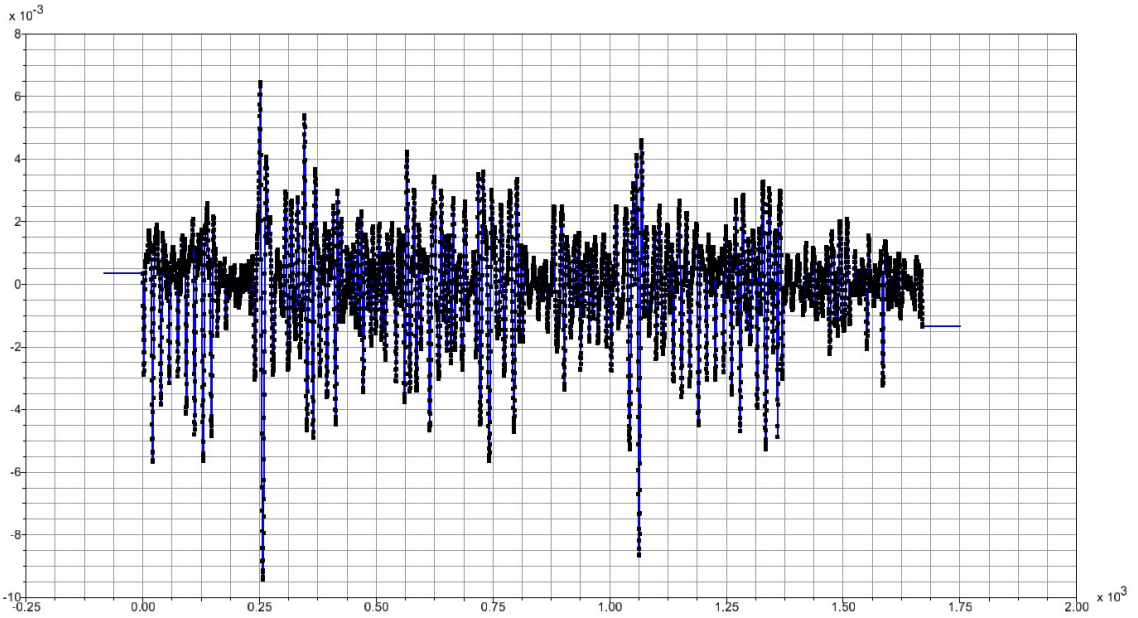

Figure C.14: Limit Alert Scenario: Excitation Vertical Right.

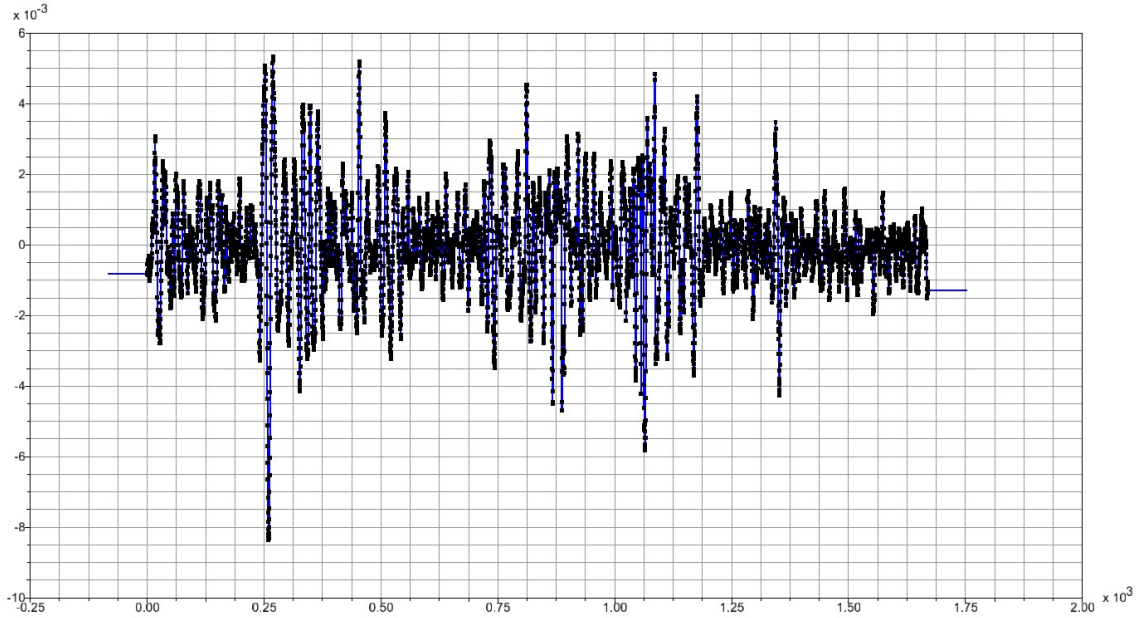

Figure C.15: Limit Alert Scenario: Excitation Lateral Left.

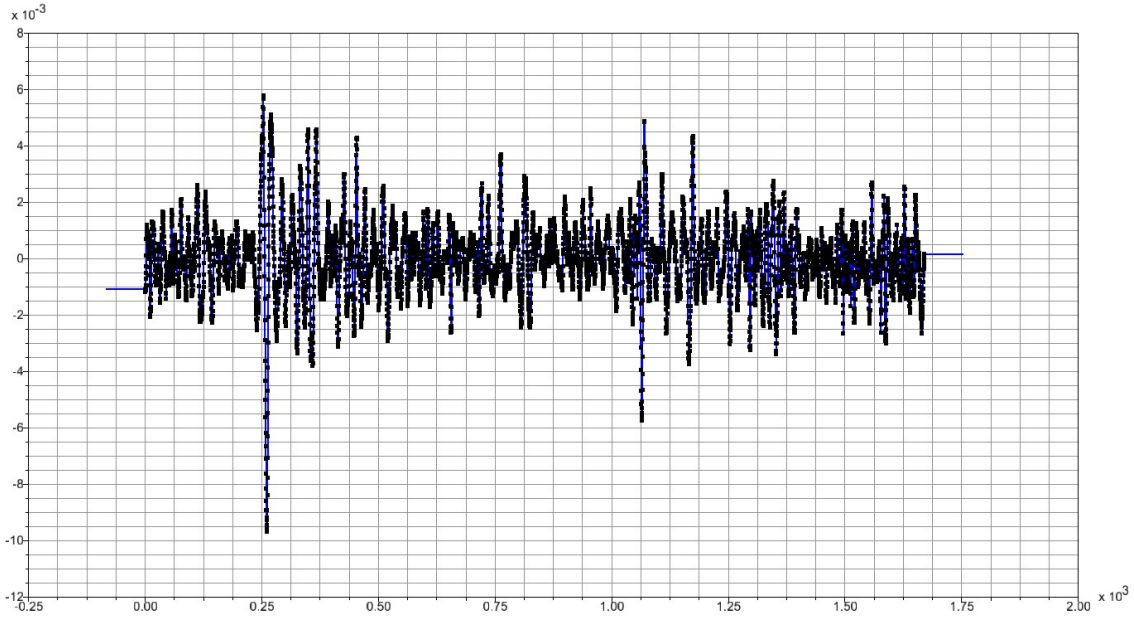

Figure C.16: Limit Alert Scenario: Excitation Lateral Right.

Appendix D

Scenario Derailment EN 14363

D.1 Horizontal properties

Horizontal				
Type	Par 1	Par 2	Par3	Lsmo/2
STR	30	-	-	1.5
CLO	30	0	150	1.5
CIR	57	150	-	1.5
CLO	30	150	0	1.5
STR	75	-	-	1.5

D.2 Superelevation properties

Superelevation				
Type	Par 1	Par 2	Par3	Lsmo/2
CST	30	0	-	1.5
LIR	30	0	0.09	1.5
CST	30	0.09	-	1.5
LIR	27	0.09	0	1.5
CST	105	0	-	1.5

D.3 Vertical properties

Vertical				
Type	Par 1	Par 2	Par3	Lsmo/2
CLS	100	-	-	1.5

D.4 Track layout

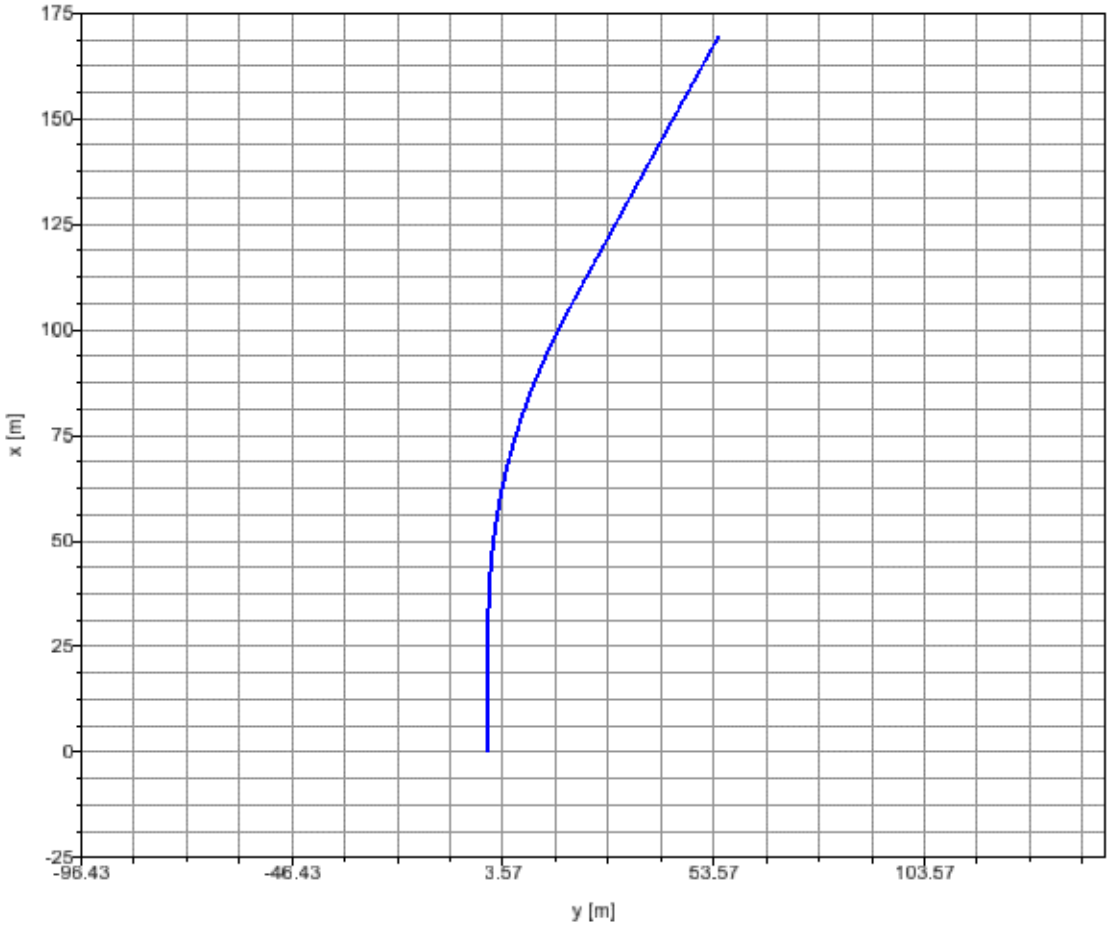

Figure D.1: Top view of track layout standard EN 14363.

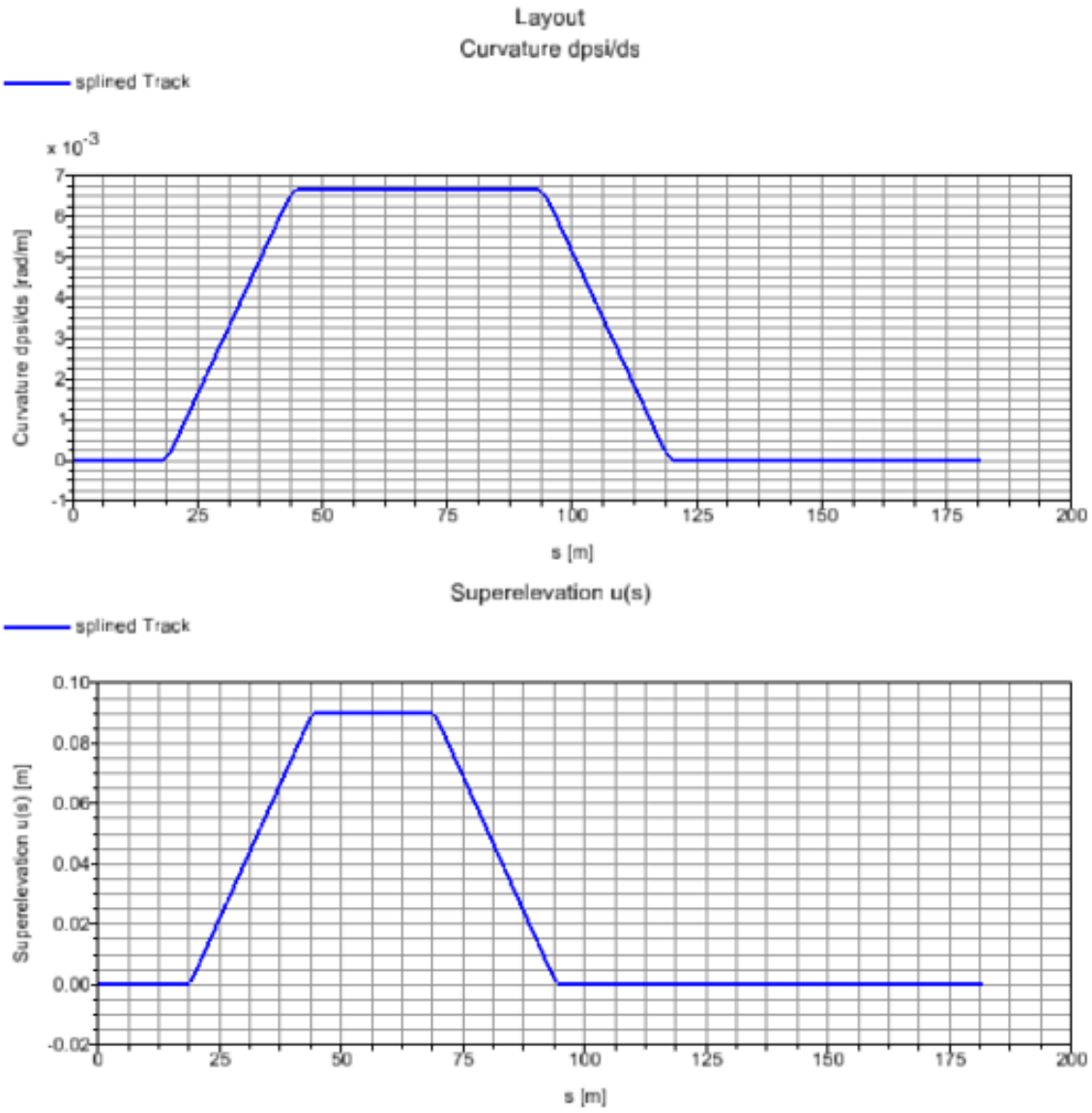

Figure D.2: Track layout of EN 14363 line: $z(s)$, Curvature $dpsi/ds$, Superelevation $u(s)$.

Appendix E

Causes of Freight Train Derailments in the United States

E.1 Top Causes of Freight Train Derailments in the United States between 2001 and 2010 [28]

Track Type	Accident Type				
	Derailment	Collision	Highway-Rail	Other	All Accident Types
Number of Freight Train Accidents					
Main	4439	302	1343	590	6674
Yard	2848	355	12	378	3593
Siding	436	23	4	40	503
Industry	369	21	6	49	445
All	8092	701	1365	1057	11215
Average Number of Cars Derailed per Accident					
Main	8.4	3.3	0.5	1.0	5.9
Yard	4.7	1.5	0.8	1.4	4.0
Siding	5.7	3.7	0.0	1.2	5.2
Industry	4.3	1.0	1.3	0.5	3.7
All	6.8	2.3	0.5	1.1	5.2
Total Number of Cars Derailed					
Main	37456	989	609	580	39634
Yard	13363	527	9	511	14410
Siding	2477	85	0	47	2609
Industry	1593	22	8	23	1646
All	54889	1623	626	1161	58299

Appendix F

Bumpstops displacements

F.1 Lateral Bumpstops

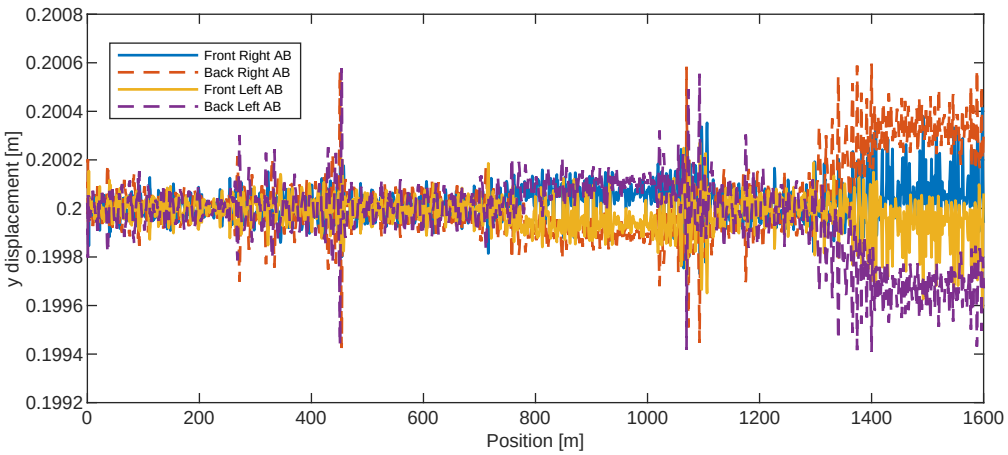

Figure F.1: Lateral Bumpstops: Front Bogie.

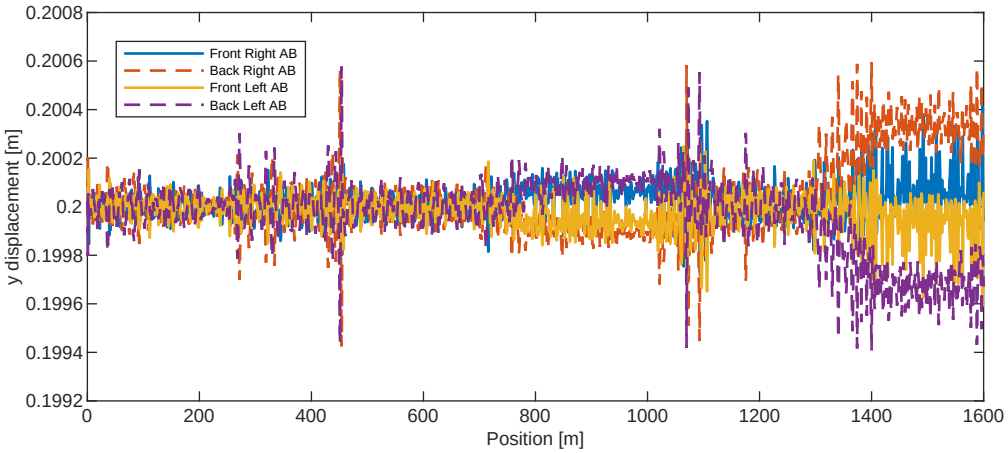

Figure F.2: Lateral Bumpstops: Back Bogie.

F.2 Longitudinal Bumpstops

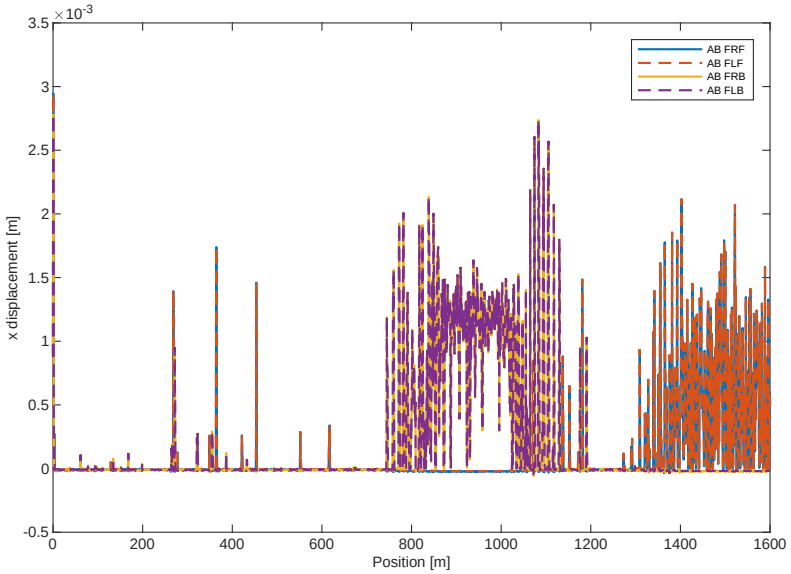

Figure F.3: Longitudinal Bumpstops: Center Bogie - Front Axleboxes.

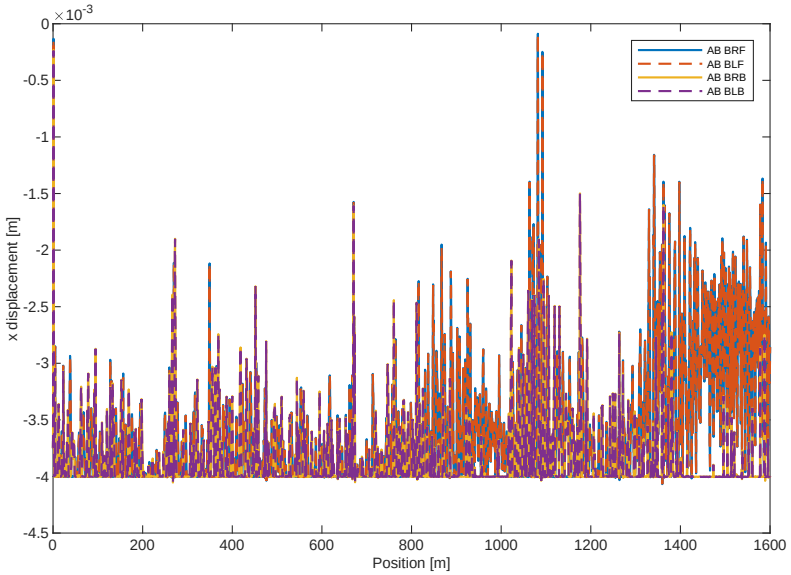

Figure F.4: Longitudinal Bumpstops: Center Bogie - Back Axleboxes.

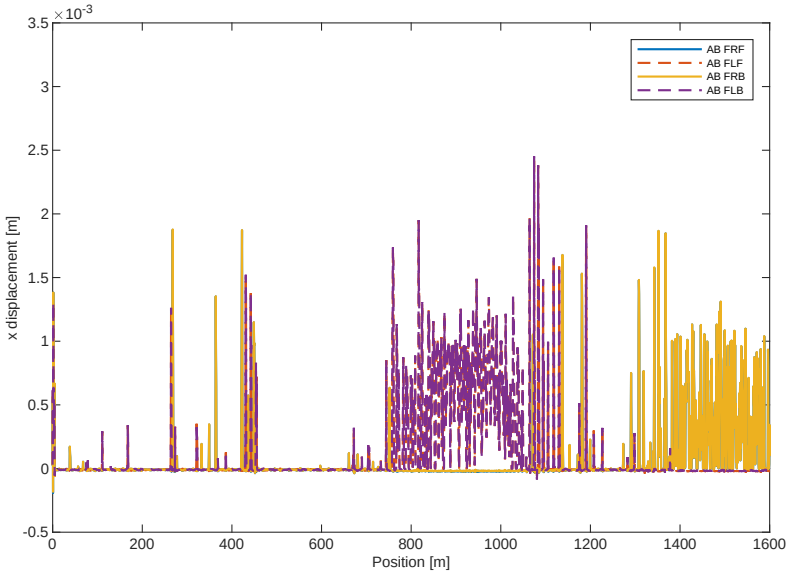

Figure F.5: Longitudinal Bumpstops: Back Bogie - Front Axleboxes.

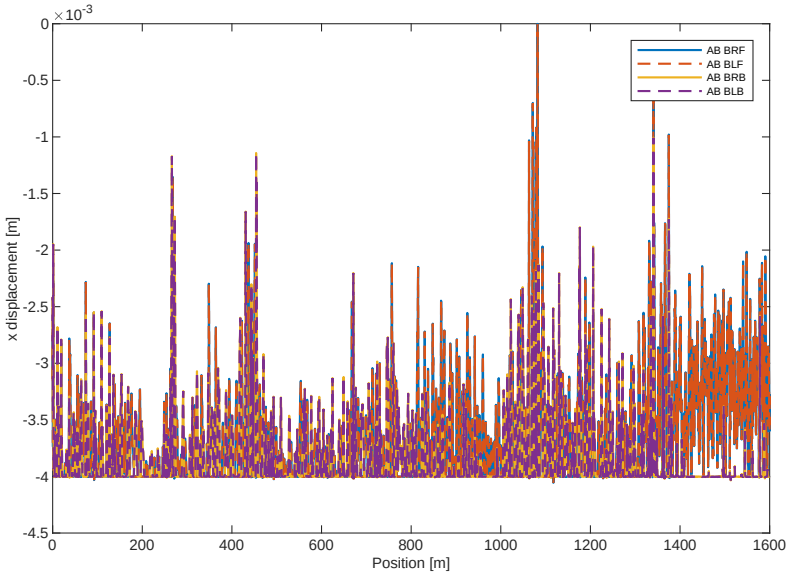

Figure F.6: Longitudinal Bumpstops: Back Bogie - Back Axleboxes.

Appendix G

Nadal Criteria

G.1 Front Bogie

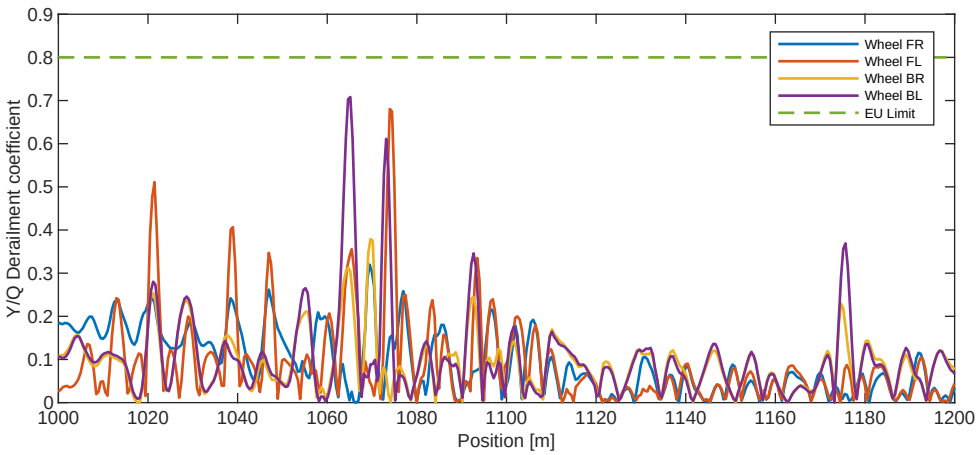

Figure G.1: Nadal criterion for the Sggrss wagon in the accident scenario.

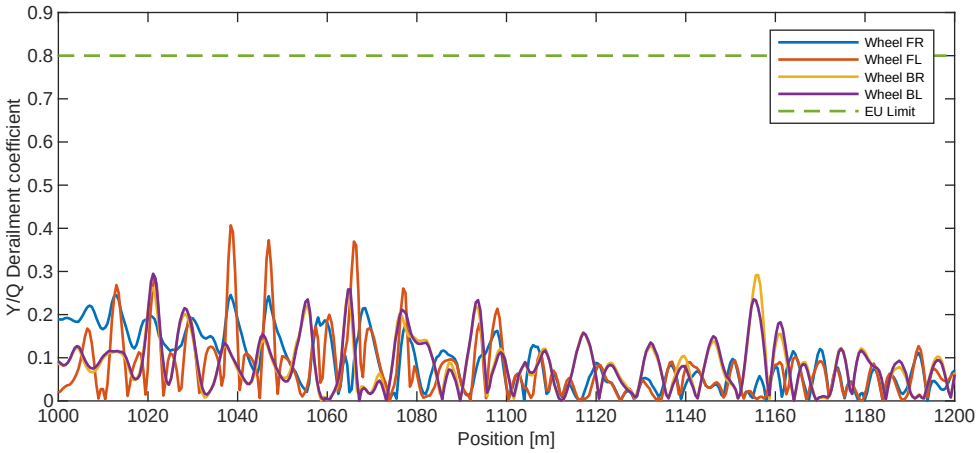

Figure G.2: Nadal criterion for the Sggrss wagon in the 2016-12-16 scenario.

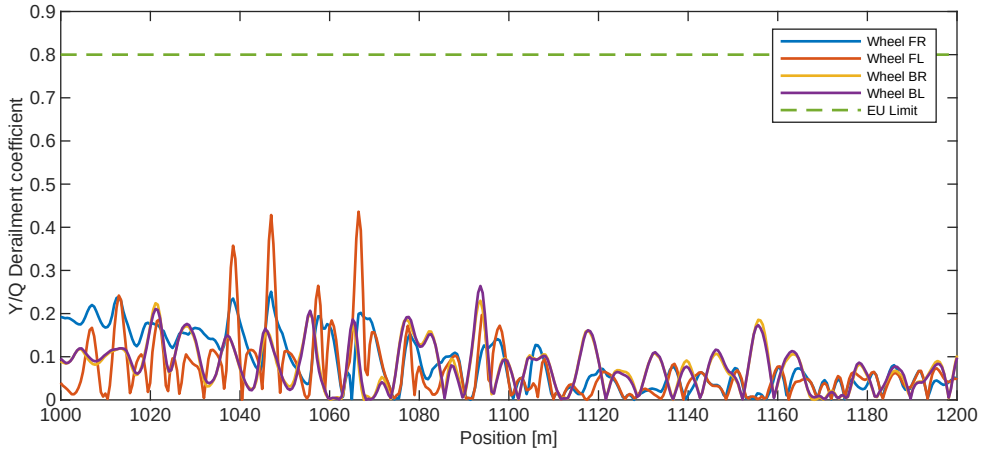

Figure G.3: Nadal criterion for the Sggrss wagon in the intervention limit scenario.

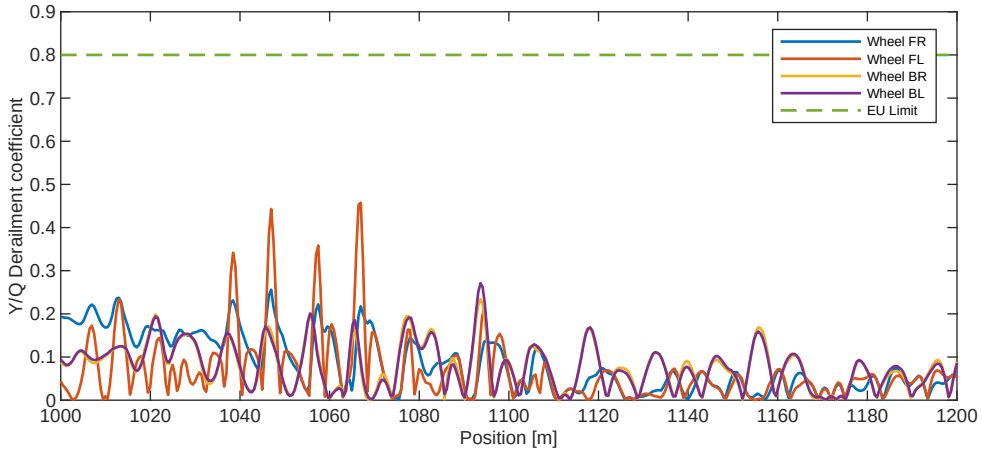

Figure G.4: Nadal criterion for the Sggrss wagon in the alert limit scenario.

G.2 Center Bogie

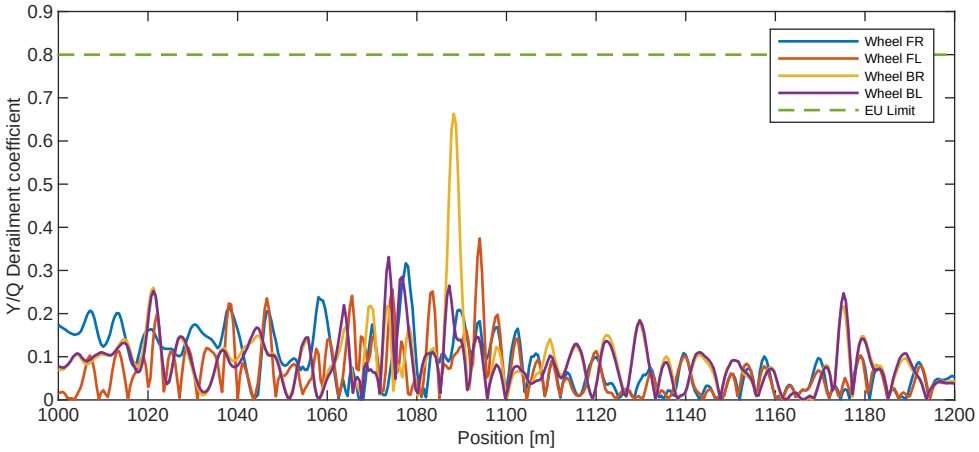

Figure G.5: Nadal criterion for the Sggrss wagon in the accident scenario.

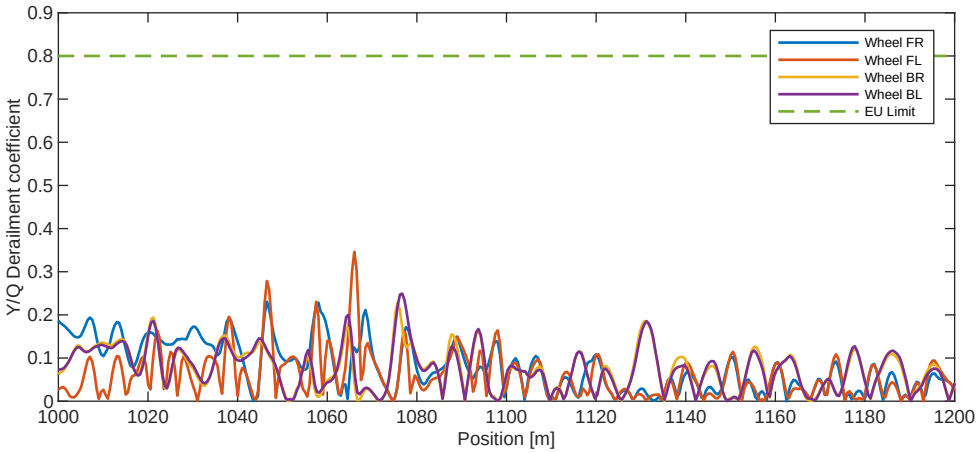

Figure G.6: Nadal criterion for the Sggrss wagon in the 2016-12-16 scenario.

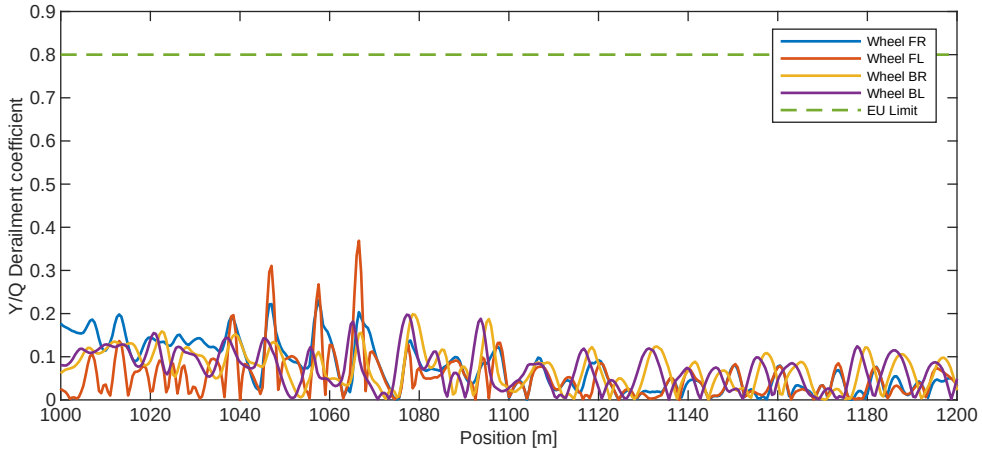

Figure G.7: Nadal criterion for the Sggrss wagon in the intervention limit scenario.

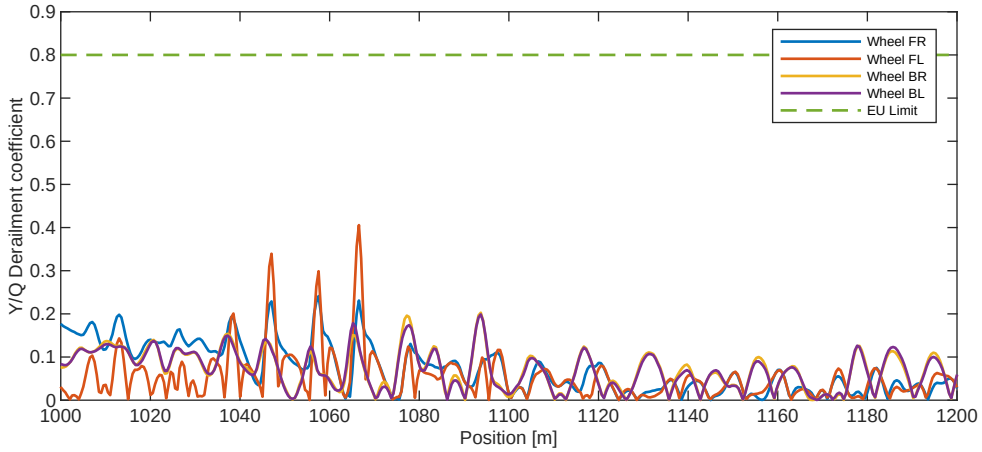

Figure G.8: Nadal criterion for the Sggrss wagon in the alert limit scenario.

G.3 Back Bogie

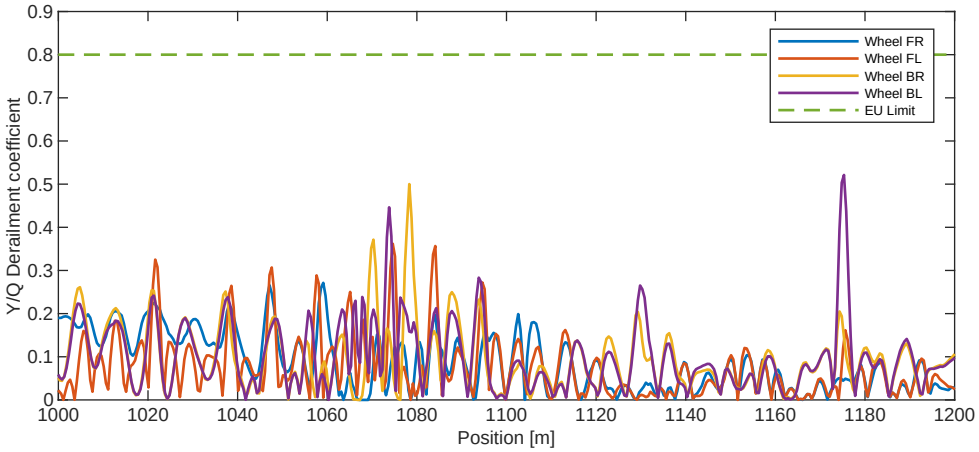

Figure G.9: Nadal criterion for the Sggrss wagon in the accident scenario.

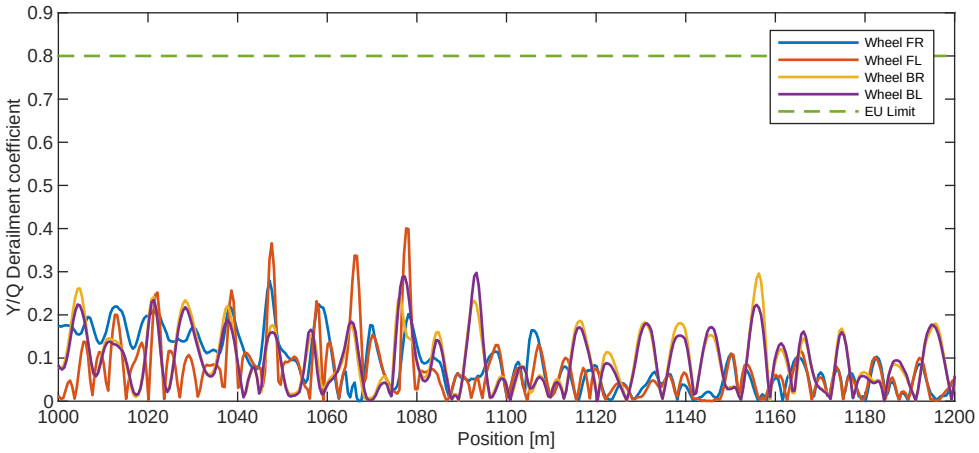

Figure G.10: Nadal criterion for the Sggrss wagon in the 2016-12-16 scenario.

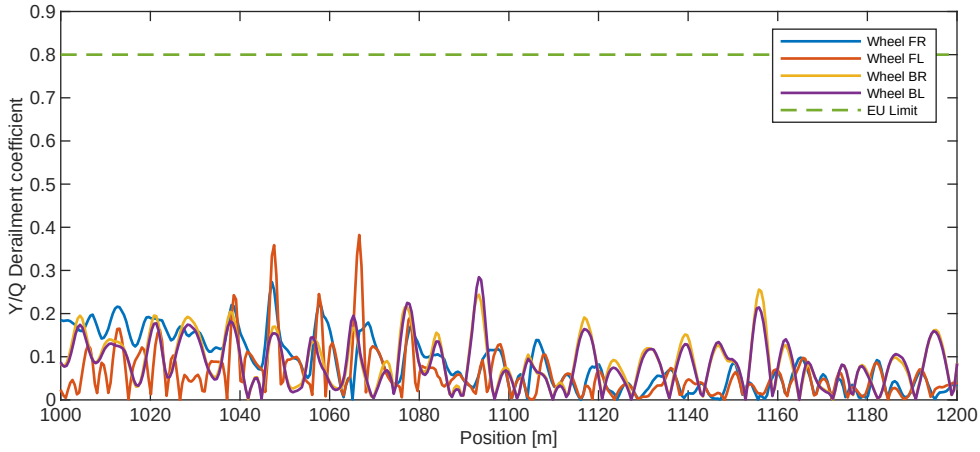

Figure G.11: Nadal criterion for the Sggrss wagon in the intervention limit scenario.

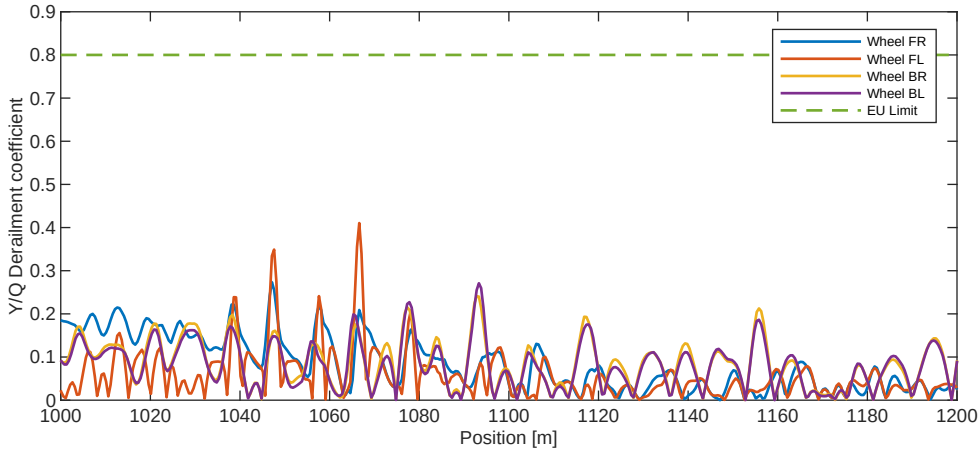

Figure G.12: Nadal criterion for the Sggrss wagon in the alert limit scenario.

Appendix H

Prud'homme Criteria

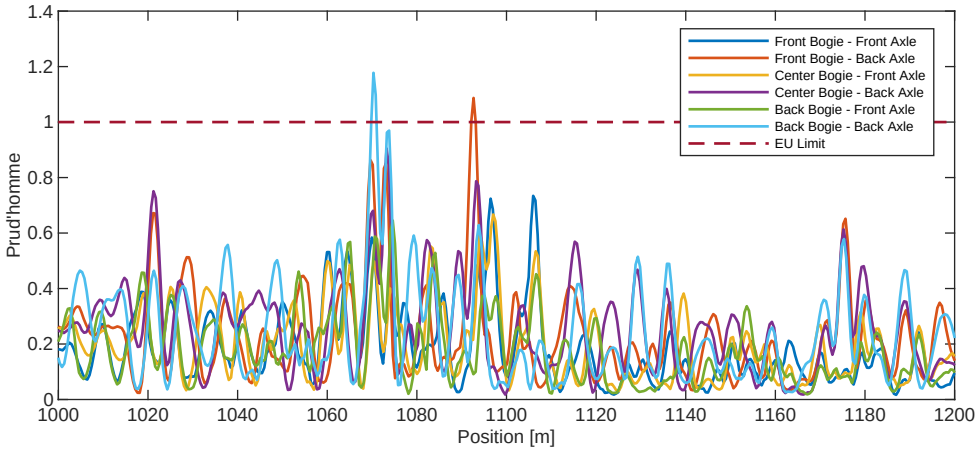

Figure H.1: Prud'homme criterion for the Sggrss wagon in the accident scenario.

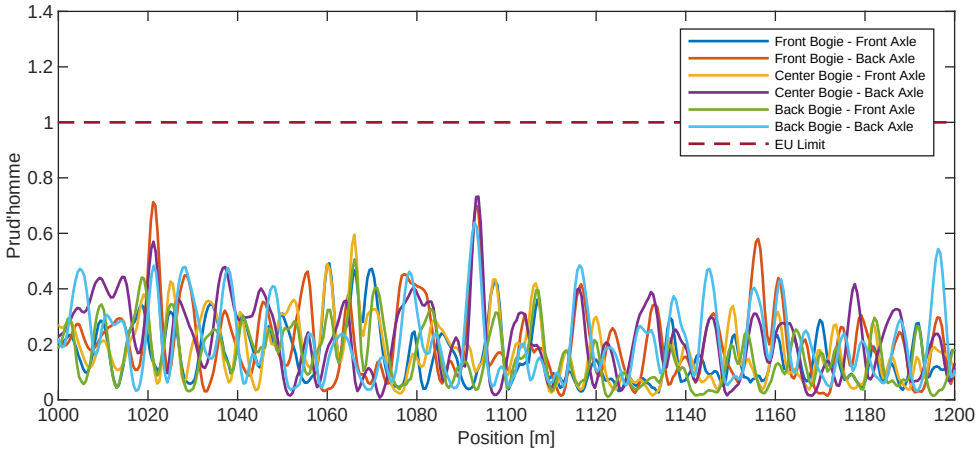

Figure H.2: Prud'homme criterion for the Sggrss wagon in the 2016-12-16 scenario.

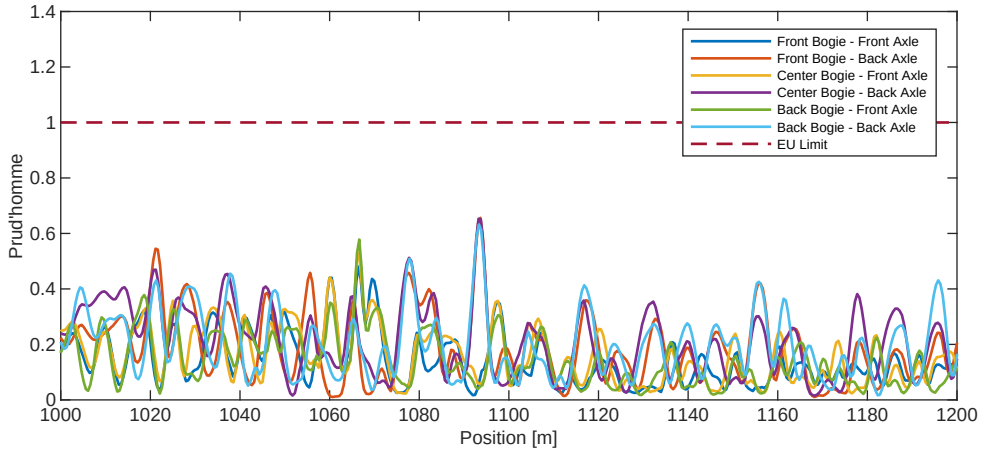

Figure H.3: Prud'homme criterion for the Sggrss wagon in the intervention limit scenario.

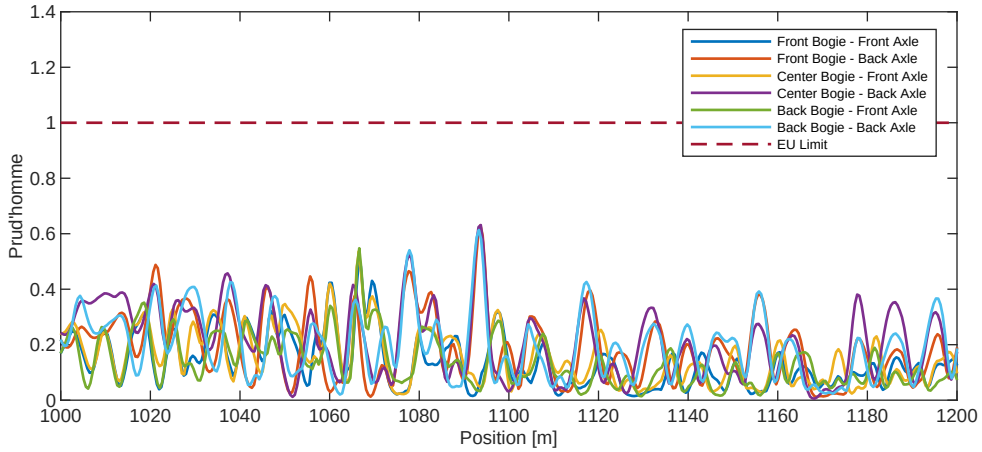

Figure H.4: Prud'homme criterion for the Sggrss wagon in the alert limit scenario.

Appendix I

Wheel Unloading Criteria

I.1 Front Bogie

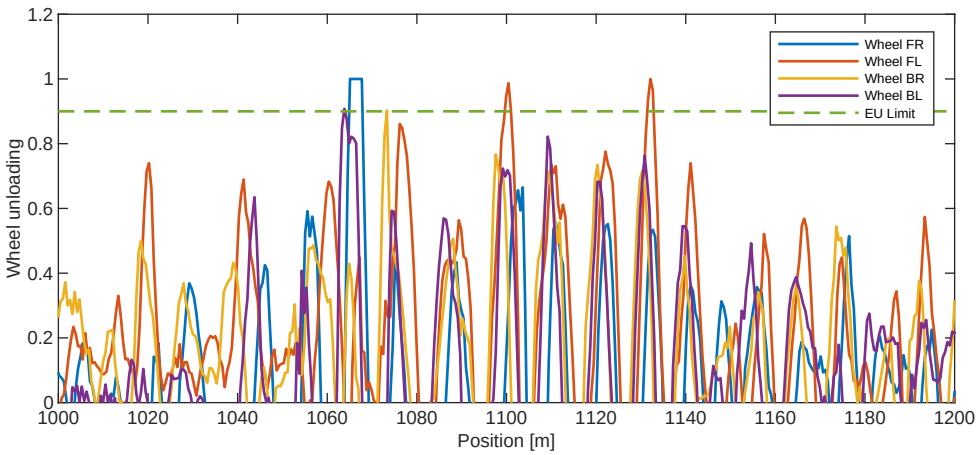

Figure I.1: Wheel Unloading criterion for the Sggrss wagon in the accident scenario.

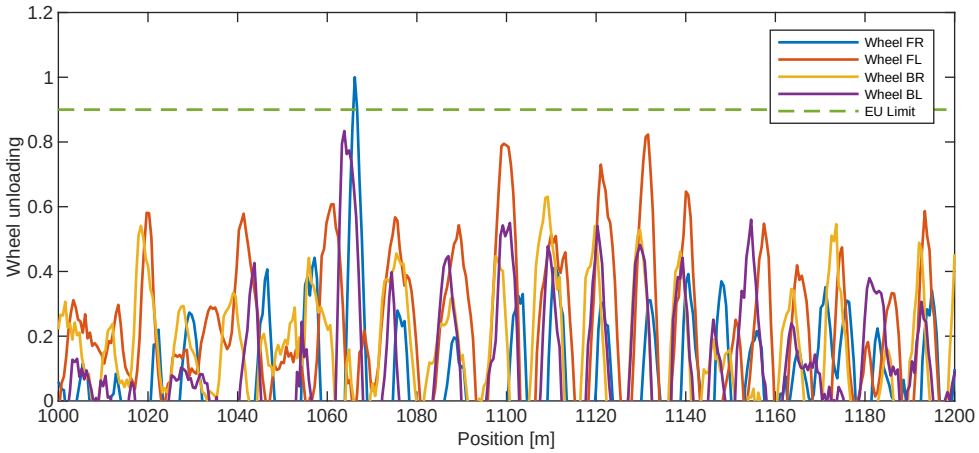

Figure I.2: Wheel Unloading criterion for the Sggrss wagon in the 2016-12-16 scenario.

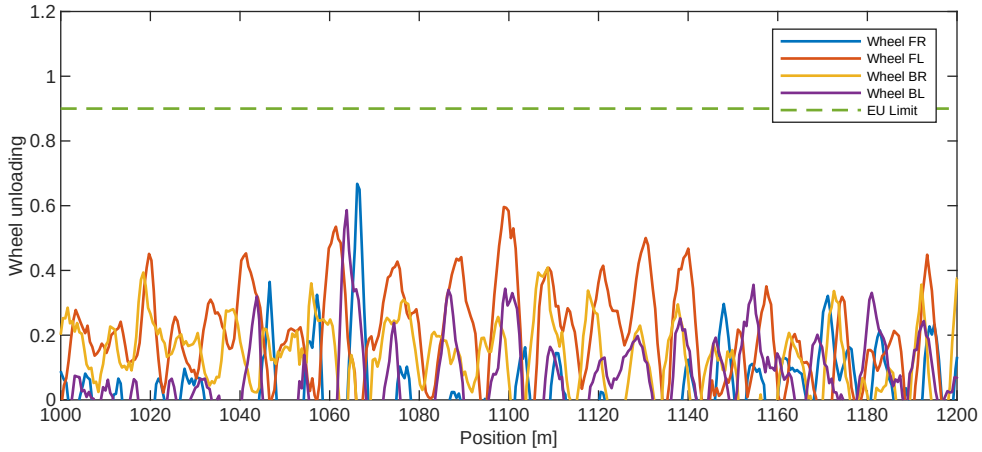

Figure I.3: Wheel Unloading criterion for the Sggrss wagon in the intervention limit scenario.

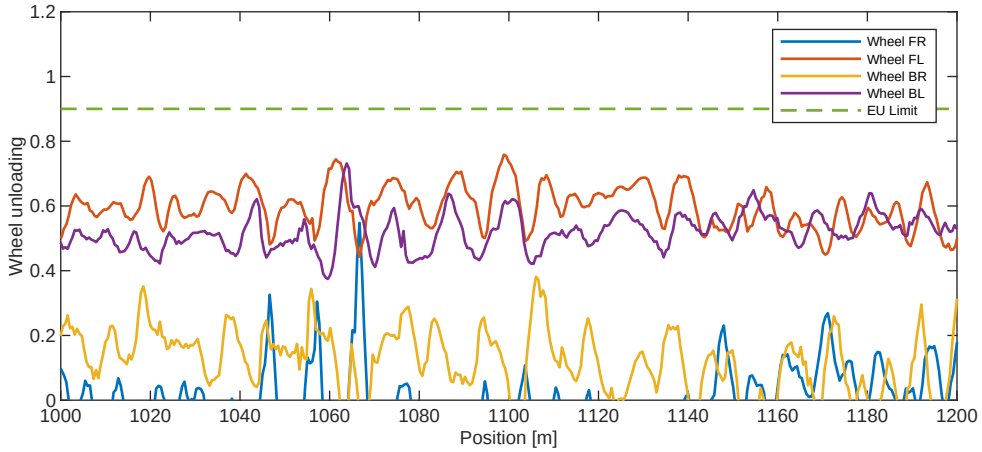

Figure I.4: Wheel Unloading criterion for the Sggrss wagon in the alert limit scenario.

I.2 Center Bogie

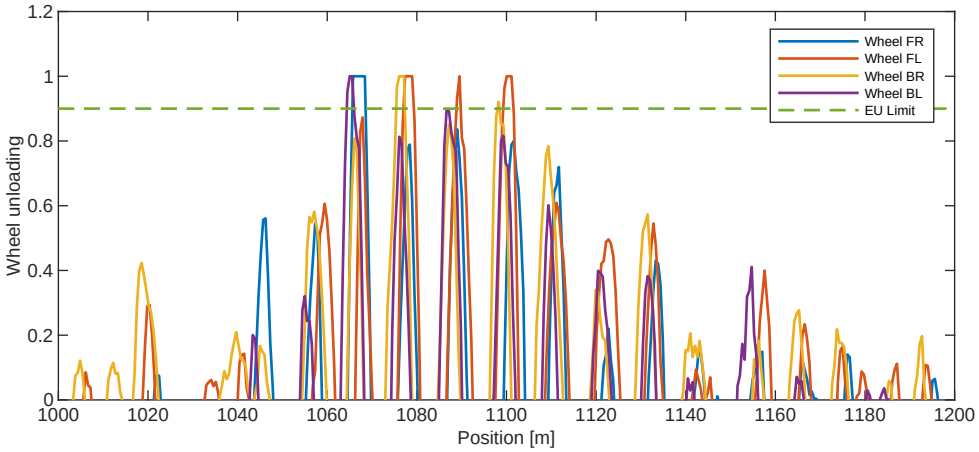

Figure I.5: Wheel Unloading criterion for the Sggrss wagon in the accident scenario.

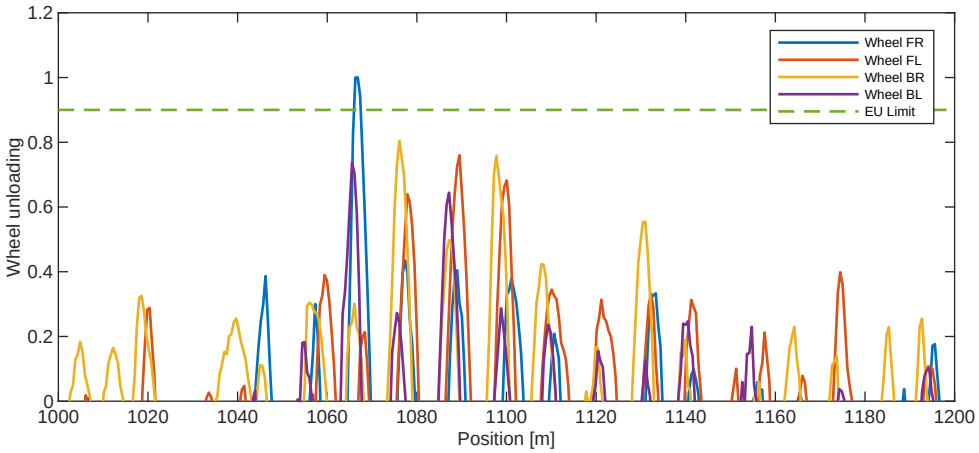

Figure I.6: Wheel Unloading criterion for the Sggrss wagon in the 2016-12-16 scenario.

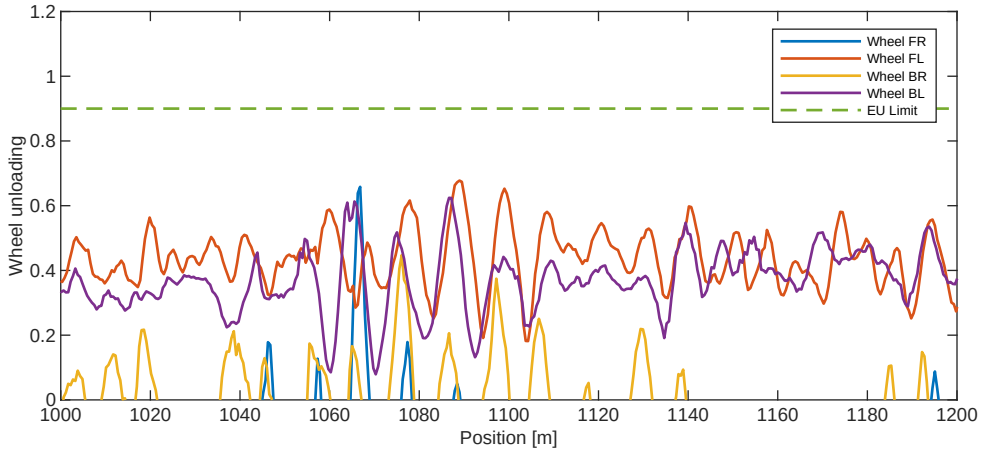

Figure I.7: Wheel Unloading criterion for the Sggrss wagon in the intervention limit scenario.

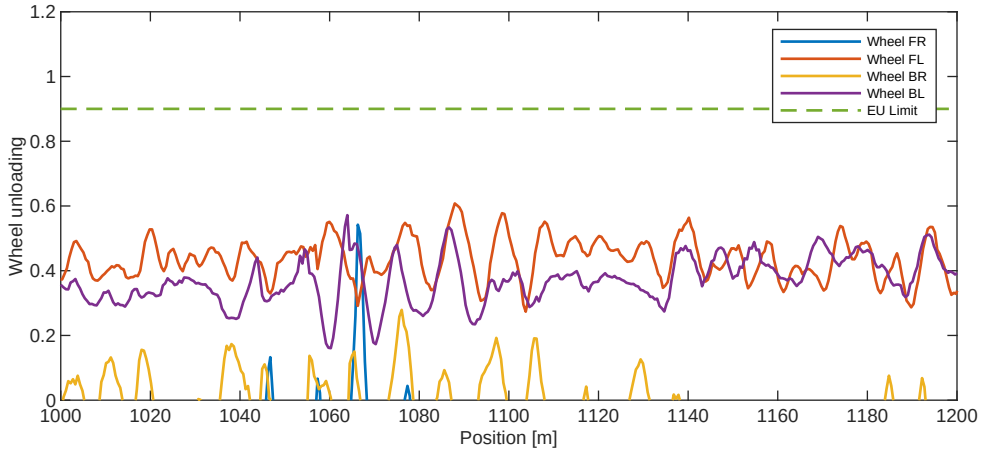

Figure I.8: Wheel Unloading criterion for the Sggrss wagon in the alert limit scenario.

I.3 Back Bogie

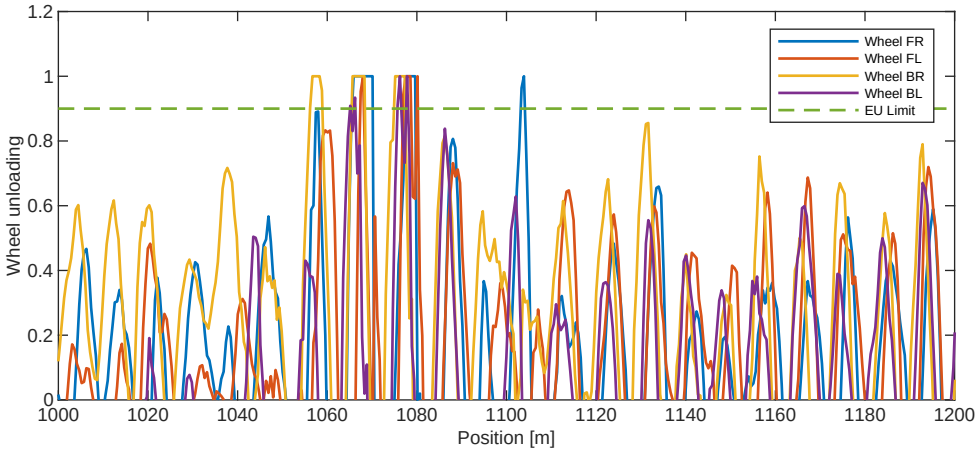

Figure I.9: Wheel Unloading criterion for the Sggrss wagon in the accident scenario.

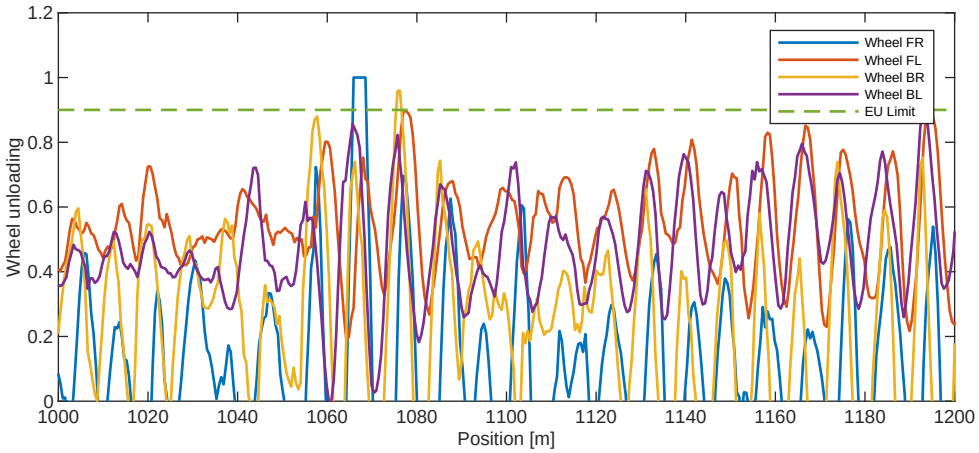

Figure I.10: Wheel Unloading criterion for the Sggrss wagon in the 2016-12-16 scenario.

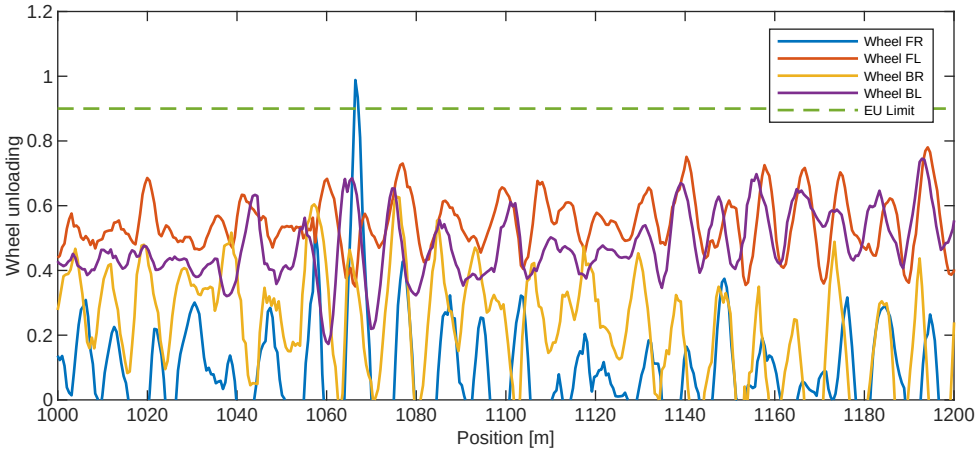

Figure I.11: Wheel Unloading criterion for the Sggrss wagon in the intervention limit scenario.

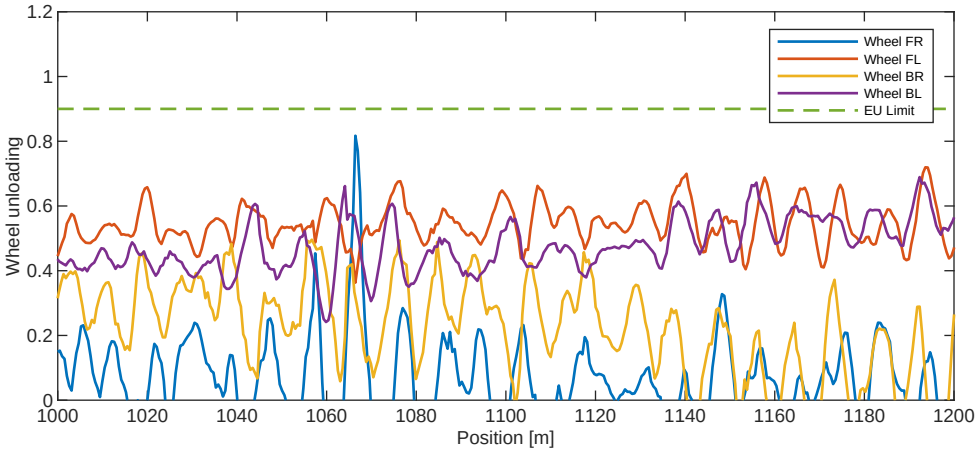

Figure I.12: Wheel Unloading criterion for the Sggrss wagon in the alert limit scenario.